

Aus dem Fachbereich Medizin  
der Johann Wolfgang Goethe-Universität  
Frankfurt am Main

betreut an der  
Dr. Senckenbergischen Anatomie  
Institut für Anatomie I (Klinische Neuroanatomie)  
Direktor: Prof. Dr. Thomas Deller

**Enhanced excitability and structural plasticity of maturing adult-born  
granule cells after LTP induction in the hippocampus**

Dissertation  
zur Erlangung des Doktorgrades der Medizin  
des Fachbereichs Medizin  
der Johann Wolfgang Goethe-Universität  
Frankfurt am Main

vorgelegt von  
Marie-Violet Laura Hawkrigde

aus Karlsruhe

Frankfurt am Main, 2018

Dekan: Prof. Dr. Josef M. Pfeilschifter

Referent: PD Dr. Stephan Schwarzacher

Korreferent: Prof. Dr. Frank Nürnberger

Tag der mündlichen Prüfung: 20. Dezember 2018

# Content

<b>1</b>	<b>LIST OF TABLES .....</b>	<b>V</b>
<b>2</b>	<b>LIST OF FIGURES.....</b>	<b>V</b>
<b>3</b>	<b>ABBREVIATIONS .....</b>	<b>VII</b>
<b>4</b>	<b>SUMMARY .....</b>	<b>- 1 -</b>
4.1	SUMMARY IN ENGLISH .....	- 1 -
4.2	ZUSAMMENFASSUNG IN DEUTSCHER SPRACHE .....	- 3 -
<b>5</b>	<b>INTRODUCTION .....</b>	<b>- 5 -</b>
5.1	ADULT NEUROGENESIS .....	- 5 -
5.2	ANATOMY OF THE HIPPOCAMPUS .....	- 6 -
5.3	THE HIPPOCAMPAL NEUROGENIC NICHE AND GRANULE CELL GENESIS .....	- 8 -
5.4	THE FUNCTION OF THE HIPPOCAMPUS .....	- 10 -
5.5	THE FUNCTION OF NEWLY BORN HIPPOCAMPAL GRANULE CELLS.....	- 11 -
5.6	REGULATION OF ADULT NEUROGENESIS .....	- 12 -
5.7	MOLECULAR MARKERS OF DIFFERENTIATION .....	- 13 -
5.8	MARKERS OF NEUROGENESIS .....	- 16 -
5.9	SYNAPTIC PLASTICITY IN MATURE GRANULE CELLS.....	- 17 -
5.10	STRUCTURAL MATURATION OF ADULT BORN GRANULE CELLS .....	- 18 -
5.11	SYNAPTIC INTEGRATION AND PLASTICITY OF NEWBORN GRANULE CELLS .....	- 19 -
5.12	QUESTIONS .....	- 22 -
<b>6</b>	<b>MATERIAL AND METHODS.....</b>	<b>- 24 -</b>
6.1	ANIMALS AND TISSUE PREPARATION.....	- 24 -
6.2	XDU PROJECT IMMUNOHISTOCHEMISTRY .....	- 25 -
6.3	SPINE PROJECT IMMUNOHISTOCHEMISTRY.....	- 28 -
6.4	MICROSCOPIC IMAGING AND ANALYSIS .....	- 29 -
6.5	SPINE ANALYSIS.....	- 31 -
<b>7</b>	<b>ADDITIONAL MATERIAL AND METHODS .....</b>	<b>- 32 -</b>
7.1	XDU PROJECT .....	- 32 -
7.1.1	<i>Injection of the cell markers .....</i>	<i>- 32 -</i>
7.1.2	<i>Electrophysiology and surgery.....</i>	<i>- 33 -</i>
7.1.3	<i>The induction of long term potentiation (LTP).....</i>	<i>- 34 -</i>
7.1.4	<i>Novel environment and perfusion .....</i>	<i>- 35 -</i>

7.2	SPINE PROJECT: .....	- 35 -
7.2.1	<i>Animals</i> .....	- 35 -
7.2.2	<i>Virus production and in vivo injection</i> .....	- 36 -
7.2.3	<i>In vivo perforant path stimulation</i> .....	- 36 -
7.2.4	<i>Tissue preparation</i> .....	- 37 -
<b>8</b>	<b>RESULTS</b> .....	<b>- 38 -</b>
8.1	XDU PROJECT .....	- 38 -
8.1.1	<i>Analysis of Egr1 immunoreactivity in adult-born granule cells</i> .....	- 38 -
8.1.2	<i>Unilateral Stimulation increases Egr1 expression in ABGCs of both hemispheres</i> .....	- 43 -
8.1.3	<i>Enhanced excitability is not an innate feature of ABGCs</i> .....	- 46 -
8.1.4	<i>Unilateral Stimulation results in similarly heightened excitability of 6, 12 and 35 week old ABGCs of both hemispheres</i> .....	- 49 -
8.1.5	<i>Higher excitability in infrapyramidal adult born granule cells</i> .....	- 52 -
8.1.6	<i>Cross reaction of antibodies</i> .....	- 56 -
8.2	SPINE PROJECT .....	- 57 -
8.2.1	<i>Egr1 expression due to HFS is lower in adult-born than in mature granule cells</i> .....	- 58 -
8.2.2	<i>Dendritic spine plasticity of adult-born granule cells following HFS</i> .....	- 60 -
8.2.3	<i>Correlation of Egr1 intensity and spine enlargement</i> .....	- 61 -
<b>9</b>	<b>DISCUSSION</b> .....	<b>- 66 -</b>
9.1	XDU PROJECT .....	- 66 -
9.1.1	<i>Early retirement vs. ongoing function in maturing granule cells</i> .....	- 66 -
9.1.2	<i>Excitability of adult born granule cells over time</i> .....	- 68 -
9.1.3	<i>Influence of experience/stimulation on excitability reactivation</i> .....	- 70 -
9.1.4	<i>Bilateral excitation by unilateral stimulation</i> .....	- 72 -
9.1.5	<i>Differences in Egr1 expression between infra- and suprapyramidal blade</i> .....	- 72 -
9.1.6	<i>Omission of cross reaction in single stainings</i> .....	- 74 -
9.2	SPINE PROJECT.....	- 75 -
9.2.1	<i>Age dependent functional integration of maturing adult born granule cells</i> .....	- 76 -
9.2.2	<i>Homo- and heterosynaptic spine plasticity in adult born granule cells following HFS</i> ...	- 77 -
9.2.3	<i>Homo- and heterosynaptic spine plasticity correlates with Egr1 expression intensity</i> ...	- 78 -
<b>10</b>	<b>CONCLUSION, CLINICAL RELEVANCE AND OUTLOOK</b> .....	<b>- 80 -</b>
<b>11</b>	<b>ACKNOWLEDGEMENTS</b> .....	<b>- 83 -</b>
<b>12</b>	<b>REFERENCES</b> .....	<b>- 85 -</b>

13	CURRICULUM VITAE .....	- 112 -
14	SCHRIFTLICHE ERKLÄRUNG .....	- 115 -

## 1 List of tables

Table 1 XdU project: Primary antibodies.....	- 27 -
Table 2 XdU project: Secondary antibodies.....	- 27 -
Table 3 Spine project: Primary antibodies .....	- 28 -
Table 4 Spine project: Secondary antibodies .....	- 28 -
Table 5 XdU project: Experimental method per animal .....	- 39 -
Table 6 XdU project: Number of all counted GCs, ipsi vs contra.....	- 40 -
Table 7 XdU project: Number of all counted GCs, supra vs infra .....	- 53 -

## 2 List of figures

Figure 1: Calbindin expression in neurons of the hippocampal formation .....	- 7 -
Figure 2: Randomized selection of mature GCs.....	- 29 -
Figure 3: Timeline. ....	- 33 -
Figure 4: Confocal images of Egr1 and NeuN positive, IdU labelled ABGCs. ....	- 39 -
Figure 5: Average per slice (unlabelled). ....	- 41 -
Figure 6: Average per slice (6 weeks).....	- 42 -
Figure 7: Average per slice (12 weeks).....	- 42 -
Figure 8: Average per slice (35 weeks).....	- 43 -
Figure 9: Average per time point .....	- 44 -
Figure 10: Merged time points .....	- 45 -
Figure 11: Control. ....	- 48 -

Figure 12: The distribution of z-score values .....	- 51 -
Figure 13: Supra vs. infra .....	- 54 -
Figure 14: Supra vs infra, merged .....	- 55 -
Figure 15: Cross reaction.....	- 57 -
Figure 16: Cell age dependent Egr1 expression .....	- 59 -
Figure 17: Layer specific structural plasticity of dendritic spines.....	- 61 -
Figure 18: Correlation of Egr1 expression and dendritic spine size .....	- 63 -
Figure 19: Egr1 expression is linked to homo- and heterosynaptic plasticity.....	- 65 -

### 3 Abbreviations

ABGC	adult born granule cell/s
BrdU	5-Bromo-2'-deoxyuridine
CldU	5-Chloro-2'-deoxyuridine
CRE	Ca <sup>2+</sup> /cAMP responsive element
CREB	cAMP response binding protein
DBS	delta burst stimulation
DG	dentate gyrus
DNA	de-oxy ribonucleic acid
dpi	days past injection
Egr1	early growth response 1, TIS, Zif268, ( <b>Z</b> inc finger protein 225, <b>E</b> gr-1, <b>N</b> GF1-A, <b>K</b> rox24)= ZENK
GC	granule cell/s
GCL	granule cell layer
GFP	green-fluorescent protein
HFS	high frequency stimulation
IdU	5-Iodo-2'-deoxyuridine
IEG	immediate early gene
IML	inner molecular layer
LTP	long term potentiation
mGC	mature granule cell
MML	middle molecular layer
MPP	medial perforant path
NeuN	neuronal nuclear protein
NeuroD	neuronal differentiation factor
SGZ	subgranular zone of the dentate gyrus
SRE	Serum response element
SVZ	subventricular zone
OML	outer molecular layer
PBS	phosphate buffered saline



PRH/LEC	perirhinal and lateral entorhinal cortex
ptd	prior to death
TBS	Tris-buffered saline
XdU	any Uridine derivativ

## 4 Summary

### 4.1 Summary in English

Throughout the entire life, new neurons of the granule cell type (GCs) are continuously generated in the mammalian hippocampal dentate gyrus (DG). As a part of the limbic system, the hippocampus is concerned with spatial and declarative memory formation. Increasing evidence exists, that adult born granule cells (ABGCs) play an important role in this process. An especially critical period, when these ABGCs are 4-6 weeks old, has come into the focus of research. It is during this specific time-span that the ABGCs express enhanced excitability and synaptic plasticity as well as a lowered threshold for the induction of long term potentiation (LTP), a mechanism associated to learning and memory formation.

This study investigates the time course and dynamics of synaptic integration in ABGCs and mature GCs together with which differences exist between them at various cell ages. Furthermore, spine plasticity following high frequency stimulation (HFS) is analysed focusing on a critical phase of enhanced excitability in 4-5 week old ABGCs.

In this thesis, two approaches at studying the synaptic integration and structural plasticity of ABGCs in rats were investigated. This work was performed on fixed brain material that was provided by two laboratories that performed the *in vivo* labelling, stimulation procedures and brain fixation. In the first project, 6, 12 and 35 weeks old XdU-labelled ABGCs were studied. Adult rats were exposed to an enriched environment and received unilateral intrahippocampal delta burst stimulation (DBS) and LTP induction. The ABGCs and a control population of mature GCs were immunohistologically analysed for Egr1 (early growth response 1) expression. Egr1 is an immediate early gene (IEG), expressed after LTP induction and marks neuronal excitation.

It was found, that unilateral stimulation of the perforant path of the hippocampus results in an increase of Egr1 expression in ABGCs of both hemispheres. It could be shown that the enhanced expression intensity of Egr1 in ABGCs is not a usual state of young GCs but a reaction to DBS. ABGCs from unstimulated control animals and ma-

ture GCs expressed lower levels of Egr1. Interestingly, the stimulation induced a similar degree of Egr1 expression intensity in all ABGC age groups. Furthermore, it was found that young ABGC from the infrapyramidal dentate gyrus (DG) express a higher excitability than those from the suprapyramidal DG.

In the second project, fixed brain sections were analysed. They stemmed from rat brains containing 28 and 35 day old ABGC that had been transfected with intrahippocampal RV-GFP (retroviral-green fluorescent protein) injections and had received unilateral high frequency stimulation of the medial perforant path *in vivo*. Nuclear Egr1 expression intensity was analysed in a cell specific manner. Dendritic spine size was measured in the inner-, middle- and outer molecular layer (IML, MML, OML). It was found that in ABGC, stimulation induced Egr1 expression increase is lower than in mature GC. Following HFS, a significant homosynaptic spine enlargement was observed in the MML indicating homosynaptic LTP, while heterosynaptic spine shrinkage was found in the adjacent IML and OML. The latter corresponds to heterosynaptic long term depression (LTD). Homosynaptic plasticity describes an input-specific potentiation of synapses that received direct activation. The weakening of synapses not stimulated during homosynaptic potentiation is oppositely coined heterosynaptic plasticity<sup>1</sup>.

A positive correlation between an increase in nuclear Egr1 expression intensity and spine enlargement due to homosynaptic plasticity induced by HFS could be shown. Concomitant heterosynaptic plasticity, as indicated by spine shrinkage was observed. Spine shrinkage in the IML and OML showed a negative correlation to a decrease in Egr1 intensity.

Taken together, the results provide detailed information on the gradual integration of ABGC with ongoing maturation. Cell specific proof for homo- and heterosynaptic plasticity following HFS was found in the critical period of synaptic integration of ABGCs.

## 4.2 Zusammenfassung in deutscher Sprache

Während des gesamten Lebens von Säugetieren werden im *Gyrus dentatus* des Hippocampus neue Neurone vom Körnerzelltyp gebildet, was als adulte Neurogenese bezeichnet wird. Als Teil des limbischen Systems ist der Hippocampus an der Verarbeitung räumlicher und zeitlicher Informationen beteiligt und spielt eine wichtige Rolle in der Gedächtnisbildung. Die adult neugeborenen Körnerzellen (ABGC) sind aktuell Gegenstand intensiver Forschung, da gezeigt werden konnte, dass sie eine Schlüsselrolle in hippocampalen Lernvorgängen einnehmen. Die ABGCs gehen aus Stammzellen hervor, die sich schrittweise zu Nervenzellen mit komplexen Dendritenbäumen entwickeln. Insbesondere das Zellalter von 4-6 Wochen hat sich für hippocampale ABGCs als interessant erwiesen. Während dieser Zeitspanne, die auch „kritische Phase“ genannt wird, zeigen die ABGCs eine verstärkte zelluläre Erregbarkeit und synaptische Plastizität sowie eine erniedrigte Schwelle für die Induktion von Langzeitpotenzierung (LTP). Letzgenannter Prozess wird mit Lernen und Gedächtnisbildung assoziiert und umschreibt die Verstärkung synaptischer Übertragungen. Im Gegensatz dazu beschreibt Langzeitdepression (LTD) die Abschwächung desselben. In der vorliegenden Dissertation wurden zwei unterschiedliche methodische Ansätze für die Erforschung der Dynamik synaptischer Integration und struktureller Plastizität von ABGCs in Ratten verfolgt. In beiden Ansätzen wurde *Egr1* (early growth response 1) als gradueller Marker für synaptische Plastizität verwendet. *Egr1* ist ein sogenanntes *Immediate early gene* welches nach der Induktion von Langzeitpotenzierung exprimiert wird und als stabiler Marker für synaptische Plastizität etabliert ist. Für das erste Projekt, wurden XdU-markierte ABGCs im Alter von 6, 12 und 35 Wochen verwendet. Adulte Ratten wurden einer anreicherten Umgebung ausgesetzt und, mittels intrahippocampaler Hochfrequenzstimulation (HFS) einer Hemisphäre, *in vivo* einer Langzeitpotenzierung unterzogen. Die *Egr1* Expression im Zellkern von ABGCs und der Kontrollpopulation aus murenen Körnerzellen wurde immunhistologisch quantifiziert.

Im Rahmen dieses Projekts wurde herausgefunden, dass die einseitige Stimulation des *Tractus perforans* des Hippocampus eine Zunahme der *Egr1* Expression in ABGCs beider Hemisphären hervorruft. Es konnte gezeigt werden, dass die verstärkte *Egr1* Ex-

pression in ABGCs kein Normalzustand junger Körnerzellen, sondern eine Reaktion auf die HFS ist. Sowohl ABGCs unstimulierter Kontrolltiere, als auch mature Körnerzellen exprimierten geringere Mengen Egr1. Interessanterweise induzierte die Stimulation ein vergleichbares Maß an Egr1 Expression in ABGCs aller Altersgruppen. Diese Resultate demonstrieren, dass die Aktivität von ABGCs mittels einer HFS auf ein langfristig erhöhtes Maß an Erregbarkeit angehoben werden konnte. Im zweiten Projekt wurden ABGCs durch intrahippocampale Injektionen eines retroviralen Vektors mit einem grün fluoreszierenden Protein markiert. Nach 28 und 35 Tagen wurde eine *in vivo* HFS durchgeführt. Die nukleäre Egr1 Expressionsintensität wurde bestimmt und mit strukturellen Veränderungen dendritischer Dornen korreliert. In der Literatur ist eine Assoziation von LTP mit einer Vergrößerung von Dornfortsätzen beschrieben ebenso wie von LTD mit einer Verkleinerung von Dornfortsätzen. Die Größe der dendritischen Dornfortsätze wurde jeweils in der inneren-, mittleren- und äußeren Molekularschicht (IML, MML, OML) ausgemessen. Die Ergebnisse konnten jeweils individuellen Körnerzellen zugeordnet werden. Nach der HFS war der Egr1 Expressionsanstieg in ABGCs geringer als in muren Körnerzellen. In der stimulierten MML kam es nach HFS währenddessen zu einer signifikanten Vergrößerung von dendritischen Dornen, die als strukturelles Korrelat homosynaptischer LTP interpretiert werden kann. Die Stärke der Vergrößerung konnte mit einer intensiveren Egr1 Expression positiv korreliert werden. Gleichzeitig kam es in der benachbarten, unstimulierten IML und OML zu einer Verkleinerung von Dornfortsätzen. Dieses Phänomen bezeichnet man als heterosynaptische LTD, sie konnte negativ mit der Egr1 Expression im Zellkern korreliert werden. Homosynaptische Plastizität beschreibt eine Input spezifische Potenzierung von Synapsen, die direkt aktiviert werden. Im Gegensatz dazu wird die Abschwächung von Synapsen, die während homosynaptischer Potenzierung nicht stimuliert wurden, heterosynaptische Plastizität genannt<sup>1</sup>. Zusammengefasst liefern die gewonnenen Resultate detaillierte Informationen über die graduelle Integration von ABGCs während ihrer zunehmenden Reifung. Es wurde ein zellspezifischer Beweis für homo- und heterosynaptische Plastizität nach HFS in der kritischen Phase der synaptischen Integration von ABGCs gefunden, die mit der nukleären Expression von Egr1 korreliert werden konnte.

## 5 Introduction

### 5.1 Adult neurogenesis

It was thought for a long time that neurons cannot be regenerated in adult organisms. This dogma was, however, overthrown with the discovery of neurogenesis in adult rats by Altman & Das in 1965. Adult neurogenesis describes the process of cell division in neurons during adulthood disclosing an entire field of research as a result of this discovery. Thanks to the unbroken enthusiasm, with which the details of adult neurogenesis were and are sought after until the present day, the knowledge of this phenomenon has greatly increased. The abovementioned authors showed adult neurogenesis in the subgranular zone (SGZ) of the dentate gyrus as well as in the subventricular zone (SVZ) by labelling newborn neurons with radioactive thymidine- $H^3$ . In the following years, adult neurogenesis was demonstrated in other animals, corroborating their results. The existence of ongoing neurogenesis in the telencephalon of canary birds and their proliferation, differentiation and functional integration was presented<sup>2,3</sup>. The first to demonstrate adult neurogenesis in the human brain was Eriksson and colleagues<sup>4</sup>. Evidence for continuing neurogenesis throughout the humans lifespan was presented by measuring the amount of  $^{14}C$  from atomic bomb tests in the genomic DNA of hippocampal neurons<sup>5</sup>. Very recent results from post-mortem- and epileptic surgery resection samples interestingly show a strong indication that, although neurogenesis in the hippocampus rapidly declines during childhood, it cannot be detected in humans beyond puberty<sup>6</sup>. On the other hand, a study from 2018 in whole hippocampi from cognitively healthy humans aged 14 - 79 revealed a decreasing but persistent adult neurogenesis<sup>7</sup>. Throughout the recent decades, adult neurogenesis has been shown in a large variety of animals<sup>8,9</sup>. Today it is widely accepted, that adult neurogenesis exists in the SVZ and the SGZ of the hippocampus, though evidence was presented that neurogenesis also exists in the striatum of humans<sup>10</sup>. The reports of adult neurogenesis in other brain regions are controversially discussed<sup>11,12</sup>.

## 5.2 Anatomy of the hippocampus

The curved structure of the hippocampal formation, a part of the limbic system, has prompted many comparisons that resulted in its given name. In the mid-sixteenth century, the Venetian anatomist Julius Caesar Aranzi saw a similarity to a seahorse and hence called it “hippocampus”, the Latin translation<sup>13</sup>. One hundred years later, the Dutch physician and anatomist Isbrand van Diemerbroeck visualized the “pes hippocampi” instead, interpreting the curved forelimb of the mythological hippocampus, a creature half horse and half fish<sup>14</sup>. Decades later, the similarity to a ram’s horn prompted the name “cornu ammonis” driven by the depiction of the Egyptian god Amun with a ram’s head<sup>15</sup>. Today, the subdivisions of the hippocampus proper are divided into three parts, called CA1, CA2 and CA3. The CA stands for “cornu ammonis”. The hippocampus proper is part of the hippocampal formation, which also comprises the dentate gyrus, the subiculum, parasubiculum, presubiculum and entorhinal cortex. In the rat and mouse, its arched structure reaches from slightly dorsal of the corpora mammilaria all the way along the lateral ventricles to the ventromedial part of the temporal lobe<sup>16</sup>. The hippocampus is widely used as a model system of cortical neural network because its features allow easier, specific observation and manipulation than other brain parts. The aforementioned features include both the formation of its main cells in a single layer and the inputs adherence to a stringent lamination. Furthermore, most of the connectivity follows unidirectional pathways and includes synapses with strong plasticity<sup>17</sup>. Many *in vivo* and *in vitro* techniques have been established using the hippocampal formation, making it possible to compare different studies. The entorhinal cortex is the main cortical source of input, consisting of a variety of sensory information. The superficial layers II and III of the six-layered entorhinal cortex provide axons that project, via the perforant path, to the dentate gyrus (DG)<sup>16,18</sup>. Here, the granule cells’ long axons, termed mossy fibers, convey the signal to CA3. The pyramidal cells give rise to the so called Schaffer collaterals which project to CA1. Those cells closer to the DG project to CA1 neurons more septal to their location, CA3 pyramidal cells closer to CA1 send their axons to CA1 neurons further temporally. Axons either directly reach the entorhinal cortex from this point or the projections take an indirect way via the subiculum, pre- or parasubiculum and then progress further to the entorhinal cortex. This circuitry is called the

trisynaptic loop<sup>19</sup>. Additionally, the entorhinal cortex projects directly to other hippocampal regions such as CA3<sup>18</sup>.

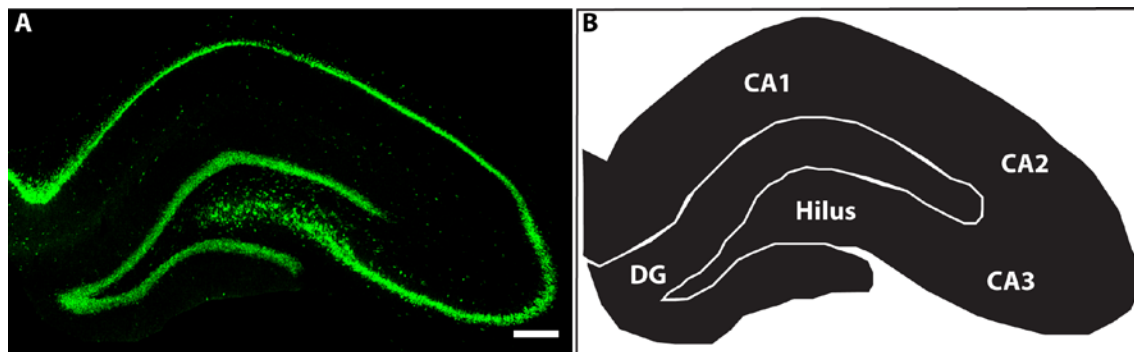


*Figure 1: Calbindin expression in neurons of the hippocampal formation (A): A coronary schema of the dentate gyrus (DG) and the hippocampus proper is depicted (B). The latter can be subdivided into CA1 – CA3 (CA stands for “cornu ammonis”). The part of CA3 enclosed by the DG is called the hilus. Scalebar: 50  $\mu$ m. Image on the right drawn according to the immunohistochemically stained hippocampal tissue on the left.*

The DG itself consists of three cell layers, the granule cell layer (GCL) curves around the polymorphic layer or hilus and thus features a lying V- or U-shape with the bend, called crest, pointing medially. Hence, the DG can be divided into a dorsal- or suprapyramidal blade and a ventral or infrapyramidal blade. On the outer side of the GCL lies the molecular layer. It is formed by the cone-shaped dendritic trees of the granule cells extending completely through to the hippocampal fissure. The molecular layer is subdivided into the inner, middle and outer molecular layer (IML, MML and OML). The lateral perforant path from the lateral entorhinal cortex terminates in the OML and conveys olfactory, visual and tactile stimuli<sup>20,21</sup>. The medial perforant path originating from the medial entorhinal cortex reaches the MML, providing input on spatial information and navigation<sup>22,23</sup>. Furthermore, a few inhibitory interneurons like chandelier cells are interspersed in the molecular layer and supply inhibitory input to GCs. The resting membrane potential of mature GCs lies at -75 mV, a more hyperpolarised state than in CA3<sup>24–26</sup>. This leads to a higher threshold for action potential generation together with a lower spontaneous firing rate in granule cells. The GCL is composed of a densely packed band of granule cells and a small amount of other cells, such as the GABAergic basket cells. The latter cell-type is positioned at the border of the GCL to



the hilus and derives its name from the basket-like plexus which its axons form around neighbouring GC somata. The GCs give rise to long axons called mossy fibres because they seemed to be “mossy” in appearance to Ramón y Cajal due to their many varicosities<sup>27</sup>. Initially, their trajectory takes them to the centre of the hilus<sup>28</sup>, which is composed of a variety of cells: GABAergic interneurons and glutamatergic mossy cells with axons terminating in the IML of the ipsi- and contralateral DG. They project to GCs as well as GABAergic interneurons and thus stimulate excitatory and inhibitory parts of the circuitry. It is hypothesized that this could fulfil a modulatory function<sup>29,30</sup>. The proximal dendrites of the mossy cells are covered with the eponymous “thorny excrescences” and receive input from GCs of the same septotemporal level. The mossy fibres from all granule cells are highly organized. From the hilus, they turn towards CA3c (division according to Lorente de Nó, 1934<sup>31</sup>) where their trajectory takes a 90° angle from ventral to dorsal as they cross CA3b. Upon arrival in CA3a the mossy fibres take a further 90° angle towards the temporal pole of the hippocampus<sup>32</sup>. Thus, all mossy fibres reach through the entire CA3 field irrelevant of the position of their soma. Each mossy fibre produces varicosities to 14-28 CA3 pyramidal cells. Since there are far more GCs than presynaptic neurons in the entorhinal cortex and postsynaptic neurons in the CA3 area, the input first diverges in the GCL only to converge on the CA3 pyramidal cells<sup>16,33-36</sup>. Apart from the abovementioned input via the perforant path, GCs receive further input from certain subcortical regions: Achetylcholinergic afferents from the septal nuclei, noradrenalinergic input from the locus coeruleus, dopaminergic input from the central tegmental area, serotonergic afferents from the raphe nuclei and afferents from the supramammillary region of the hypothalamus with the transmitter substance P which has a modulatory function<sup>18,29</sup>.

### **5.3 The hippocampal neurogenic niche and granule cell genesis**

The term “neurogenic niche” describes the microenvironment in which adult neurogenesis takes place in the subventricular zone (SVZ) of the lateral ventricles and the subgranular zone (SGZ) within the hippocampus. It consists of cellular and molecular components that regulate neurogenesis. Microglia, macrophages, ependymal- and endo-

thelial cells as well as mature neurons, progenitors and astrocytes all participate in the complex equilibrium that promotes the birth of new neurons<sup>37,38</sup>. Non-cellular components such as cytokines, neurotransmitters and growth factors are equally indispensable for a stable regulation<sup>39,40</sup>.

The neural stem cells of the hippocampus can be found in the SGZ of the dentate gyrus, which lies adjacent to the GCL at its hilar border. The neural stem cells are radial glia-like precursor cells, so called type 1 cells, that express the distinct neuronal stem cell markers Nestin (a type VI intermediate filament protein), GFAP (glial fibrillary acidic protein), Sox1 (Sry-related HMG box transcription factor) and BLBP (brain lipid-binding protein). Their end-feet are in contact with blood vessels and their dendrites reach through the granule cell layer (GCL). The type 1 cell has astrocytic properties and although it scarcely divides, it gives rise to intermediate progenitor cells, the type 2 cells<sup>41-43</sup>. The fate choice decision of type 2 cells is already fixed. Those of glial lineage are the type 2a cells, although they express the same four markers as the glia-like precursor cell<sup>44</sup>, their morphology differs greatly. The type 2b cells have a neuronal phenotype and express NeuroD, Nestin and Tbr2. At this point in time the expression of DCX (Doublecortin) and PSA-NCAM (polysialylated neuronal cell adhesion molecule) begins, which overlaps completely. The type 2b cells divide quickly and provide the large number of new neuronal progenitor cells<sup>45</sup>. They generate neuroblast-like cells, the type 3 cells, that start to migrate into the GCL. They have exited the cell cycle and still express DCX, PSA-NCAM, NeuroD and Prox1. Through the extension of an axon through the hilus to the CA3 region of the hippocampus together with the stretching of an elongating dendrite towards the molecular layer, a change in cell marker expression develops as a result. During the postmitotic maturation stage, DCX gives way to Calretinin in mice, accompanied by NeuN (Neuronal Nuclei). At about 3 weeks of cell age, Calretinin expression switches to Calbindin and DCX expression is finally concluded<sup>46</sup>. The GC is functionally mature enough from this point onward to participate in the network<sup>47,48</sup>.

## 5.4 The function of the hippocampus

One of the main functions of the hippocampus is memory formation<sup>49,50</sup>. More explicitly, two kinds of memories are dependent on the hippocampal formation: Spatial memory, which is responsible for the orientation in the environment, and declarative memory. The latter can be divided into semantic memory, which concerns factual information, and episodic memory which includes autobiographical events and their context<sup>49</sup>. Furthermore, the hippocampal formation takes part in other brain functions, such as the regulation of the hypothalamic-pituitary axis<sup>51</sup>, behavioural inhibition<sup>52</sup>, anxiety<sup>53</sup> and sensorimotor function<sup>18</sup>. A well-established method for studying the function of an anatomical structure is to carefully administer a lesion and to then observe the results. Different approaches to this method exist, each with varying precision and adverse effects. Impairment of associative memory and spatial learning has been reported in animals with lesion of the hippocampal formation<sup>54-56</sup>. The most famous human with deliberate hippocampus lesions was the patient H.M. In order to cure his epilepsy; a bilateral medial temporal lobectomy was performed effectually blocking his ability to form new memories. Although he could remember everything predating the operation, the formation of episodic, semantic and spatial memories was completely lost, with only implicit content being learned as a result<sup>57</sup>. Other studies have focused on the role of ABGCs in the hippocampal function by impeding adult neurogenesis as thoroughly as possible using irradiation, application of antimetabolic drugs or genetic alteration<sup>58-60</sup>. A variety of studies have shown deficits in hippocampus dependent tasks like spatial navigation in the Morris-Water-Maze<sup>61,62</sup>, exploration of novel environment<sup>63</sup>, trace fear conditioning<sup>64,65</sup> and pattern separation<sup>55,66</sup> (see below). Interestingly, there are contradictory results for certain functions. After inhibition of adult neurogenesis contextual fear conditioning was found to be impaired by some<sup>60,67-69</sup>, but not by other researchers<sup>64,70,71</sup>. Furthermore, spatial learning and memory seemed to be compromised to some investigators<sup>70,71</sup>, but appeared normal to others<sup>60,67,72</sup>. This may be due to fundamental differences existing between mice and rats, i.e. animal strains and age as well as variation in the type of behavioural tests used.

Certain hippocampal properties have been found to be relevant for memory formation. Pattern separation is a process that differentiates between differences of highly

similar input. In order to disambiguate the characteristics of events, objects and locations, minimal differences have to be noted. Thus, through computational conversion, similar input is transformed into more distinct output within the network<sup>73</sup>. As previously described, the input to the EC diverges on a multitude of dentate gyrus GCs only to converge on a smaller number of CA3 pyramidal cells<sup>33,35,36</sup>. Through neural circuits from local interneurons, the GCs not only receive constant feedback inhibition<sup>74,75</sup>, they are also more hyperpolarized<sup>24</sup>. These factors lead to a low activity which allows for a separation of incoming similar input and a representation in very few neurons<sup>76,77</sup>. It has been proposed, that the connectivity between the DG and CA3 plays an important part in pattern separation<sup>78</sup>. It is of interest to note, that the precision of memory encoding improved with increased DG-CA3 feedforward inhibition<sup>79</sup>. Opposed to pattern separation is pattern completion, a process that allows the recall of an entire memory from any cue<sup>80</sup>. The completion of a memory imprint, starting from an incomplete part, has been attributed to CA3. The CA3 region receives input from mossy fibres as well as directly from layer 2 of the EC via the perforant path. Furthermore, the pyramidal neurons give rise to recurrent projections, which function as an auto associative memory. This enables the completion of a memory starting from a small part of the representation<sup>80-82</sup>.

## 5.5 The function of newly born hippocampal granule cells

Various theories have been formed as a result of considering the role of adult neurogenesis in pattern discrimination. Whilst Marín-Burgin and colleagues argued that old GCs could be apt pattern separators due to their high activation threshold and input specificity<sup>83</sup>, other groups reported that although mature GCs are necessary for differentiating between distinct input, new born GCs are indispensable for disambiguating similar information<sup>36,84</sup>. Disregarding these discrepancies, it has been made clear that adult neurogenesis is relevant for several aspects of memory. Increasing adult neurogenesis in the dentate gyrus resulted in enhanced memory formation and acquisition<sup>64,68,70,85</sup> as well as recall capacity<sup>72,86</sup>. Animals with reduced adult neurogenesis showed impaired pattern separation which became evident in their deficits discriminating similar contexts<sup>63,84,87</sup>. Conversely, results in pattern separation dependent tasks were improved in mice with enhanced neurogenesis<sup>88</sup>. The role of adult neurogenesis in forgetting has re-

cently been investigated. It has been demonstrated that increasing neurogenesis correlates with forgetting in adult mice. Infants, with an inherent high rate of neurogenesis, quickly forget new memories (infantile amnesia). This observation led to the experimental decrease of adult neurogenesis in infant mice resulting in attenuated forgetting. Inducing stronger adult neurogenesis in two species with naturally low hippocampal adult neurogenesis resulted in the appearance of infantile amnesia<sup>89</sup>. These conclusions suggest that the integration of newborn neurons could result in replacement of pre-existing neurons. A careful measure of adult neurogenesis would therefore appear necessary to provide a balance between new memory formation and forgetting<sup>73</sup>.

## 5.6 Regulation of adult neurogenesis

Adult neurogenesis is regulated by countless intrinsic and extrinsic factors. The complexity of this process stems from the levels of regulation that begin at the initiation of proliferation and its rate, proceed to the variety in differentiation and integration and reach the determination of neuron survival. On single cell level, various cell cycle genes and signalling pathways have been identified as key regulators in adult neurogenesis<sup>85,90-92</sup>. Furthermore, hormones and growth factors like VEGF and BDNF belong to the mediators that orchestrate its equilibrium<sup>93-95</sup>. Epigenetic factors also influence adult neurogenesis in order to provide adaptation to the environment<sup>85</sup>. Several studies have presented certain mechanisms that have a positive effect on adult neurogenesis, including differentiation and survival. Hippocampus dependent learning tasks have proved to increase ABGC survival<sup>96-98</sup>. It has been demonstrated that the exposition of rats and mice, especially during a critical phase, to enriched environment equally boosts survival of newborn GCs<sup>99-103</sup>. It is of interest to note, that a positive correlation between the area size explored by the animal and the amount of hippocampal neurogenesis was observed by Freund et al<sup>104</sup>. Voluntary physical exercise, such as wheel-running, augmented cell proliferation in the SGZ and lead to enhanced mushroom spine formation<sup>105,106</sup>. Casting a closer look at the hippocampal circuitry, it can be noted that neurogenesis is tuned by excitatory and inhibitory neuronal activity. GABAergic signalling from interneurons lead to improved ABGC survival as well as dendritic growth and synapse formation. These effects were maintained via the CREB pathway and through

Calcium-dependent expression of NeuroD, a neuronal differentiation factor<sup>107,108</sup>. Conversely, the application of Calcium agonists or antagonists leads to an increase or decrease of neuronal differentiation<sup>109</sup>. Promoted ABGC survival and proliferation could be observed after LTP induction at the perforant path<sup>110,111</sup>. It has been shown that during the critical period, NMDA receptor dependent neuronal activity is decisive for the survival of ABGCs<sup>95,112</sup>. The NMDAR subunit NR2B, which is expressed during the critical period, is necessary for enhanced synaptic plasticity of ABGCs<sup>47,63</sup>. Contrary to the abovementioned effects, several conditions influence adult neurogenesis in a negative way. It has been noted remarkably long ago that neurogenesis declines with increasing age<sup>113,114</sup>. Furthermore, various forms of stress pose a derogatory influence on ABGC proliferation through over-activation of the hypothalamic-pituitary-adrenal axis<sup>115-118</sup>. Although temporal lobe epilepsy initially enhances progenitor cell proliferation, this pathological state of stimulation also causes a defective differentiation and often results in erroneous morphology<sup>119</sup>. The increased neurogenesis following ischemia together with the migration of the newly formed neurons to the destructed locus is a compensatory reaction of the organism but long lasting cell survival mostly fails due to a lack in synaptic integration<sup>120,121</sup>. The abundance of regulatory mechanisms in adult neurogenesis takes effect on the fate of the continuously born precursor cells. In the two weeks following this event, it can be observed that the majority succumb to apoptosis until only a few succeed to fully differentiate and integrate into the existing network<sup>122,123</sup>.

## 5.7 Molecular markers of differentiation

In order to analyse brain function and development on single cell basis, tools are necessary to determine different cell types and their stage of maturation. Furthermore, individual cells of specific age should be analysed with regard to their participation in the circuitry. At the close of the 19<sup>th</sup> century, Camillo Golgi and Ramón y Cajal laid the foundations for the analysis of single neurons. The silver staining method is still in use today but in the meantime an entirely new toolbox has been added: molecular cell markers. In the following section, a small selection of cell markers that are essential for researching adult neurogenesis will be presented. Doublecortin (DCX) is expressed by

neuronal precursor cells and immature neurons starting at about three days of cell age<sup>124</sup>. It is a microtubule associated protein that plays an important role in the migration of newborn neurons and lamination of the cortex<sup>125</sup>. DCX is widely used as a surrogate marker for neurogenesis<sup>45</sup>. PSA-NCAM (polysialylated neuronal cell adhesion molecule) is a member of the immunoglobulin superfamily and participates in the maturation and differentiation of young neurons in the hippocampus<sup>113,126</sup>. It modulates cell-to-cell interactions and has been shown to take part in the regulation of axonal outgrowth<sup>127,128</sup>. PSA-NCAM is expressed in all DCX positive GCs but more DCX expressing cells exist that are PSA-NCAM negative<sup>44,48</sup>. Therefore, DCX is often preferred to label young maturing neurons. When the expression of DCX and PSA-NCAM is down-regulated at approximately three weeks, most neurons start synthesizing NeuN (Neuronal Nuclei) with some exceptions including Golgi cells and cerebellar Purkinje cells<sup>129</sup>. Due to its strong and almost ubiquitous expression in neurons of the central nervous system, NeuN is a widely used neuron marker. Although the dentate gyrus of the hippocampus consists mainly of granule cells, interneurons are sparsely scattered throughout the molecular layer and a variety of neurons lie adjacent to the subgranular zone. NeuN is not sufficient enough to distinguish granule cells precisely from other neurons; hence a different marker must be employed: Prox1 (Prospero homeobox protein 1) is specific for granule cells<sup>130</sup>. It determines the fate of granule cells, if Prox1 is absent, immature neurons differentiate into pyramidal cells such as those of the CA3 region of the hippocampus<sup>131</sup>. The earliest expression of Prox1 can be found in the type 2b intermediate progenitor cell<sup>45,132</sup>. The abovementioned cell markers provide the means to identify GCs and vaguely determine their stage of maturation. In order to analyse the GCs reaction to neuronal activity, cell markers termed immediate early genes (IEG) are employed. The IEGs consist of more than 40 gene products of various functions<sup>133</sup>. Among these are transcription factors such as Early growth response protein 1 (Egr1), DNA-binding proteins, cytoskeletal and secreted proteins as well as receptor subunits. Whilst not actually being dependent on protein synthesis, these genes are rapidly and transiently activated after synaptic stimulation and therefore play a key role in genomic response<sup>134-137</sup>. It has been shown that IEG expression is responsive to diverse physiological and pathological stimuli<sup>135,138-141</sup>. Increasing evidence points out that

many IEG play an important role in hippocampus dependent information processing and memory formation.

Egr1 is a regulatory IEG, meaning that in contrast to effector IEG, it maintains regulatory tasks rather than having a more direct function at the synapse. Immunohistological staining reveals a nuclear location. Egr1 belongs to the Egr family consisting of four members. Prominent features of these are the three Zinc finger sequences in the DNA binding domain, which show a high homology among the Egr family<sup>142,143</sup>. The gene product of Egr1 is a protein of 82 or 88 kDa, depending on where its translation is initiated<sup>144</sup>. The activation of transcription hails from a plethora of stimuli. All subtypes of glutamate receptors, as well as dopaminergic, adrenergic and opiate receptors can convey the activating signal<sup>145,146</sup>. It is forwarded via several different signaling pathways like the CaMK, MEK, PI3K and essentially the MAP kinase cascade. Most pathways converge on the activation of the transcription factor ELK-1, which in turn, binds to the regulatory sequence SRE (Serum response element) or on CREB, which binds to CRE (Ca<sup>2+</sup>/cAMP responsive element), to finally initiate the transcription of Egr1<sup>147</sup>. Although early studies reported an upregulation of Egr1 30-60 min after perforant path stimulation<sup>134,148</sup>, Egr1 mRNA can be found as early as 10 minutes after LTP induction<sup>137</sup>. Following high frequency stimulation of one hemisphere, Egr1 was preferentially expressed in the dorsal part of the hippocampus in the same hemisphere<sup>134,149,150</sup>. When evaluating the role of Egr1 in synaptic plasticity, it has been shown that especially the late phase of LTP and long term memory consolidation seem to be contingent on adequate Egr1 as well as Arc (activity-regulated cytoskeleton-associated protein) expression<sup>135,137,150,151</sup>. In comparison with other IEGs such as c-Fos, c-jun and Jun-B for example, Egr1 expression correlates best with LTP maintenance, especially with regard to its persistence<sup>149,150</sup>. Several studies have demonstrated the importance Egr1 plays in learning and memory. In Egr1 knockout mice the formation of long term memory did not occur, even though short term memory was flawless<sup>152,153</sup>. Tasking homozygous Egr1 knockout mice with spatial learning in the Morris Water Maze, conditioned taste aversion and object recognition showed a general impairment in long term memory formation that was not task specific but indicated a deficit in memory consolidation. When heterozygous mice performed the same tasks, some accomplished comparable re-



sults to those of wildtype mice, but a shortcoming was apparent if the task had a pronounced spatial component. This appoints Egr1 an important role in spatial learning<sup>147</sup>. In addition, in this study, the impairment in spatial learning and recognition could be overcome by excessive training. Further studies with Egr1 knockout and heterozygous mice described a compensation of deficits in spatial learning<sup>152</sup>, recognition memory<sup>137</sup> and ABGC survival<sup>154</sup> by enhanced training. Contrary to this, Veyrac and colleagues reported no effect of excessive training on 9 day old ABGC survival<sup>153</sup>. Their investigation of the effects of Egr1 knockout, however showed a missing recruitment of ABGCs, linked to shortcomings in long term memory formation. Whilst the basic structure of the dentate gyrus, together with its synaptic functions was normal, the morphology and function of ABGCs was impaired. Glutamatergic and GABAergic properties were delayed in their maturation. The absence of Egr1 resulted in faulty dendritic development and a reduced spine density<sup>153</sup>. The complex association of functional and structural changes of ABGCs in long term memory formation, with Egr1 in a key position, opens many possibilities in which these processes can be influenced or disturbed.

## 5.8 Markers of neurogenesis

The necessity to study single neurons with precise knowledge of their age is inherent to researching adult neurogenesis. Especially *in vivo* cell labelling faces many obstacles concerning the adverse effects of the utilised label. One of the earliest approaches was to use the radioactive nucleoside 3H-thymidine which is incorporated into the DNA of dividing cells during mitosis<sup>2</sup>. Cells labelled in this manner can be visualized by autoradiography. A method based on the same principle but without the disadvantage of radiation, is to employ the synthetic Thymidine analogue 5-bromo-2'-deoxyuridine (BrdU). It was established by M. Miller and R. S. Nowakowski in 1988 to study the proliferation and migration of neurons<sup>155</sup>. Today, further Thymidine analogues like Chlorodeoxyuridin (CldU) and Iododeoxyuridin (IdU), which can be used concordantly have been developed. In order to label a maximal number of cells, a certain amount, depending on the analogue, must be injected<sup>156</sup>. A single low dose injection would label all cells born in the ensuing 24 hours but not many would remain. This is due to XdU (any Uridine derivative) degradation and rarefication of the analogue each time a cell

divides<sup>157</sup>. The Thymidine analogue can later be visualized by immunostaining. Since the Uridin derivative is incorporated in the DNA, it is passed on to the daughter cells and persists for several years<sup>4,158</sup>. It is therefore impossible to determine the exact age of cells labelled in this manner. It can only be stated, that the “birthday” of an XdU labelled cell does not precede the injection date. The methods described above, however, only label the nucleus. By transducing neurons with the green-fluorescent protein gene (GFP), the entire cell can be distinguished. Depending on which viral vector is used, even cells that are not dividing can be labelled<sup>159</sup>. Contrary to the Thymidine analogue incorporation method, cells labelled with the GFP gene increase over time. Adding a few more colours and alterations to the technique, Lichtman and colleagues even produced a mouse brain that resembled a piece of art: the Brainbow<sup>160</sup>.

## 5.9 Synaptic plasticity in mature granule cells

The ability to alter existing synaptic structures and their efficacy as a result of neuronal activity is called synaptic plasticity. This is thought to be the foundation for memory storage in the brain. Change in synaptic efficacy can be brought about in two directions: The strengthening of established and formation of new synapses is described as long-term plasticity (LTP), whereas their retrenchment, called long-term depression (LTD), weakens the synaptic connection<sup>161–163</sup>. In an experimental setting, LTP can be excited by brief high-frequency stimulation. LTD on the other hand, is evoked by low-frequency stimulation over an extended period of time<sup>164</sup>. LTP as well as LTD can be divided into an early and a late phase. During the early phase, synaptic input causes Calcium influx through N-methyl D-aspartate (NMDA) receptors, but only when the postsynaptic membrane is depolarised and glutamate has bound to the NMDA receptor. This prompts the recruitment of further Calcium channels, namely  $\alpha$ -amino-3-hydroxy-5-methyl-4-isoxazolepropionic acid (AMPA) receptors, to the postsynapse<sup>165,166</sup>. The induction of LTP can be abolished by pharmaceutically blocking the NMDA receptor<sup>134,167</sup>. The later phase requires additional structural changes in spine morphology and synapse organisation<sup>168–171</sup>. This process encompasses *de novo* protein synthesis. Among the earliest synthesised proteins are immediate early genes such as Egr1. In Egr1 knock out animals, long-term memory was severely impaired whilst short-term

memory remained unaffected<sup>172</sup>. LTP and LTD as synaptic forms of plasticity can be further discriminated into homo- and heterosynaptic plasticity. Homosynaptic plasticity is input specific in that the efficacy of a synapse is changed by the activation of its pre-synaptic partner<sup>165</sup>. Heterosynaptic plasticity, on the other hand describes the change of efficacy in synapses from neurons receiving no input in the vicinity of activated neurons. The dentate gyrus has proven to be a good model for studying homo- and heterosynaptic plasticity<sup>17,173</sup>. HFS induced LTP in the stimulated medial perforant path whilst LTD was elicited in the non-stimulated lateral perforant path<sup>173,174</sup>. Furthermore, neuronal activity not only has modulating effects on neurons in geographical vicinity but also over the course of time. It has been hypothesized by Bienenstock, Cooper and Munro<sup>175</sup> that preceding activation of the same neurons can shift the threshold of LTP and LTD for successive stimulation. This phenomenon is termed metaplasticity<sup>176,177</sup>.

## 5.10 Structural maturation of adult born granule cells

The structural maturation of adult born granule cells (ABGCs) describes the outgrowth of the axon and the formation of the dendritic tree with its spines<sup>178,179</sup>. The development of the granule cells axons, called mossy fibers, begins ~ 3 days prior to that of the dendrites<sup>32</sup>. In the first 10 days of cell age, the axon gains much of its final length although no boutons are yet formed<sup>180</sup>. Its path can be traced to the hilus from which it turns to the more lateral and temporal CA3 region of the hippocampus. At 10-17 days of age, the mossy fibres terminate at CA3 pyramidal neuron and begin to form boutons<sup>181</sup>. The axonal outgrowth continues until the third week when the bouton density reaches its maximum<sup>32</sup>. Apart from the large boutons that provide contact to the CA3 pyramidal neurons, two other types of mossy fibre terminals can be found: small filopodial extensions and *en passant* varicosities that project to inhibitory interneurons<sup>182,183</sup>. The dendritic development is closely linked to that of the axon<sup>184</sup>. Distinct stages, correlating with cell age, have been classified to describe the outgrowth of dendritic tree till it reaches its characteristic cone shaped form<sup>48</sup>. A tiny protrusion appears within the first 12 hours which reaches the molecular layer in the second day after injection. At 4 dpi the apical dendrites are extended to the MML<sup>185</sup>. Although dendritic growth lags behind in GCs born in the adult brain, the process is similar to that in

the embryonic phase<sup>184</sup>. The dendrites accretion shows similarities to the outgrowth of the mossy fibres. The first three weeks are devoted to rapid increase of length and complexity, after which only minimal growth can be witnessed<sup>32</sup>. Dendritic spine formation only starts at about 16 days, the dendritic ramifications having mostly reached the OML<sup>184</sup>. At the same time, mossy fibres reach the CA3 area. Since GCs receive the majority of their excitatory input via dendritic spines, their morphology and number largely reflect the connectivity of these GCs<sup>184,186</sup>. Four categories have been established to distinguish granule cell dendritic spines: large mushroom-shaped spines with a big spine head and a stout neck, thin spines with a small head and long neck, filopodial spines consisting of an elongated protrusion without head and stubby spines without any neck<sup>187,188</sup>. During early development, stubby spines and filopodia predominate but with ongoing maturation, however, they give way to mushroom spines, which are the most common in mature GCs<sup>189,190</sup>. This transition is concomitant with several changes in connectivity and synapse efficacy: Although small spines are similarly reactive to stimulation as large spines, they are more likely to show long lasting spine enlargement<sup>169</sup>. Thin protrusions (< 0.4 µm) are more dynamic and therefore more probable to form synapses with boutons already connected to other spines whereas thick spines rather form synapses with single synapse boutons<sup>191</sup>. The spine size and density incrementally grow until 70 dpi when a steady state is attained<sup>191</sup>. It has been shown that with augmenting spine head size the density of glutamate receptors increases as well as the size of the post-synaptic density together with the amount of docked vesicles at the presynapse<sup>192,193</sup>.

## **5.11 Synaptic integration and plasticity of newborn granule cells**

The morphological maturation of adult born GCs in the adult hippocampus is accompanied by the synaptic integration into the existing circuitry. This process occurs in a very similar way to that in hippocampal development<sup>194</sup>. Two neuronal messengers play an important role in orchestrating the synaptic integration: the inhibitory transmitter GABA ( $\gamma$ -aminobutyric acid) and the excitatory transmitter Glutamate. Although ABGCs do not react to stimulation in the first week, they still however already express GABA and Glutamate receptors<sup>194</sup>. The newborn GCs are subject to tonic activation by

ambient GABA from local interneurons<sup>195</sup>. Starting at 8 dpi they receive GABAergic afferents which are located at the dendrites and therefore elicit a slow response. After 2-3 weeks the first postsynaptic currents are generated by glutamatergic input from newly formed spines. A high intrinsic excitability compensates the initially rather weak glutamatergic input strength<sup>196</sup>. At 28 dpi perisomatic GABA terminals have formed and induce a fast response<sup>107,184,194,197-199</sup>. Initially, GABA input leads to depolarization of the GC. This is due to the expression of the Cl<sup>-</sup> importer NKCC1. Only when it slowly yields to the expression of KCC2, a Cl<sup>-</sup> exporter, does GABA induce hyperpolarization<sup>200</sup>. The switch from Cl<sup>-</sup> import to export leads to a significant change in its gradient and therefore in a different GABA response polarity. The GABA<sub>A</sub> receptor itself is permeable to Cl<sup>-</sup>, but does not influence the direction of ion passage. The effect of GABA on immature GCs evolves over time. In contrast to mature GCs, GABAergic inhibition does not impair the activation of young GCs<sup>83</sup>. Consequently, blocking GABA<sub>A</sub> receptors in mature GCs resulted in a lower activation threshold but left the required input strength in immature GCs unchanged. This alteration in susceptibility to GABAergic inhibition occurs at about 7 weeks of age<sup>47,195</sup>. A concomitant increase in membrane capacitance and decrease in input resistance can be explained by changing channel density and membrane proportions<sup>194,201</sup>. It has been demonstrated that K<sup>+</sup>-inward rectifier channel (Kir) conductance reduces membrane resistance and therefore diminishes the excitability of a GC as a result. Kir conductance is far higher in mature GCs leading to a higher excitation threshold. The deduction that Kir blockade with Ba<sup>2+</sup> in mature GCs increased their excitability to the same level as young GCs and that Kir overexpression in immature neurons induced a state of low excitability equal to that of mature GCs corroborates the conclusion that Kir decidedly regulates spiking behavior of GCs<sup>196</sup>. The transition from excitatory to inhibitory GABA activation is accompanied by a phase of competitive survival of ABGCs at 2-3 weeks of age<sup>195</sup>. The activation of NMDA receptors is indispensable for cell survival<sup>112</sup>. The NMDA receptor consists of two subunits with multiple variants expressed at different stages of hippocampal development<sup>202</sup>. The process of adult neurogenesis is similar to prenatal development in the preferential expression of the NMDA subunits NR1 and NR2B during the early phase of neurogenesis<sup>203</sup>. It has been shown that the induction of LTP by MPP stimulation (see 5.9 Synaptic plasticity in mature granule cells) is dependent on the presence of the

NR2B subunit and that this plays an instructive role in enhanced synaptic plasticity of immature GCs<sup>47,204</sup>. In contrast to NR1, a deletion of NR2B does not result in cell death but in impaired LTP similar to neurogenesis ablation models as well as diminished dendritic complexity and deficits in certain forms of hippocampal learning tasks<sup>63,112</sup>. The differential expression of NMDA subunits and their individual effect on various forms of synaptic plasticity, synaptic integration and ABGC survival plays an important role in context discrimination and novelty encoding<sup>63,205,206</sup>. Several studies established that ABGCs play an important role in pattern separation: Enhanced neurogenesis led to improved pattern separation; a smaller number of ABGCs resulted in inferior pattern separation<sup>87,88</sup>. Elaborate experiments with transgenic mice allowed the differentiation between certain mechanisms of information processing of young ABGCs and old GCs. It was shown that old GCs are not important for maintaining pattern separation (see 5.4 The function of the hippocampus), a task which requires ABGCs of 3-4 weeks of age. Rapid pattern completion was found to be facilitated by old GCs<sup>84</sup>. Pattern separation was impaired in mice with excitotoxic perirhinal and lateral entorhinal cortex (PRH/LEC) lesions. This is in accordance to the finding that the PRH/LEC is an important source of input to ABGCs as well as septal cholinergic cells and various intra hippocampal neurons: interneurons, mossy cells, area CA3 and even mature GCs. The input from mature GCs persists only during the first month after injection while afferents from local interneurons increased from 21 dpi on<sup>207</sup>. Interestingly, a subsequent study demonstrated that enriched environment during a critical time window of 2-6 weeks of GC age raised the number of afferents from local interneurons and cortical neurons. Although the presynaptic local interneurons decreased to baseline after returning the mice to standard housing conditions, new input from CA3 and CA1 inhibitory neurons was established that was scarcely found in control animals<sup>100</sup>. These results corroborate that structural plasticity is experience dependent and takes place during a particular period in ABGCs. It has been shown by several authors that young GCs of a certain age express enhanced sensitivity to stimulation. Although the process of maturation and integration of ABGCs differs slightly in rats and mice<sup>123</sup>, several studies demonstrated that GCs of both species aged 4-6 weeks exhibit a lower LTP induction threshold, a higher LTP amplitude than mature GCs and are more likely to be integrated into

the established circuitry<sup>47,184,201,204</sup>. This period of superior synaptic integration and plasticity has been termed “the critical phase”.

From this, the following questions for this thesis project can be formulated:

## 5.12 Questions

Though the change in excitability of ABGCs during the course of their maturation has been studied in some detail, a number of questions remain. In order to harmonize previous findings and to investigate missing evidence, the following specific questions were asked in this thesis work.

1. What are the characteristics of excitability of ABGCs over the time of the critical period (4-6 weeks of cell age) and beyond, viewed at different time points?
2. Can stimulation of the perforant path change the excitability of a maturing GC?
3. Can stimulation of the medial perforant path induce a layer specific homo- and heterosynaptic plasticity at dendritic spines?
4. Can stimulation retrieve the enhanced excitability shown by young ABGCs in older ABGCs and preserve it for a longer duration than that of the stimulation itself?
5. Can the IEG Egr1 be correlated to homo- and heterosynaptic plasticity and if so, how strong is this correlation?
6. Is the IEG Egr1 an appropriate indicator of subtle differences in synaptic activity and structural plasticity?
7. Do ABGCs of the suprapyramidal blade of the DG show different sensibility to stimulation than those of the infrapyramidal blade?

In order to solve these questions, the following anatomical and histological methods were used:

- Detection of ABGCs and mature GCs by application of histochemical stainings of Egr1 and NeuN, labelling of ABGCs by IdU and CldU administration.
- Detection of ABGC and portrayal of the dendritic tree including spines with retroviral GFP transfection.
- Immunohistochemical expression analysis of synaptic activity and plasticity marker Egr1 following stimulation.
- Grid-based, cell-specific analysis of spine size dynamics in the IML, MML and OML.



## 6 Material and methods

For this work, brain tissue was processed for histological examination with immunocytochemical stainings. The analysed brains in this study came from two different sources:

1. XdU project: Prof. Wickliffe Abraham, Department of Psychology, University of Otago, Dunedin, New Zealand
2. Spine project: Dr. Tassilo Jungenitz, Institut für klinische Neuroanatomie, Centre of Neuroscience, Frankfurt, Germany

The *in vivo* methodology used by these two laboratories to label and stimulate the hippocampal dentate gyrus is described in chapter 7 Additional material and methods. All methods performed by these laboratories can be found there. In the following, the methods for this work performed by myself are described.

### 6.1 Animals and tissue preparation

For the XdU project, brains from thirteen adult male Sprague-Dawley rats which underwent various experimental procedures including injection of mitotic markers and *in vivo* stimulation (see 7 Additional material and methods) were fixated by perfusion with 4 % paraformaldehyde in the laboratory of Prof. Wickliffe Abraham, University of Otago in New Zealand. The fixated brains were sent to Germany submerged in phosphate buffered saline (PBS). After washing them in Tris-buffered saline (TBS) for one night they were marked on the right side. The brains were sliced in to series of 40  $\mu\text{m}$  coronal sections with a vibratome (Leica VT 1000S). Only sections containing the hippocampus in the area from -2.40 to -4.44 mm posterior to Bregma<sup>208</sup> were used. All sections were stored in cryoprotection (30 % ethylene glycol [Sigma Aldrich], 25 % glycerine [AppliChem] in phosphate buffered saline [PBS]) at -20 °C. Histological procession and analysis was performed while blinded to the experimental group.

For the spine project, selected 50 µm brain sections were provided by Dr. Tassilo Jungenitz. To this end, 11 adult male Sprague-Dawley rats which underwent various experimental procedures including injection of RV-GFP and *in vivo* stimulation (see 7 Additional material and methods) were fixated by perfusion with 4% paraformaldehyde in the Institut für klinische Neuroanatomie by Dr. Tassilo Jungenitz. The fixated brains were marked on the right side. The brains were sliced in series of 50 µm coronal sections with a Vibratome (Leica VT 1000S). Only sections containing the hippocampus in the area from -2.40 to -4.45 mm posterior to Bregma<sup>208</sup> were used. All sections were stored in cryoprotection (30 % ethylene glycol [Sigma Aldrich], 25 % glycerine [AppliChem] in phosphate buffered saline [PBS]) at -20 °C. Histological procession and analysis was performed while blinded to the experimental group.

## 6.2 XdU project immunohistochemistry

The immunohistological analysis of the rat brains provided by Prof. Wickliffe Abraha was performed with three different groups of antibodies that were co-applied on series of 40µm coronal brain sections. Firstly: The identification of different populations of adult born granule cells was performed with antibodies against CldU (rat-anti-CldU from Accurate, OBT 0030) and IdU (mouse-anti-IdU from BD Biosciences, 347580). Secondly: The detection of the *immediate early gene* (IEG) Egr1 was performed with the antibody (rb-anti-Egr1 from Cell Signalling). Thirdly: In order to insure that the stained structures were actually neurons NeuN was detected with the antibody (guinea pig-anti-NeuN from Synaptic Systems). The final protocol for the immunohistological staining of the IEG, XdU and granule cells was developed after several staining tests and combination samples.

The stainings in free floating sections were performed according to a basic schema. Depending on the staining some steps were repeated or added.

- Four times washing with 0.1 M TRIS buffered saline (TBS) (pH 7.5; 0.1 TRIS [AppliChem] in distilled water) for 10 minutes at room temperature.

- Blocking of non-specific staining (0.25 % Triton-X [Merck]; 5 % bovine serum albumin (BSA) [Roth] in 0.1 M TBS) for 60 minutes at room temperature.
- Incubation with the primary antibody (solved in 0.1M TBS) for 48 hours at 4 °C
- Four times washing with 0.1 M TBS for 10 minutes at room temperature.
- Incubation with the secondary antibody (solved in 0.1 M TBS) for 24 hours at 4 °C
- Four times washing with 0.1 M TBS for 15 minutes at room temperature.
- Mounting the stained sections on glass slides and covering them with *Dako Fluorescence Mounting Medium* under a thin cover slip.

For the XdU stainings a pre-treatment was needed:

- Four times washing with 0.1 M TBS for 15 minutes at room temperature.
- Incubation with 2 N hydrochloric acid (HCL) [VWR Chemicals] for 30 minutes at 30 °C.
- Incubation with 0.1M boric acid (pH 8.5) [AppliChem] for 10 minutes at room temperature.
- Four times washing with 0.1 M TBS for 15 minutes at room temperature.

Initially, the pre-treatment was tested at two time points in the schema. Once it was applied directly at the beginning of the protocol followed by a synchronous incubation with the primary antibodies against XdU and the IEG. For the other test the pre-treatment was applied after the incubation with the primary and secondary antibodies against the IEG. In the following, the incubation with the primary and secondary antibodies against the XdUs was performed. All relevant staining were performed using the latter schema including the pre-treatment after the IEG staining.

*Table 1 XdU project: Primary antibodies*

<b>Antibody</b>	<b>Host</b>	<b>Manufacturer</b>	<b>Kind</b>	<b>Workingconc.</b>	<b>Cataloguenr.</b>
CldU	rat	Accurate	monoclonal	1:250	OBT 0030
IdU	mouse	BD Bioscience	monoclonal	1:250	347580
NeuN	guinea pig	Synaptic Systems	polyclonal	1:500	266 004
Egr1 (15F7)	rabbit	Cell Signalling	monoclonal	1:1000	4153

*Table 2 XdU project: Secondary antibodies*

<b>Conjugation</b>	<b>Host</b>	<b>Antigen</b>	<b>Manufacturer</b>	<b>Workingconc.</b>	<b>Cataloguenr.</b>
Alexa Fluor® 488	goat	mouse	Vector Labs	1:1000	A-11001
Alexa Fluor® 488	goat	rat	Vector Labs	1:1000	A-11006
Alexa Fluor® 568	goat	rabbit	Vector Labs	1:1000	A-11011
Alexa Fluor® 568	goat	guinea pig	Vector Labs	1:1000	A-11075
Alexa Fluor® 568	goat	rat	Vector Labs	1:1000	A-11077
Alexa Fluor® 568	goat	mouse	Vector Labs	1:1000	A-11004
Alexa Fluor® 633	goat	guinea pig	Vector Labs	1:1000	A-21105
Alexa Fluor® 633	goat	rabbit	Vector Labs	1:1000	A-21070

*The staining with XdU, Egr1 and NeuN was done in two sessions with the same primary antibodies (see Table 1 XdU project: Primary antibodies), but different combinations of secondary antibodies (see*

Table 2 XdU project: Secondary antibodies) in order to rule out changes in marker intensities due to different detection protocols. In the first session three brain slices per

animal, each six slices apart, were stained. The selection of the secondary antibodies was as follows:

- IdU and CldU => Alexa Fluor® 488
- NeuN => Alexa Fluor® 568
- Egr1 => Alexa Fluor® 633

In the second session, three other slices per animal were stained but this time the colour spectrum of the secondary antibodies for NeuN and Egr1 was exchanged:

- IdU and CldU => Alexa Fluor® 488
- NeuN => Alexa Fluor® 633
- Egr1 => Alexa Fluor® 568

### 6.3 Spine project immunohistochemistry

The immunohistochemical stainings for GFP 44 and Egr1 in the 50 µm coronal rat brain slices provided by Dr. Tassilo Jungenitz were performed using the same schema as elaborated in chapter 6.2 only with different antibodies. The primary and secondary antibodies used for spine analysis are listed below.

*Table 3 Spine project: Primary antibodies*

Antibody	Host	Manufacturer	Kind	Workingconc.	Cataloguenr.
GFP488	mouse	Sigma-Aldrich	monoclonal	1:500	SAB 4600051
Egr1 (15F7)	rabbit	Cell Signalling	monoclonal	1:1000	4153

*Table 4 Spine project: Secondary antibodies*

Conjugation	Host	Antigen	Manufacturer	Workingconc.	Cataloguenr.
-------------	------	---------	--------------	--------------	--------------

Alexa Fluor® 488	goat	mouse	Vector Labs	1:1000	A-11001
Alexa Fluor® 568	goat	rabbit	Vector Labs	1:1000	A-11011

## 6.4 Microscopic imaging and analysis

For the XdU project, stained 40  $\mu\text{m}$  coronal brain sections were analysed with a confocal microscope (Nikon Eclipse 80i) under an objective with a 40-fold magnification (oil immersion, numeric aperture 1.3). The dentate gyrus was screened for XdU positive cells in both the suprapyramidal and the infrapyramidal blade. Every XdU positive and NeuN positive cell within the GCL was captured including the tissue surrounding this marked cell. Using the Software EZ-C1 3.60, picture sequences in the z axis, called z-stacks, were made with 1  $\mu\text{m}$  intervals between each image. Z-stacks contained between 20 and 40 images equivalent to 20 - 40  $\mu\text{m}$  in the z-axis. The image resolution was 1024 x 1024 Pixel. This allowed a detailed inspection of the XdU positive cells and their location in the granule cell layer. The XdU and NeuN positive cells of the GCL were called “labelled GCs” and the XdU negative NeuN positive cells of the GCL were called “unlabelled GCs”.

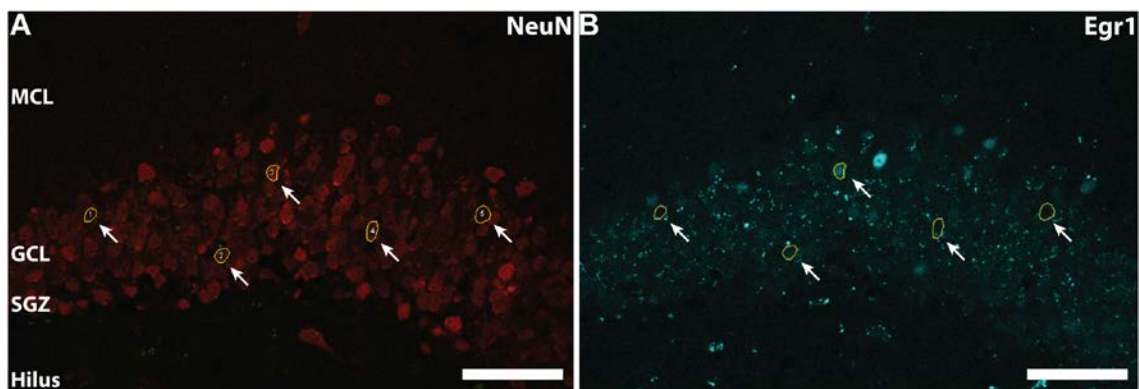


*Figure 2: Randomized selection of mature GCs. Five XdU negative NeuN positive GCs were chosen randomly while only the NeuN colour channel was invisible. The subgranular zone and the top most cell layer of the granule cell layer were excluded. The circumference was marked at the largest diameter, allowing measuring the Egr1 intensity only in the area of the nucleus. The unlabelled GCs served as control. MCL: molecular layer, GCL: granule cell layer, SGZ: subgranular layer. Scale bar: 50 $\mu\text{m}$ .*

The z-stacks were then screened for labelled GCs using the program *ImageJ* (<http://fiji.sc/>). At the level of their largest soma diameter, the circumference of the cell-soma was marked and the Egr1 intensity in the marked area was analysed. For each z-stack five XdU negative GCs from the same z-stack at the level of the labelled GCs were marked randomly and analysed in a similar way. While marking the circumference, the colour channel of the Egr1 signal was deactivated with the *Channels Tool*. By doing so, the selection of the unlabelled GC was blind towards their Egr1 intensity. For the co-localisation analysis the plugin *Cell Analyser* was used. The XdU negative GCs were used as control. This method was first established by Dr. T. Jungenitz<sup>48</sup> (Figure 2).

The Egr1 intensities were converted into so called z-scores as a means of further normalisation. The following formula was used:

$$z\text{-score} = (x - \mu) / \sigma$$

x is the measured Egr1 intensity value,  $\mu$  is the mean of all Egr1 values from the unstimulated side of the rat and  $\sigma$  is the standard deviation of all Egr1 values for each animal separately<sup>209</sup>. In order to compare the data of this thesis work with that of the collaborative laboratory in New Zealand, the conversion into this z-score proved sufficient. There, the Egr1 expression was categorized in Egr1 positive or negative; a graded intensity measurement did not take place. Therefore, GCs with a Z-score of > 2.0 were defined as being Egr1 positive.

In order to relativize the Egr1 intensity regarding different slices and animals, the Egr1 signal of each XdU positive GC was compared to the average Egr1 intensity of all unlabelled GCs of their z-stack.

The statistical analysis was performed with *GraphPad Prism Version 6*® for *Microsoft Windows*®. The significance tests are outlined in the description of each figure. The significance was fixed on  $P < 0.05$ . Group values are demonstrated as means  $\pm$  SEM.

## 6.5 Spine analysis

For the spine project, stained 50µm coronal brain sections were analysed with a confocal microscope (Nikon Eclipse 80i) under an objective with a 40-fold magnification (oil immersion, numeric aperture 1.3). The dentate gyrus was screened for RV-GFP positive ABGCs in both the suprapyramidal and the infrapyramidal blade. The identification of each ABGC was possible due to careful numbering and description of the location. It was made sure that only dendrites with visible connection to the GC soma within the 50 µm section were imaged. Images were made with a confocal microscope with a 60 x oil immersion objective (N.A. 1.3; Nikon). The dendritic segment was zoomed in with a 5 x field zoom. Z-stacks (see 6.4) were made with a step size of 0.5 µm. Z-stacks were made in the IML (inner molecular layer), MML (middle molecular layer) and OML (outer molecular layer). The location of the imaging window for the IML was adjoining the GCL. For images of the OML, the z-stack bordered the hippocampal fissure with a distance of 5 - 10 µm. The imaging window for the MML was at the centre between IML and OML. 2 - 5 dendritic segments were imaged in each layer.

The ensuing image analysis was performed with the program *ImageJ* (<http://fiji.sc>). The length of each segment was measured in a two-dimensional z-projection by manually tracing its trajectory along the centre of the dendrite. The mean length was roughly 42 µm. Firstly, the spines were categorized. For this the stack was examined using a grid of 0.2 µm<sup>2</sup>. Large spines were defined as being larger than one grid element; small spines were equal or smaller than one grid element. They were referred to as “mushroom spines”. Spines whose head was not larger than their spine-neck were identified as stubby and filopodial spines. They were sorted out as “non-mushroom spines”. Normalization was applied using the following formula:

$$x = \# / \mu\text{m}$$

X being the spine number (#) per segment length (µm). Secondly, the spine diameter was captured by manually circling the largest cross-sectional area. A graphic tablet (Wacom, Kozo, Saitama, Japan) was utilized for this.



## 7 Additional material and methods

### 7.1 XdU project

The cell marker injections, surgery, tetanus application and perfusion of all rats were performed by the team of Professor Wickliffe Abraham of the University of Otago in Dunedin, New Zealand.

#### 7.1.1 Injection of the cell markers

Thirteen male Sprague-Dawley rats were used for this study. They were sourced from the University of Otago Animal Breeding Station. Eleven of these rats received two injections of different markers at varying time points prior to their death at 10 months of age. These markers were two Thymidin analogues: Ioddeoxyuridin (IdU) and Chlordeoxyuridin (CldU). The term XdU will be used to describe either Thymidine analogue. The Thymidin analogues were integrated into the DNA of all cells which were in the state of mitosis at the injection time. Therefore, the adult newborn granule cells of the hippocampus were marked as well. Collectively, three populations of granule cells were to be compared that were born at three different time points. These three populations consisted of six, twelve and 35 week old adult born granule cells. At the age of two months a rat received an intraperitoneal injection of one of the XdUs equivalent to 200 mg/kg Bromodeoxyuridine (BrdU) at 20 mg/ml. At the age of six or eight and a half months, the other XdU was injected. These times the application was spread over five days with two intraperitoneal injections per day at the equivalent of 50 mg/kg BrdU at 50 mg/ml. Therefore, every rat contained two populations of adult born granule cells of different age. The animals received injections either at 35 and six weeks or at twelve and six weeks prior to death (ptd). Since all animals were injected at six weeks and the other injection was either at twelve or 35 weeks ptd,  $n = 8$  for the six week old ABGC population and  $n = 4$  for the other time points. In order to minimize any influence on the number of labelled cells due to the little difference of the Thymidine analogues, the assignment of either XdU to each time point was different in every rat. For the simulation procedure and novel environment exposition see below.

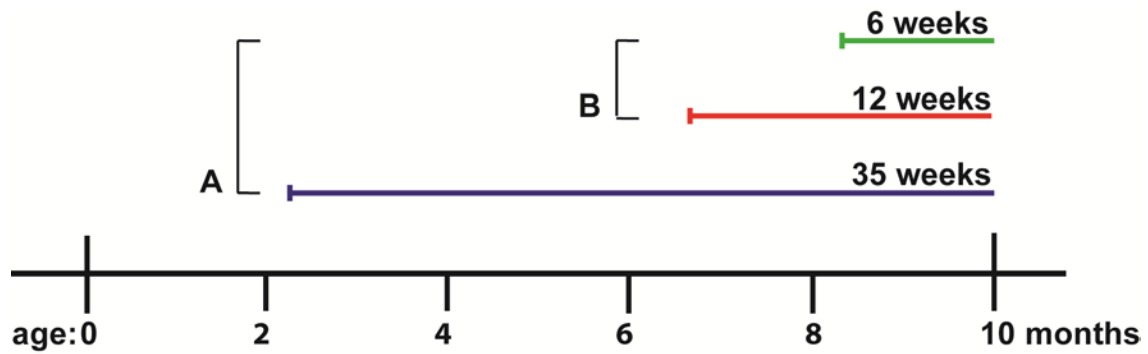


Figure 3: Timeline. The protocol of XdU labelling is shown. Each rat was injected with CldU and IdU at two time points, either at 2 months and 8 ½ months of age (A) or at 7 months and 8 ½ months of age (B). Thus, three populations of ABGCs were labelled: 6 week, 12 week and 35 week old ABGCs. The rats were killed when they were 10 months old. Animal numbers: (6+35 weeks)  $n = 6$ , (6+12 weeks)  $n = 5$ .

The two remaining rats were to be practice animals. Only one XdU was applied at the age of twelve weeks. The rat Ng 71 received two intraperitoneal injections of 42.5 mg/kg CldU per day for two days equivalent to 50 mg/kg BrdU. The rat Ng 70 received two intraperitoneal injections of 57.75 mg/kg IdU per day for two days equivalent to 50 mg/kg BrdU. These rats were exposed to the same kind of novel environment like the other rats. They were transcardially perfused four weeks after the injections at the age of 16 weeks. However, they were not given any intracerebral stimulation. Thus, the practice animals contained only one population of adult born granule cells which was four weeks old at the time of death.

### 7.1.2 Electrophysiology and surgery

The anaesthesia was carried out with ketamine (75 mg/kg, 100 mg/ml) and Domitor (0.5 mg/kg, 1 mg/ml). At the time of surgery the weight of the rats was about 500 g. Normally, the surgery time was about 1 h. Separate sterile needles were used for each rat. Once a surgical plane of anaesthesia and sedation was obtained, the surgery was executed under aseptic conditions. The rat's head was immobilized with a standard stereotaxic instrument and disinfected with alcohol. The area for the incision was furthermore anaesthetized with subcutaneous injections of lignocaine. After waiting for the effect of

the local anaesthetic, the skin and periosteum was cut to expose the skull. At the location for the electrodes small holes with a diameter of 1.2 mm were drilled. Both electrodes were made of stainless steel wire (125  $\mu$ m diameter) and insulated except for the cut tip. The stimulation electrode was placed in the medial perforant path fibres where they meet the angular bundle. The stimulus-evoked field potentials were recorded by the electrode in the hilus of the dentate gyrus. The bilateral location of the electrodes was based on stereotaxic coordinates and physiological responses. Once the electrodes were in a satisfactory position the electrode leads were inserted into a plastic head plug. The device was then fastened to the skull with 5 sterile stainless steel anchor screws which were inserted into the bone but did not perforate it. The head plug was additionally adhered to the skull with dental acrylic. The skin was then sutured in a strainless manner as far as the head plug allowed. Finally the animal was released from the stereotaxic instrument. The rat received a subcutaneous injection of 10-15 ml of warmed 0.9 % saline and afterwards an antisedan to antagonize the Domitor. One day after surgery, Carprofen and amphoprim were re-administered. For the two following weeks the rats were allowed to recover. Three control animals also received a head plug with implanted electrodes but no high frequency stimulation.

### **7.1.3 The induction of long term potentiation (LTP)**

The fixed head plug with the implanted electrodes permitted to record field potentials and stimulate the perforant path in freely moving animals. A minimum of four days of baseline recording was begun. The recording lasted 30 minutes each day. The perforant path was stimulated with single-pulse (1/20 s) stimulations and the baseline evoked responses were recorded and measured in the dentate gyrus. In order to induce long term potentiation (LTP) a protocol of brief high frequency stimulation (HFS: delta-burst stimulation, 50 trains, each 10 pulses at 400 Hz) was applied to one hemisphere via the stimulation electrode to the perforant path<sup>210</sup>. The HFS was given on two consecutive days. The opposite hemisphere served as unstimulated control since only test pulses were applied. After the stimulation the responses were monitored for further 30 minutes to assert the LTP induction. Then the rats were left undisturbed for 48 h after which they received the exposition to novel environment.

#### **7.1.4 Novel environment and perfusion**

The rats that received HFS, as well as the control rats were exposed to a standardized novel environment before the perfusion. This treatment was administered to increase the expression of the immediate early gene (IEG) Egr1. Since all animals had been handled regularly before the necessary handling that came with the novel environment did not pose a new stress factor. The novel environment consisted of an open box of 60 x 60 x 20 cm which was divided into nine equal squares of 20 x 20 cm that were arranged in a 3 x 3 grid. Every rat stayed five minutes in the novel environment during which it was placed in a new square every 15 seconds to provide enough exploration opportunities. One hour after the novel environment exposure the rats were anesthetized with isoflurane. In the following 0.01 M phosphate buffered saline (100 ml) was used for the transcardial perfusion, then the fixation was achieved by perfusing with 4 % paraformaldehyde in 0.01 M phosphate buffer (PB: 100 ml). At this time the rats were ten months old.

### **7.2 Spine Project:**

The virus production and intra-hippocampal injection as well as the perforant path stimulation and following fixation of the rat brain tissue was performed by Dr. Tassilo Jungenitz of the Institute of Clinical Neuroanatomy in Frankfurt, Germany.

#### **7.2.1 Animals**

Eleven adult male Sprague-Dawley rats (8 - 13 weeks, 220 - 459 g; Charles River, Sulzfeld, Germany) were used. The animals were housed in large cages (30 x 40 cm) according to standard laboratory conditions. The German guidelines for the use of laboratory animals were applied to all animal experiments.

## 7.2.2 Virus production and *in vivo* injection

The retrovirus was produced by transfecting HEK293T cells with pCAG-GFP, pCMV-GP and pCMV-VSV (3:2:1) plasmids using Calcium-Phosphate precipitation. After 48h of incubation, the supernatant containing the retrovirus was separated and centrifuged at 3200 x g for 10 min and filtrated through a 0.22 µm filter. This insured a separation from cell detritus. The retrovirus was concentrated using ultra-centrifugation at 160000 x g for 2 h (Sorvall WX Ultracentrifuge and SureSpin 630 swinging bucket rotor, Thermo Fisher Scientific, Waltham, MA, USA). The pellet containing the retrovirus was then suspended in 200 µl phosphate buffered saline (PBS, Sigma-Aldrich, St. Louis, MO, USA). Storage at -80 °C was provided in aliquots containing the retroviral suspension with a titer of 10<sup>5</sup> colony forming units.

The anaesthesia for surgery consisted of Fentanyl (Janssen Pharmaceutica, Beerese, Belgium), Midazolam (Dormicum; Roche, Basel, Switzerland) and Medetomidin (Domitor; Pfizer, New York City, NY, USA) in conformance with the German law on the use of laboratory animals (5 µg Fentanyl, 2 mg Midazolam, 150 µg Medetomidin per kg body weight i.m. initially plus further injections as needed). The animals head was stabilized in a Kopf stereotaxic instrument (Kopf instruments, Tujunga, CA, USA). At -3.8 mm from Bregma and 2.2 mm laterally from the median, two holes (1.5 - 2.0 mm diameter) were drilled in the skull on both hemispheres. Through these holes 0.75 µl of the retroviral solution was slowly injected to a depth of 3.2 and 3.7 mm below brain surface. The injections into the dentate gyrus of the hippocampus were performed bilaterally using a NanoFil syringe (World Precision Instruments, Inc., Sarasota, FL, USA).

## 7.2.3 *In vivo* perforant path stimulation

The perforant path stimulation was performed under deep urethane anaesthesia (1.25 g/kg body weight s.c. initially plus further injections as needed; 250 mg urethane/ml 0.9 % saline, Sigma-Aldrich) conformant with the German law on the use of laboratory animals. During surgery and stimulation the animal was immobilised in a Kopf stereotaxic instrument (Kopf instruments, see above). Body temperature was de-

tected rectally and maintained at  $37.0 \pm 0.5$  °C. A bipolar stainless steel stimulation electrode (NE-200; Rhodes Medical, Woodland Hills, CA, USA) was inserted in the angular bundle of the perforant path (coordinates measured from Lambda: L: 4.5 mm, AP: +0.5 mm at 3.5 mm depth in brain tissue) through two holes (1.5 – 2.0 mm diameter) drilled through the skull. The recording microelectrode (glass, 1.5 mm outer diameter) was made with a Zeitz (Munich, Germany) electrode puller. It was placed in the dorsal blade of the granule cell layer (coordinates from Bregma: L: 2.0 mm, AP: - 3.5 mm at 3.5 mm depth in brain tissue) while filled with 0.9 % saline. The correct depth of the recording electrode was optimized by viewing the typical shape of evoked potentials using low voltage control stimulation of the perforant path.

In the following, HFS was applied for 2 h with one HFS train consisting of 8 pulses (500  $\mu$ A, 0.1 ms pulse duration) of 400 Hz once per 10 s. 10 retrovirally GFP (green fluorescent protein) labelled rats received HFS at 28 dpi (n = 6) and at 35 (n = 4). Subsequently, the animals were deeply anaesthetized with urethane and transcardially perfused using a fixative with 4 % PFA in 0.1 M PBS, pH 7.4. After brain removal they were postfixed for 12 – 18 h. This method has been established previously<sup>48,211</sup>.

## 7.2.4 Tissue preparation

Initially, the fixated brains were cut into serial frontal slices (300  $\mu$ m) using a Vibratome (Leica VT 1000S), rinsed in 0.1 M TRIS buffered saline (TBS, AppliChem, Darmstadt, Germany) and stored in cryoprotectant solution (30 % ethylene glycol, 25 % glycerin in PBS) at -20°C. These thick slices were used for dendritic tree analysis which is not part of this dissertation. In order to execute spine analysis, the slices were cut to 50  $\mu$ m with a Vibratome. Washing and storing of the thin slices was performed with the same methods as described above. The immunohistological stainings and spine analysis was only performed on the thin slices.

## 8 Results

### 8.1 XdU project

#### 8.1.1 Analysis of Egr1 immunoreactivity in adult-born granule cells

All experiments were performed on rat brains fixated by perfusion with 4% paraformaldehyde from the laboratory of Prof Wickliffe Abraham, University of Otago, New Zealand. The brains were sent to Germany submerged in phosphate buffered saline (PBS). A total of thirteen brains were used. The experimental procedures can be found in chapter 6 and 7. The brains were sectioned into series of 40  $\mu\text{m}$  slices. The immunoreactivity of XdU, Egr1 and NeuN was analysed.

Six brain sections were stained and analysed per rat. In order to verify that no outer influences regarding staining, storing and imaging was apparent between the sections of each animal, they were analysed independently. In each brain section, the Egr1 intensity of cell somata in the GCL was measured either in XdU labelled GCs or in unlabelled GCs. Unlabelled GCs were used as control.

This analysis was performed for GCs of distinct categories: the unlabelled GCs and the three populations of ABGCs aged 6 weeks, 12 weeks and 35 weeks. The average Egr1 intensities of every section were compared by side (Figure 1 - Figure 4). It has to be taken into consideration that the number of counted GCs per section side varied greatly; occasionally no labelled GCs could be found in a section. This explains why six dots per side for each animal were not always ostensible in the Figures 1 - 4. The numbers of counted GCs per rat is listed in

*Table 6.* The six stained sections per animal were stained in two sessions with two different sets of secondary antibodies. No detected difference in immune intensities between these two groups was indicated, thus the secondary antibodies had no apparent effects.

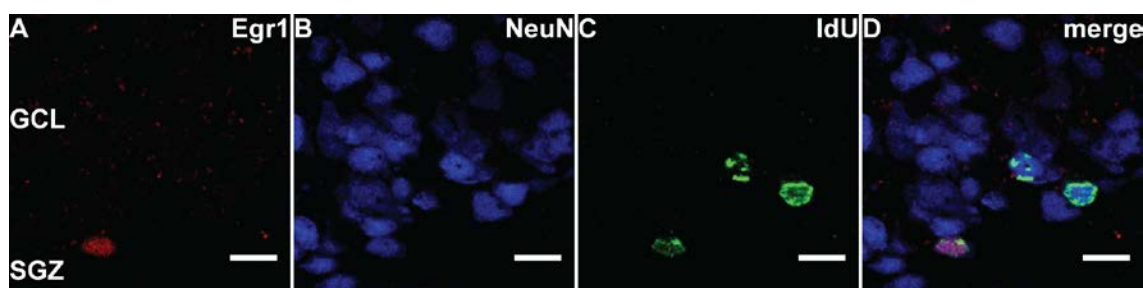


Figure 4: Confocal images of *Egr1* and *NeuN* positive, *IdU* labelled ABGCs. The merged image serves as verification of co-localization. GCL: granule cell layer, SGZ: subgranular zone. Scale bar: 20µm

Table 5 *XdU* project: Experimental method per animal

Number	Injection time point in weeks ptd			Procedure		Purpose	Age in months
	6	12	35	HFS for two days, 48h rest	5 min novel environment, 1h rest, perfusion		
Ng 44	IdU		CldU	X	X	HFS	9,9
Ng 45	IdU		CldU		X	control	9,9
Ng 46	IdU		CldU		X	control	9,9
Ng 47	CldU		IdU	X	X	HFS	9,9
Ng 48	CldU		IdU	X	X	HFS	9,9
Ng 49	CldU		IdU	X	X	HFS	9,9
Ng 61	IdU	CldU			X	control	9,9
Ng 62	IdU	CldU		X	X	HFS	9,9
Ng 63	IdU	CldU		X	X	HFS	9,9
Ng 65	CldU	IdU		X	X	HFS	9,9
Ng 66*	IdU	CldU		X	X	HFS	9,9
Ng 70	IdU 4 weeks ptd				X	practice	3,7
Ng 71	CldU 4 weeks ptd				X	practice	3,7

\*) Ng 66 was excluded from the analysis due to extremely few labelled cells.



Table 6 XdU project: Number of all counted GCs, ipsi vs contra

	Unlabelled		6 weeks ptd		12 weeks ptd		35 weeks ptd	
	Ipsi	Contra	Ipsi	Contra	Ipsi	Contra	Ipsi	Contra
<b>Ng 44</b>	125	124	16	47			27	40
<b>Ng 45<sub>c</sub></b>	50	55	6	15			5	8
<b>Ng 46<sub>c</sub></b>	170	85	21	15			44	17
<b>Ng 47</b>	75	110	4	7			24	45
<b>Ng 48</b>	170	74	41	13			77	21
<b>Ng 49</b>	140	175	27	22			55	83
<b>Ng 61<sub>c</sub></b>	55	60	18	23	29	32		
<b>Ng 62</b>	190	175	60	50	36	59		
<b>Ng 63</b>	120	30	16	4	14	5		
<b>Ng 65</b>	115	140	24	27	21	78		
<b>Ng 66<sup>*</sup></b>	15	40	1	4	2	7		

c) Ng 45, 46 and 61 are control animals, they did not receive stimulation.

\*) Ng 66 was omitted due to extremely few labelled cells.

Ng 70 and 71 were practice animals which were used for establishing the methodology, but not further used for the analysis. No cells were counted.

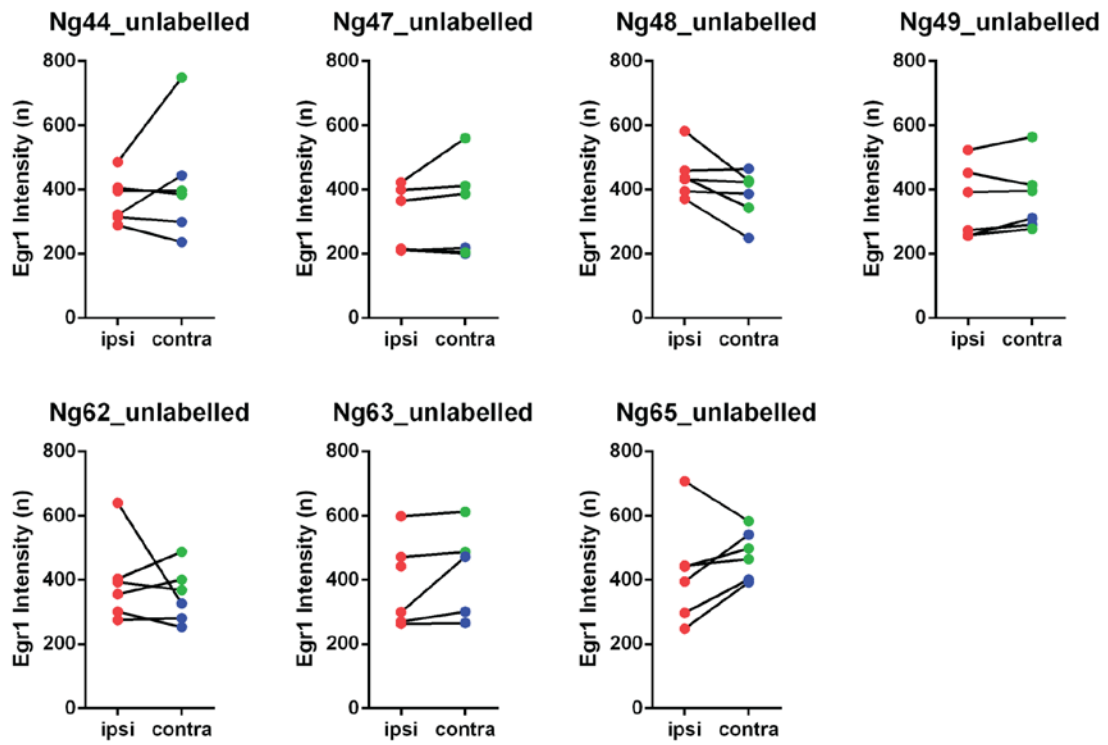


Figure 5: Average per slice (unlabelled): The average Egr1 intensity of the unlabelled control population of granule cells (GCs, unlabelled = not labelled with XdU) of every brain slice per animal is shown. The linked pairs depict the stimulated and the unstimulated side of every slice. Animal number:  $n = 7$ .

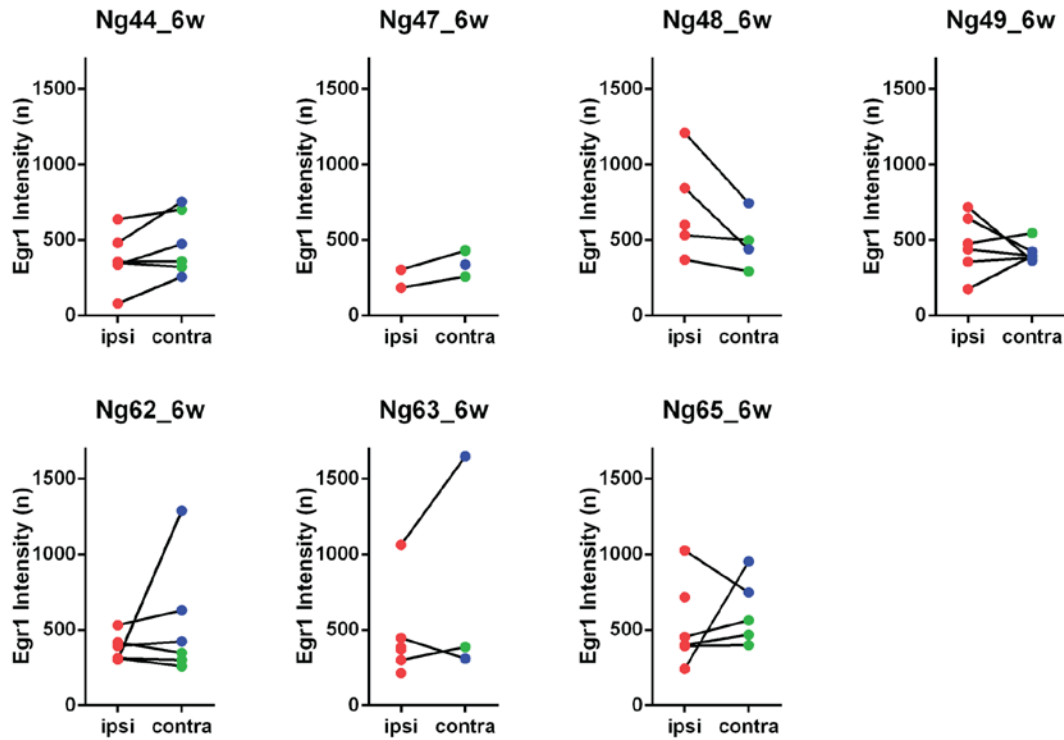


Figure 6: Average per slice (6 weeks): The average *Egr1* intensity of the adult born granule cells (ABGCs) labelled at 6 weeks ptd (labelled = received XdU injections) of every brain slice per animal is shown. The linked pairs depict the stimulated and the unstimulated side of every slice. Although six slices of each animal were stained, XdU labelled ABGCs were not found in each side and every slice. Animal number:  $n = 7$ .

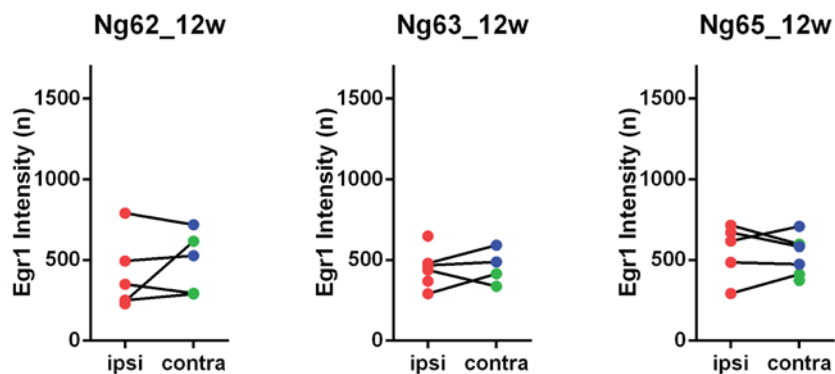


Figure 7: Average per slice (12 weeks): The average *Egr1* intensity of the adult born granule cells (ABGCs) labelled at 12 weeks ptd of every brain slice per animal is shown. The linked pairs depict the stimulated and the unstimulated side of every slice.

Although six slices of each animal were stained, XdU labelled ABGCs were not found in each side and every slice. Animal number:  $n = 3$ .

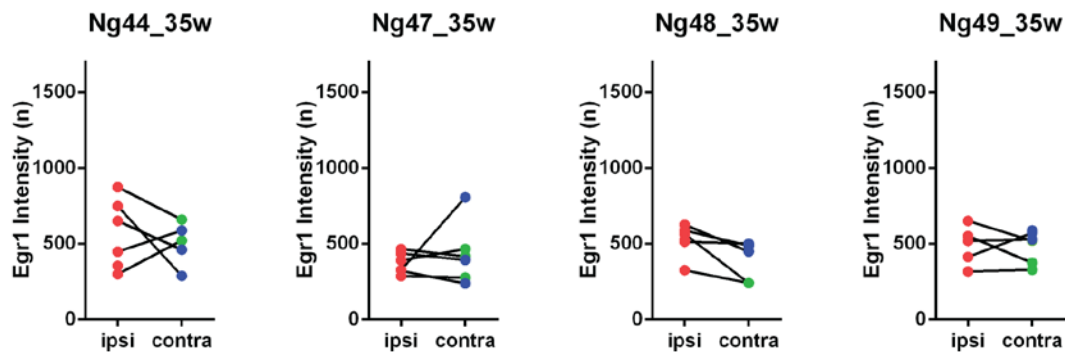


Figure 8: Average per slice (35 weeks): The average *Egr1* intensity of the 35 week old adult born granule cells (ABGCs) of every brain slice per animal is shown. The linked pairs depict the stimulated and the unstimulated side of every slice. Although six slices of each animal were stained, XdU labelled ABGCs were not found in each side and every slice. Animal number:  $n = 4$ .

### 8.1.2 Unilateral Stimulation increases *Egr1* expression in ABGCs of both hemispheres

The *Egr1* intensity values of all animals were pooled for each age group of ABGCs and for the unlabelled GCs (Figure 9, A - E). The average *Egr1* intensities of every side were compared. There was no significant difference in the *Egr1* intensity between the stimulated and the unstimulated side. The next step was to reciprocally contrast the ABGCs of each time point and with the unlabelled GCs. This was done for each brain side (Figure 9, F - G) using the absolute and relative average *Egr1* intensity of every animal. A significantly higher *Egr1* intensity could be observed in all ABGCs of the contralateral side and in the 12 and 35 week old ABGCs of the ipsilateral side. This revealed that the stimulation significantly enhanced the expression of *Egr1* in ABGCs. This effect was apparent in both hemispheres.

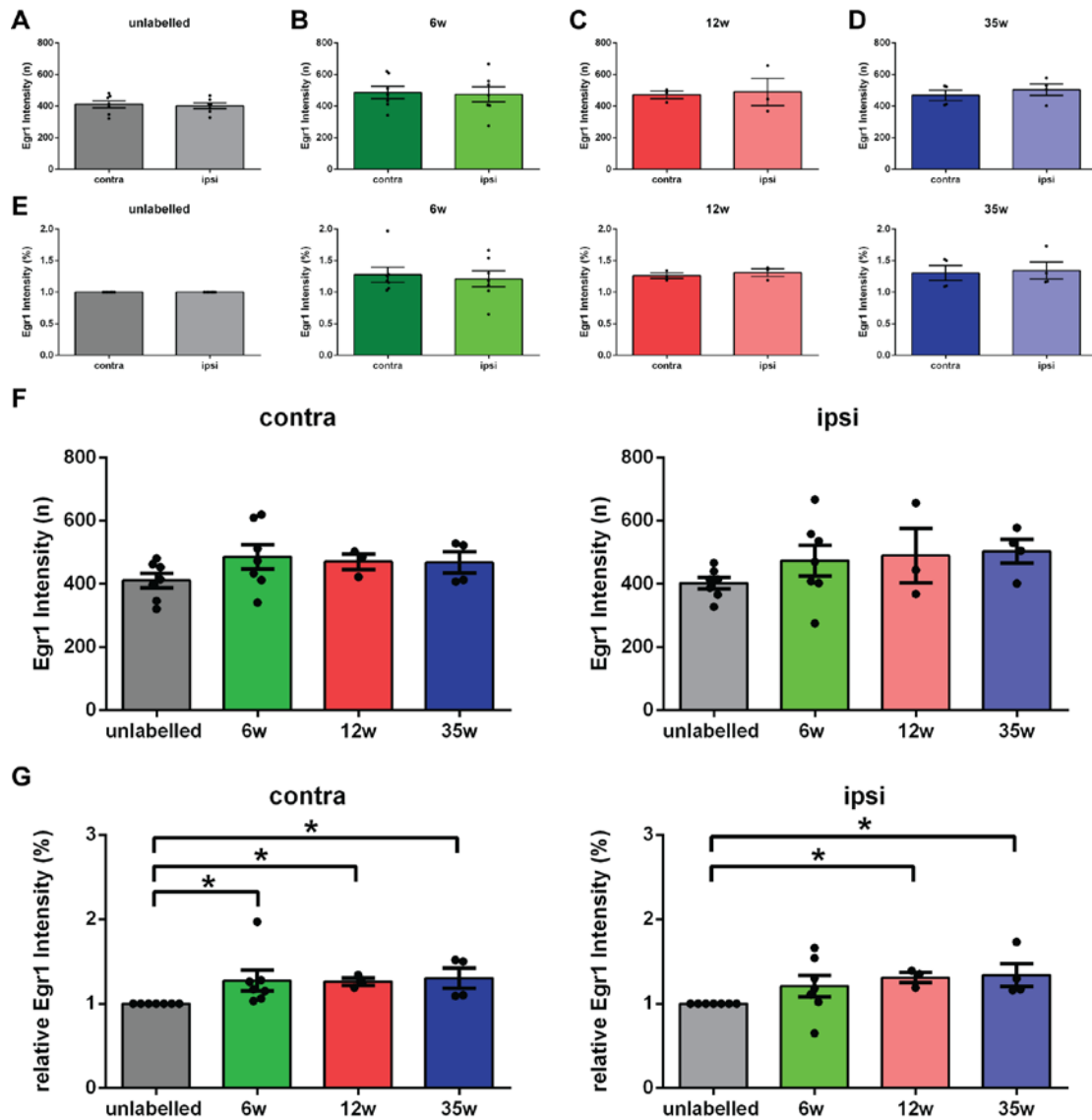


Figure 9: Average per time point: The average Egr1 intensity of all unlabelled GCs (A), all ABGCs XdU labelled at 6 week (B), 12 week ptd (C) and 35 week ptd (D) of every animal is compared by side. The same comparison is made with relative values (E). Showing the same Egr1 intensities as in A-E, the differences between the three time points and the unlabelled GCs are contrasted (F). The same comparison was conducted with relative values (G). The dots represent the average Egr1 intensity value per animal. Animal number: (unlabelled)  $n = 7$ , (6 w)  $n = 7$ , (12 w)  $n = 3$ , (35 w)  $n = 4$ . Asterisk indicate significance between time points, Kruskal-Wallis test, (unlabelled vs 6 w, vs 12 w and vs 35 w)  $*P < 0.05$ .

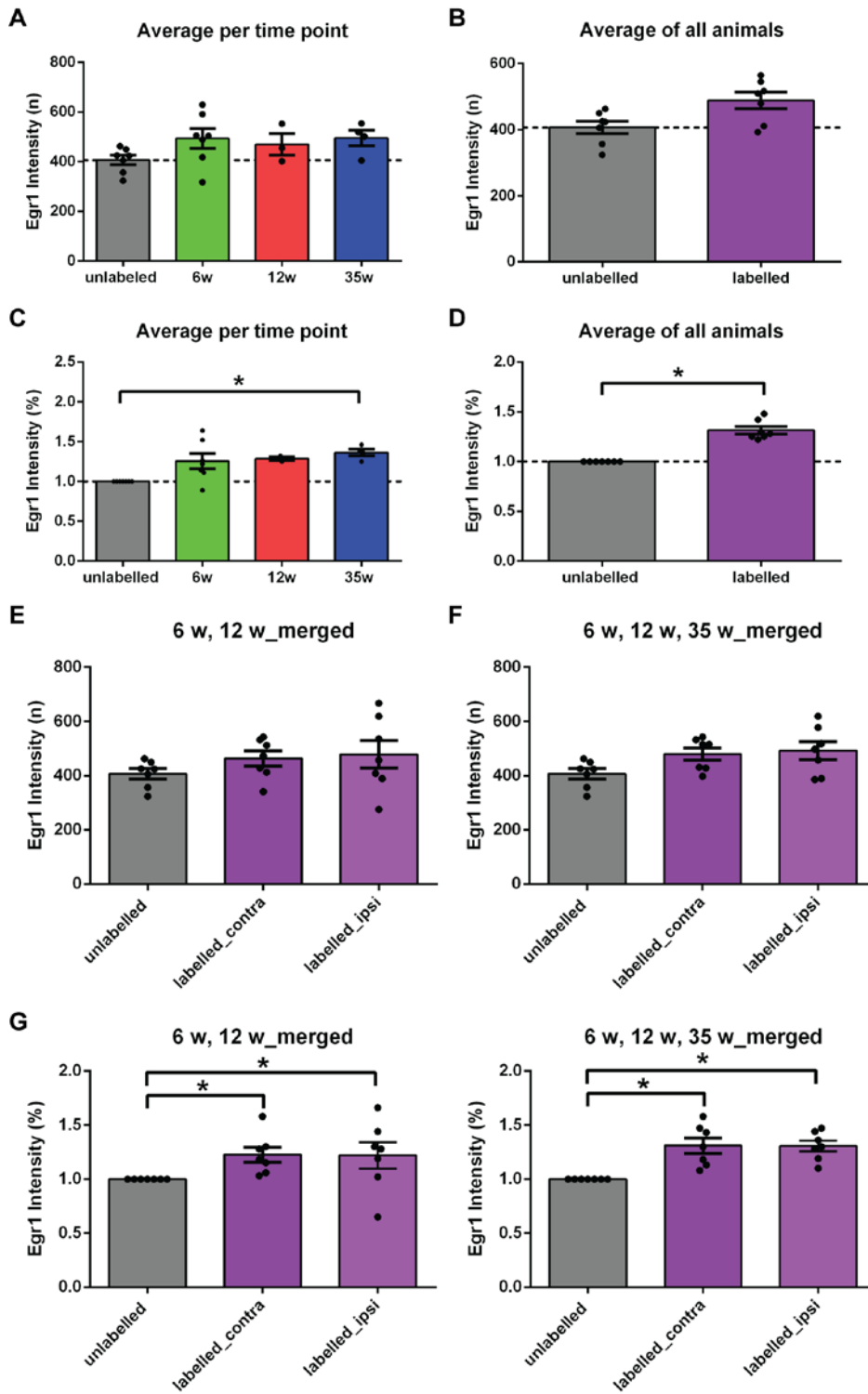


Figure 10: Merged time points: (A) The average Egr1 intensity of all GCs from the stimulated and the unstimulated side of every animal is depicted for the unlabelled GCs and the ABGCs labelled at 6, 12 and 35 weeks ptd. (B) The average Egr1 intensity of all unlabelled GCs from both sides of every animal is compared with the average Egr1 in-

*intensity of all ABGCs from both sides of every animal and every time point. The same comparison was conducted using relative values (C + D). The dashed line shows the Egr1 intensity of the unlabelled column and serves as orientation. The average Egr1 intensity of the ABGCs aged 6 weeks and 12 weeks (E) is compared by side. The average Egr1 intensity of the unlabelled GCs serves as control. The same comparison is made including the average Egr1 intensity of the 35 week old ABGCs (F). The bottom row (G) shows the same analysis with relative values. The dots represent the average Egr1 intensity value per animal. Dotted line marks level of unlabelled GCs. Animal number: (unlabelled) n = 7, (6 w) n = 7, (12 w) n = 3, (35 w) n = 4. Asterisk indicate significance between GC populations, (B+D) Mann-Whitney test, (A, C, E - G) Kruskal-Wallis test, Dunn's multiple comparison rank test (unlabelled vs 6 w, vs 12 w and vs 35 w; unlabelled vs labelled\_contra and vs labelled\_ipsi) \*P < 0.05.*

Egr1 intensities of both sides were pooled for each time point (Figure 10, A + C). Interestingly, a significant stimulation effect could only be observed for 35 week old ABGCs. The slightly higher average Egr1 intensity of the younger ABGCs could indicate a trend but was not significant if both sides were pooled. The average Egr1 intensity among the ABGCs was similar. In order to distinguish the effect on ABGCs, the Egr1 intensity of all ABGCs of every animal and side was pooled (Figure 10, B + D). Now, a significant distinction could be made between the unlabelled GCs and the labelled ABGCs (Figure 10, D). This finding led to the question of whether this distinction could also be made when the pooled ABGCs were re-split into an ipsi- and contralateral group? Figure 10, G demonstrates that the average Egr1 intensity from all ABGCs was significantly higher than that of all unlabelled GCs for both ipsi and contra. This result also remained for the merged 6 and 12 week old ABGCs (Figure 10, G left).

### **8.1.3 Enhanced excitability is not an innate feature of ABGCs**

Apart from the stimulated rat brains, three brains taken from control rats were analysed. These rats had been implanted with the same head plug but received no HFS. Just as the stimulated animals, the control rats were exposed to novel environment one hour prior to perfusion. All control rats were injected with XdU at 6 weeks prior to death.

The second XdU injection was at 35 weeks prior to death for one rat and at 12 weeks prior to death for the other two. Therefore, it was made possible to match every ABGCs population with a control population. As in the case of the stimulated animals, no outer influence on the quality of staining could be found by analysing the average Egr1 intensities of each brain section (Figure 11, A - D). As expected, no difference between the average Egr1 intensity of the unlabelled GCs and the ABGCs of any age group in the control animals was found (Figure 11, E). The ABGCs of both sides and of all age groups were pooled. The average Egr1 intensity of these labelled GCs was equivalent to that of the unlabelled GCs (Figure 11, F). This analysis showed that in control conditions, the Egr1 intensity of ABGCs was similar to that of unlabelled GCs. Therefore, the possibility that a heightened excitability is an innate feature of ABGCs was ruled out. In the next step, the control values were compared to the values from the stimulated animals. The Egr1 intensity of the unlabelled cells of both hemispheres was equal in both stimulated and control animals (Figure 11, G). This showed that XdU labelling does not alter the cells excitability. The average Egr1 intensity of all labelled ABGCs from both sides was significantly higher for the stimulated animals (*Figure 11, H*). This confirmed that the stimulation significantly enhanced Egr1 expression in ABGCs. It has been shown that the average Egr1 intensity of the control animals GCs was equal to that of the unlabelled GCs from the stimulated rats (*Figure 11, F*). It has also been demonstrated that there was a significant difference in average Egr1 intensity between all ABGCs from stimulated rats and those from control rats (Figure 10, G). This raised the expectancy that the average Egr1 intensity of all ABGCs from stimulated rats divided into an ipsi- and a contralateral group would be higher than the average Egr1 intensity of control ABGCs. But for this comparison (Figure 11, I), however, no significant difference could be shown.



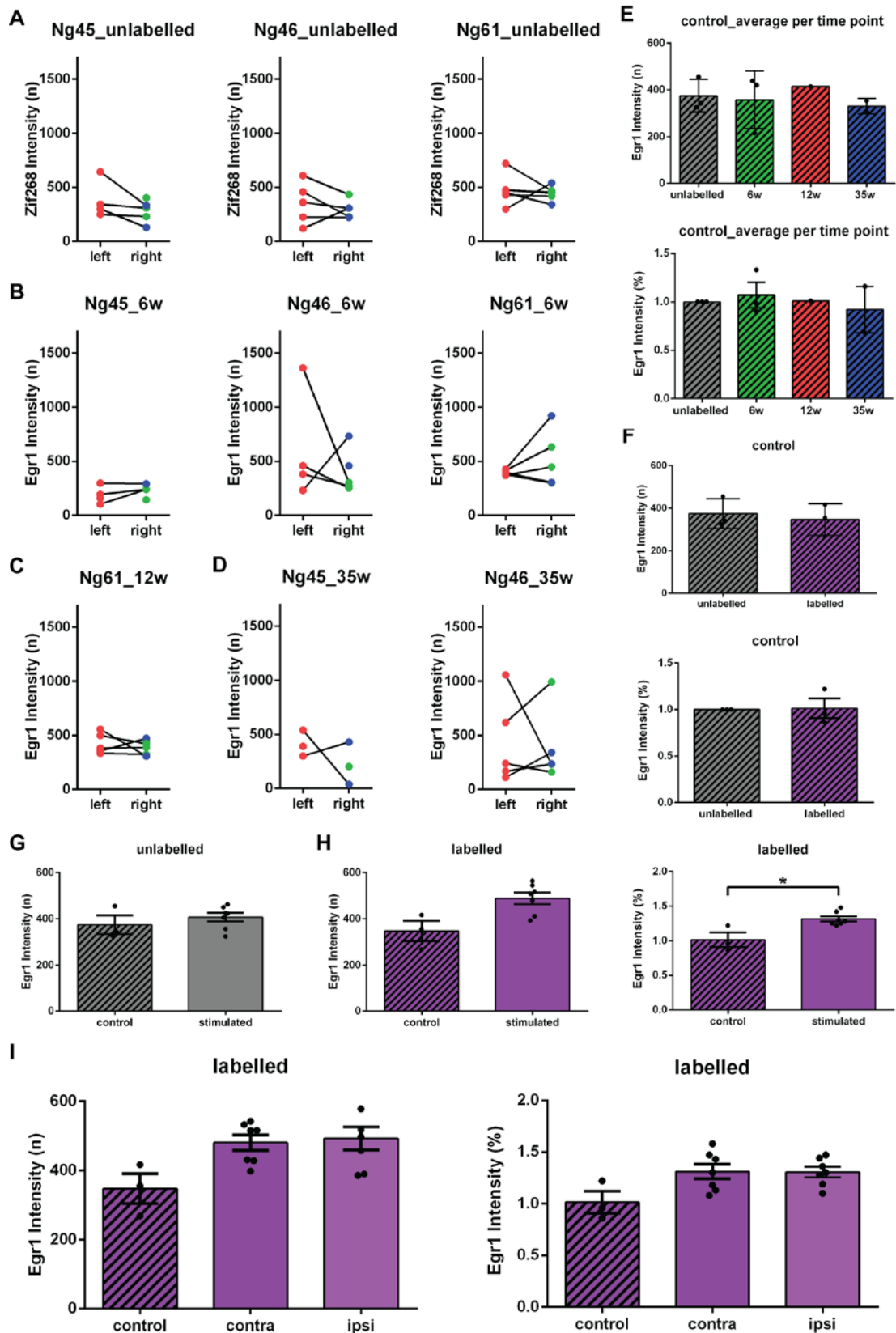


Figure 11: Control: This figure shows only values from control animals. The average Egr1 intensity of the unlabelled GCs (A), the ABGCs labelled at 6 weeks ptd (B), at

12 week ptd (C) and at 35 week ptd (D) of every brain slice per animal is shown. The linked pairs depict the right and the left side of every slice. (E) The average Egr1 intensity of all GCs from both sides of every animal is depicted for the unlabelled GCs, and the ABGCs labelled at 6, 12 and 35 weeks ptd. The same comparison is made with absolute and relative values. (F) The average Egr1 intensity of all unlabelled GCs from both sides of every animal is compared with the average Egr1 intensity of all ABGCs from both sides of every animal and every time point. This comparison is made with absolute and relative values. (G) The comparison between the average Egr1 intensity of the unlabelled GCs from the control animals is made with that from all stimulated animals. (H) The average Egr1 intensity of all ABGCs from the control animals is compared with that of all simulated animals. This analysis is made with absolute and relative values. (I) The average Egr1 intensity of all ABGCs is depicted. The average Egr1 intensity of the contra- and ipsilateral side of the stimulated animals is compared with the average Egr1 intensity of the control rats. This comparison is made with absolute and with relative values. The dots represent the average Egr1 intensity value per animal. Control animal number: (unlabelled)  $n = 3$ , (6 w)  $n = 3$ , (12 w)  $n = 1$ , (35 w)  $n = 2$ . Asterisks indicate significance between control and stimulated, (H) Mann-Whitney test, (I) Kruskal-Wallis test, Dunn's multiple comparison rank post-hoc test (control vs contra, control vs ipsi)  $*P < 0.05$ .

#### **8.1.4 Unilateral Stimulation results in similarly heightened excitability of 6, 12 and 35 week old ABGCs of both hemispheres**

In order to further normalise the absolute Egr1 intensities, they were converted into z-scores using the following formula:

$$z\text{-score} = (x - \mu) / \sigma$$

$x$  is the measured Egr1 intensity value,  $\mu$  is the mean of all Egr1 values from the unstimulated side of this animal and  $\sigma$  is the standard deviation of Egr1 values for each separate animal<sup>209</sup>. The conversion to the z-score was necessary in order to compare the

data from my analysis with that conducted for animals analyzed in New Zealand. There, the Egr1 expression of GCs was not measured on a scale of intensity but simply categorized in Egr1 positive or negative. GCs with a Z-score of  $> 2.0$  were defined as being Egr1 positive. By scrutinizing the z-scores distribution of the different GCs groups, it is apparent that the distribution of Egr1 expression is significantly right-shifted for the three ABGCs time points (Figure 12, A) ( $P < 0.005$  Bonferroni corrected Kolmogorov-Smirnow tests). This indicated that HFS identically enhances the excitability of ABGCs across all three cell ages. The possibility that increased Egr1 expression is an inherent feature of ABGCs was considered. Considering that the majority of the unlabelled GCs were born perinatally in rats<sup>212-214</sup>, the equal alignment of the z-score distribution curves in the control animals, with the exception of the 35 week old ABGCs, demonstrated no enhanced Egr1 expression of ABGCs in control animals (Figure 12,B). A distinct increase of Egr1 expression compared to unlabelled GCs and control animals could be noted when merging all ABGCs of the ipsilateral hemisphere (Figure 12,C) ( $p < 0.0083$ , Bonferroni-corrected Kolmogorov-Smirnov tests). Interestingly, the z-score distribution of the contralateral hemispheres ABGC was also right-shifted (Figure 12, D). The mean percentage of the combined age groups further distinguished the enhanced responsiveness of ABGCs ( $19.2 \pm 3.4 \%$ ) compared to the unlabelled GCs of the same hemisphere ( $4.7 \pm 0.5 \%$ ) and to the ABGCs ( $3.7 \pm 0.7 \%$ ) and unlabelled GCs ( $3.7 \pm 0.7 \%$ ) of the control animals (all  $p < 0.05$ , Figure 12, E). A similarly significant increase in responsiveness could be observed in the contralateral hemisphere for the combined ABGCs ( $15.4 \pm 3.1 \%$ ) compared to the unlabeled GCs of the same hemisphere ( $4.4 \pm 0.7 \%$ ) and the ABGCs and unlabeled GCs of the control animals (all  $p < 0.05$ , Figure 12, F). This proposes a long-term stimulation effect of increased excitability on both hemispheres following unilateral stimulation.

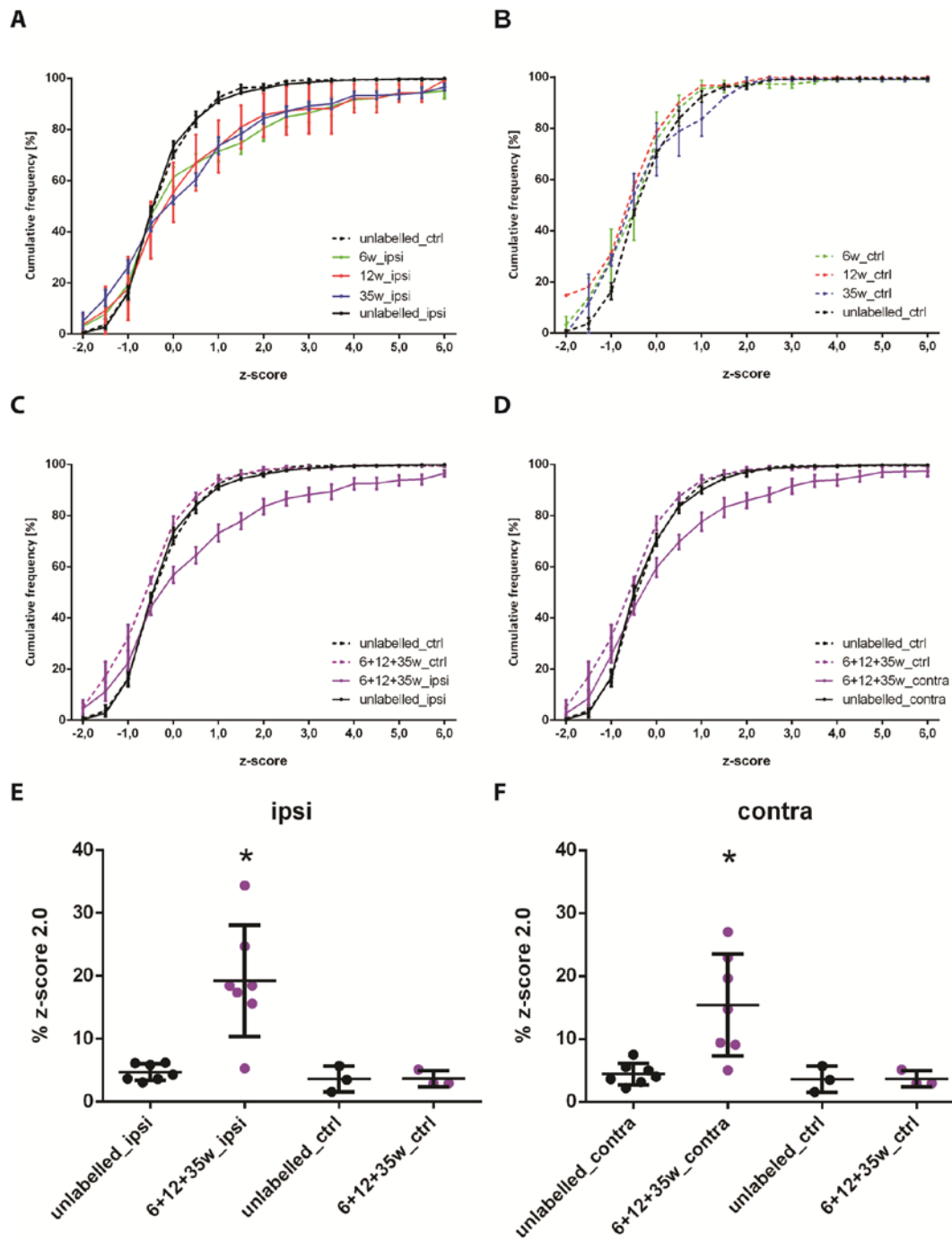


Figure 12: The distribution of z-score values (see text) from 6 ( $n = 7$ ), 12 ( $n = 3$ ) and 35 ( $n = 4$ ) week old ABGCs is equivalent. Compared to the distribution of the unlabelled GCs of the stimulated and the control animals, a significant right-shift can be observed (A). The Z-score distributions of the control groups are all similar except for a significant right shift of the 35 week old ABGCs (B). When merging all ABGCs age groups of the ipsilateral hemisphere, they appear significantly right-shifted compared to

*the unlabelled GCs and merged ABGCs of the control animals (C). The same right-shift can be observed on the contralateral hemisphere (D). The percentage of the merged ipsilateral ABGCs with a Z-score of >2.0 shows a significant increase ( $19.2 \pm 3.4\%$ ,  $n = 7$ ) when comparing that of the GCs from the contralateral side with the control animals. Figures adapted after Ohline et al<sup>209</sup>. Animal number: (unlabelled)  $n = 7$ , (6 w)  $n = 7$ , (12 w)  $n = 3$ , (35 w)  $n = 4$ . (A-D) Bonferroni- corrected Kolmogorov-Smirnov test, (E+F) one-way ANOVA, Sidak-Holm post-hoc tests, \* $P < 0.05$ .*

### **8.1.5 Higher excitability in infrapyramidal adult born granule cells**

In the following analysis the suprapyramidal GCs were compared with the infrapyramidal GCs. The average Egr1 intensity of each ABGC population varied among the rats. This was due to two factors. Firstly, the amount of labelled ABGCs counted per age group differed between the animals and age groups (Table 7 XdU project: Number of all counted GCs, supra vs. infra). Secondly, the Egr1 intensity is quite stable for the majority of GCs, some ABGCs however appear with a very strong Egr1 expression as well as some ABGCs having almost none. These fluctuations were diminished by pooling all ABGCs of every age population, separated into ipsi and contra (Figure 13, A+B). Again, there was no difference in the average Egr1 intensity between supra- and infrapyramidal GCs. Unfortunately only three rats could be used for the analysis of the 12 week old ABGCs. The fourth rat (Ng66) was excluded due to the fact that only very few labelled GCs could be found (Table 7 XdU project: Number of all counted GCs, supra vs. infra). The average Egr1 intensity of the suprapyramidal ABGCs of each age group appeared to be higher, but this inclination was not significant (Figure 13, A+B). The comparison of the average Egr1 intensity from the supra- and infrapyramidal GCs of the control animals showed that the intensity levels were equal for each ABGCs population as well as for the unlabelled GCs (Figure 13, C+D). In order to overcome the problem of low animal number per age group, the 6 week and 12 week old ABGCs were merged (Figure 14, D). The average Egr1 intensity of the infrapyramidal young ABGCs was significantly higher than that of the suprapyramidal young ABGCs. The Egr1 intensity of the infrapyramidal young ABGCs was also significantly higher than that of the unla-

belled GCs. The intensity of the suprapyramidal young ABGCs was equivalent to that of the unlabelled GCs of either side. It could therefore be concluded that the stimulation effect was clearly visible in the 6 week and 12 week old ABGCs of the infrapyramidal blade but not in those of the suprapyramidal blade of the dentate gyrus (Figure 13, D). It is also important to singularly interpret the results attained in the 35 week old ABGCs. It has already been shown that there was no significant difference of the average Egr1 intensity between the supra- and infrapyramidal ABGCs at 35 weeks of age (Figure 13, A, rightmost graph). Here it could be demonstrated that the Egr1 intensity of the infrapyramidal ABGCs of this age group was significantly higher than that of the unlabelled GCs from the infrapyramidal blade. Interestingly, the 35 week old suprapyramidal ABGCs also showed a significantly higher Egr1 intensity than the unlabelled suprapyramidal GCs (Figure 14, E). In contrast to the younger ABGCs, it was visible that the HFS affected the 35 week old ABGCs from the infrapyramidal as well as from the suprapyramidal blade. The control rats clearly showed no difference of Egr1 intensity between supra- and infrapyramidal or unlabelled GCs and labelled ABGCs (Figure 14, F).

*Table 7 XdU project: Number of all counted GCs, supra vs. infra*

	Unlabelled		6 weeks old		12 weeks old		35 weeks old	
	Supra	Infra	Supra	Infra	Supra	Infra	Supra	Infra
<b>Ng 44</b>	150	140	48	29			30	43
<b>Ng 45<sub>c</sub></b>	35	50	7	12			3	7
<b>Ng 46<sub>c</sub></b>	145	95	18	16			46	13
<b>Ng 47</b>	140	50	11	0			42	26
<b>Ng 48</b>	150	140	24	28			41	46
<b>Ng 49</b>	220	125	28	30			93	42
<b>Ng 61<sub>c</sub></b>	170	85	28	13	39	18		
<b>Ng 62</b>	260	60	88	25	67	28		
<b>Ng 63</b>	100	45	13	5	16	6		
<b>Ng 65</b>	180	105	41	14	52	80		
<b>Ng 66*</b>	30	20	3	1	5	4		

c) Ng 45, 46 and 61 are control animals, they did not receive stimulation.

\*) Ng 66 was omitted due to extremely few labelled cells.

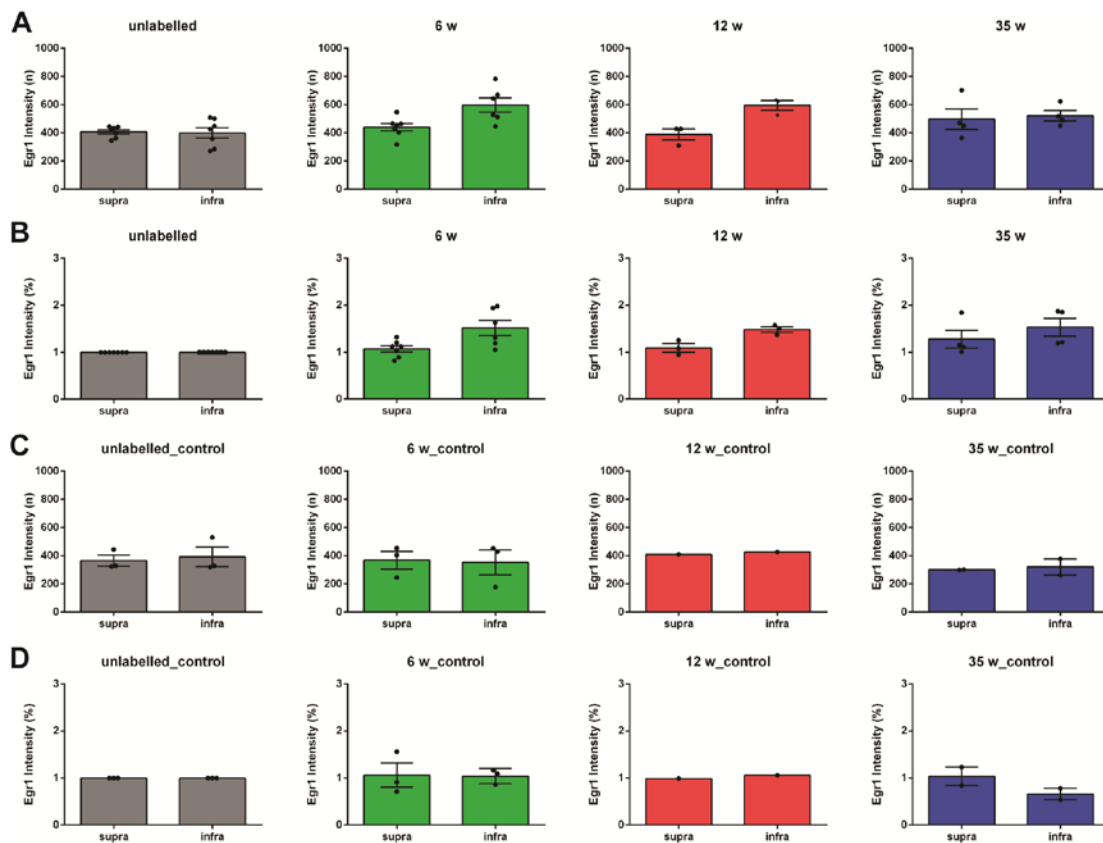


Figure 13: *Supra vs. infra: The average Egr1 intensity of the GCs counted in the suprapyramidal blade of the dentate gyrus is compared with that of the infrapyramidal GC. (A) These graphs show the average Egr1 intensity of all ABGCs of every animal labelled at 6, 12 and 35 weeks ptd. (B) The same comparison is made with relative numbers. (C) These graphs show the average Egr1 intensity of all ABGCs of every control animal labelled at 6, 12 and 35 weeks ptd. (D) The same comparison is made with relative numbers. The dots represent the average Egr1 intensity value per animal. Animal number: (unlabelled) n = 7, (6 w) n = 7, (12 w) n = 3, (35 w) n = 4.*

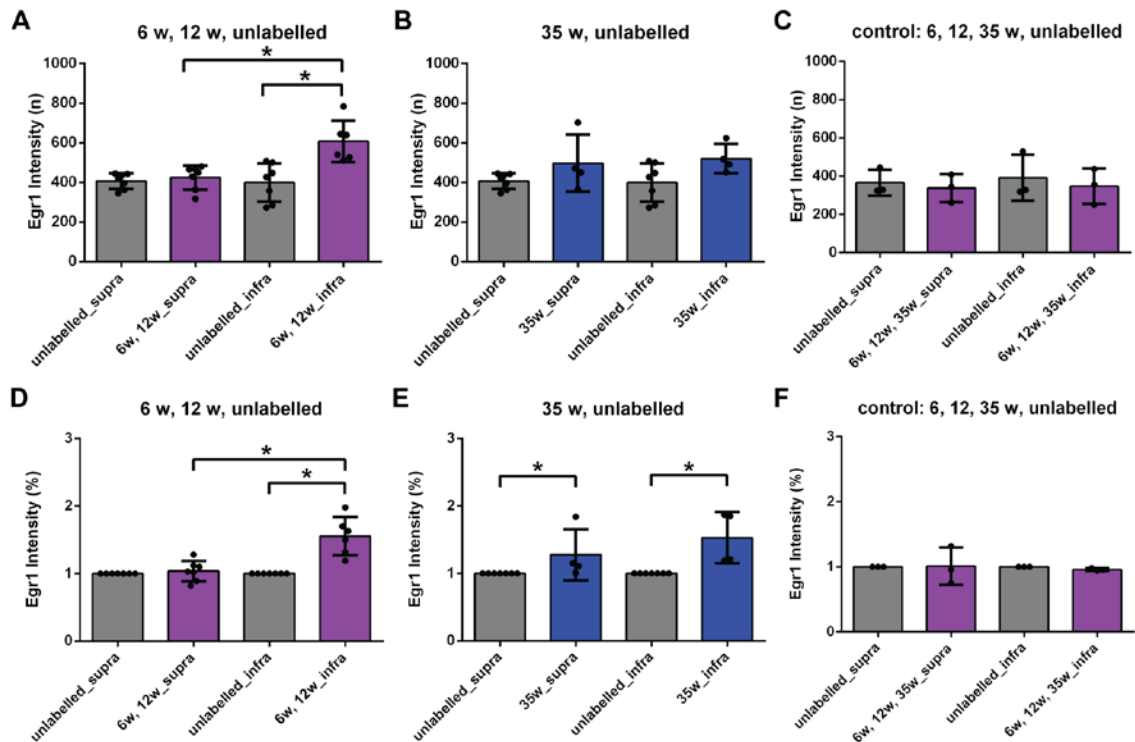


Figure 14: Supra vs infra, merged: The average Egr1 intensity of suprapyramidal GCs is compared to that of infrapyramidal GCs for the following GC populations: (A) The Egr1 intensity of the unlabelled GCs from all animals is contrasted to the merged Egr1 intensity of ABGCs labelled at 6 and 12 weeks ptd. (B) The Egr1 intensity of the unlabelled GCs from all animals is compared to that of the ABGCs labelled at 35 weeks ptd. (C) This graph shows the Egr1 intensity from GCs of the control rats. The values from the unlabelled GCs are compared with the average Egr1 intensity of all ABGCs. The bottom row (D-F) shows the same analysis with relative numbers. The dots represent the average Egr1 intensity value per animal. Animal number: (unlabelled)  $n=7$ , (6w)  $n=7$ , (12w)  $n=3$ , (35w)  $n=4$ , (control)  $n=3$ . Kruskal-Wallis test, Dunn's multiple comparison rank post-hoc test (6 w, 12 w\_infra vs unlabelled\_infra, vs 6 w, 12 w\_supra and unlabelled vs 35 w\_supra, unlabelled vs 35 w\_infra)  $*P < 0.05$ .



### **8.1.6 Cross reaction of antibodies**

The distinction of two populations of ABGCs in each rat is possible due to the fact that each one received two injections of differing XdUs. Initially double stainings with antibodies against CldU and IdU were performed. However, a very slight cross reaction was noted. Test stainings with the training animals, which had only received injection of a single XdU, revealed the exact nature of the cross reaction: The mouse-anti-IdU antibody (AB) from BD Bioscience stained few cells in brain sections from Ng 71, which only received CldU injections. This could be shown with the secondary AB Alexa Fluor goat-anti-mouse 488 and 568. The rat-anti-CldU AB from Accurate stained very few cells in IdU labelled tissue from Ng 71 (which had received only IdU injections). This was made visible with Alexa Fluor 488 goat-anti-rat AB. Interestingly, when applying the secondary AB Alexa Fluor 568 and 488 goat-anti-mouse as well, the signal of rat-anti-CldU was also brightly visible. Although the abovementioned stainings indicated the adherence of rat-anti-CldU to IdU labelled tissue, Alexa Fluor 488 and 568 goat-anti-mouse AB signalled the presence of rat-anti-CldU only in CldU labelled tissue. This could be due to the stronger adherence of rat-anti-CldU AB to CldU labelled tissue since this is its main epitope. In conclusion it can be noted that although the anti-IdU and anti-CldU AB show a very slight cross reaction, the real problem in clear identification lies in the secondary AB Alexa Fluor 488 and 568 goat-anti-mouse since they intensify the incorrect signal from Alexa Fluor goat-anti-mouse to rat-anti-CldU. By reverting to single stainings for the stimulated animals, the intensification of a very slight cross reaction was omitted, because Alexa Fluor goat-anti-mouse and rat-anti-CldU were never administered in one brain section. Alexa Fluor 488 and 568 goat-anti-rat did not show a cross reaction.

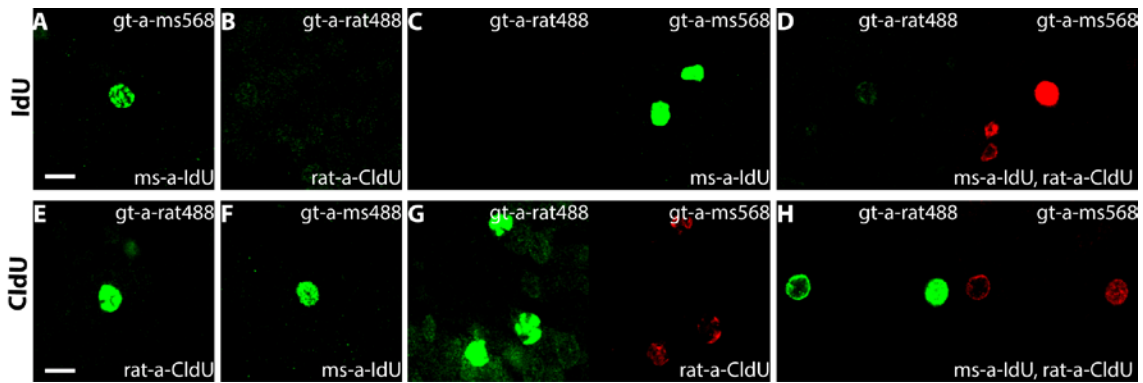


Figure 15: Cross reaction: Upper row: Ng70, only IdU injections: (A) ms-a-IdU and gt-a-ms568, correct, (B) rat-a-CldU and gt-a-rat488, correct, (C) ms-a-IdU, gt-a-rat488 and gt-a-ms568, correct, (D) ms-a-IdU, rat-a-CldU, gt-a-rat488 and gt-a-ms568, Cross reaction, left. Lower row: Ng71, only CldU injections: (E) rat-a-CldU and gt-a-rat488, correct, (F) ms-a-IdU and gt-a-ms488, Cross reaction, (G) rat-a-CldU, gt-a-rat488 and ms-s-568, Cross reaction, G, right, (H) ms-a-IdU, rat-a-CldU, gt-a-rat488 and gt-a-ms568, Cross reaction H, right. Scale bar: 10 $\mu$ m.

## 8.2 Spine Project

Egr1 fluorescence and spine analysis constituting to the following results provide additional data for a larger project from Dr. Tassilo Jungenitz of the Institute of Clinical Neuroanatomy in Frankfurt, Germany. The point of interest of this project was the critical phase for homo- and heterosynaptic structural plasticity and synaptic integration in ABGCs. In order to analyse the dendritic structure of individual GCs, selective GC labelling was executed with a retrovirus based approach. Rats received HFS of the MPP in *in vivo* conditions, this elicited homosynaptic LTP in the middle molecular layer (MML). Heterosynaptic LTD was observed in the neighbouring inner- and outer molecular layer (IML and OML). By analysing Arc and f-actin expression in differently aged ABGC, conclusions were drawn on their developing structural plasticity and integration into the existing GC network<sup>215</sup>. Here, the role of IEGs as a marker of synaptic activity and plasticity was investigated by using Egr1 labelling. Some immunohistochemical staining and all the imaging, Egr1 intensity measurement and spine analysis were done by me, all prior work leading to this was performed by Dr. T. Jungenitz.

### **8.2.1 Egr1 expression due to HFS is lower in adult-born than in mature granule cells**

This study was performed on fixed brain sections of eleven adult male Sprague-Dawley rats that had received intrahippocampal injections of a GFP-expressing murine leukemia retrovirus (RV-GFP) at 28 or 35 days prior to transcardial perfusion. In these animals, 2 h of unilateral HFS of the medial perforant path had been applied directly prior to transcardial perfusion. After fixation, brains were sliced with a vibratome. The provided brain sections were immunohistochemically stained for Egr1 and, in order to enhance the GFP signal, with an additional antibody directed against GFP. Egr1 fluorescence intensity was measured with the same method used for the XdU labelled GCs (chapter 6.4): In three dimensional image stacks, the soma of a labelled GC was marked at its largest diameter by outlining the circumference. Egr1 intensity was measured only in the thus selected area. Sample ABGC at 28 and 35 dpi with strong and weak Egr1 expression can be seen in Figure 16 (A - D). When comparing the cumulative Egr1 intensity of ABGCs at 28 dpi, 35 dpi and mature GCs, it was apparent that the average intensity of the ABGC was less than that of the mature GCs (Figure 16, E). At 28 dpi, 50 % of the ABGC population expressed an Egr1 intensity of less than ~20 %. 100 % was set as the average Egr1 expression intensity of all mature GCs. With ongoing maturation the average Egr1 intensity increased. At 35 dpi half the population expressed an Egr1 intensity of up to 40 %. The mature GCs clearly showed the highest Egr1 intensity (Figure 16, E). Figure 16 F depicts the same data set revealing the detailed Egr1 intensity distribution of the GCs of each age group. The difference in Egr1 intensity between ABGCs and mature GC is significant for both 28 dpi ( $p = 0.0001$ ) and 35 dpi ( $p = 0.0114$ ) (Figure 16, H). This data indicated a stimulation induced increase of Egr1 intensity which was dependent from the age of ABGC. It was apparent that with increasing maturation, the Egr1 intensity increased although at 35 dpi, it did not reach the expression level of mature GC.

Overall, the peak distribution of nuclear Egr1 intensity values from ABGCs differed from that of the mature GCs. The best differentiation between the two groups could be made at 70 % Egr1 expression intensity (Figure 16, F dotted line). This key value was

used as a threshold to divide ABGCs and mature GCs into groups with nuclear Egr1 expression higher or lower than 70 %. The distribution of the ABGCs at 28 and 35 dpi is opposite to that of the mGCs, marking a considerably lower Egr1 expression in the majority of ABGCs compared to mGCs (Figure 16, G).

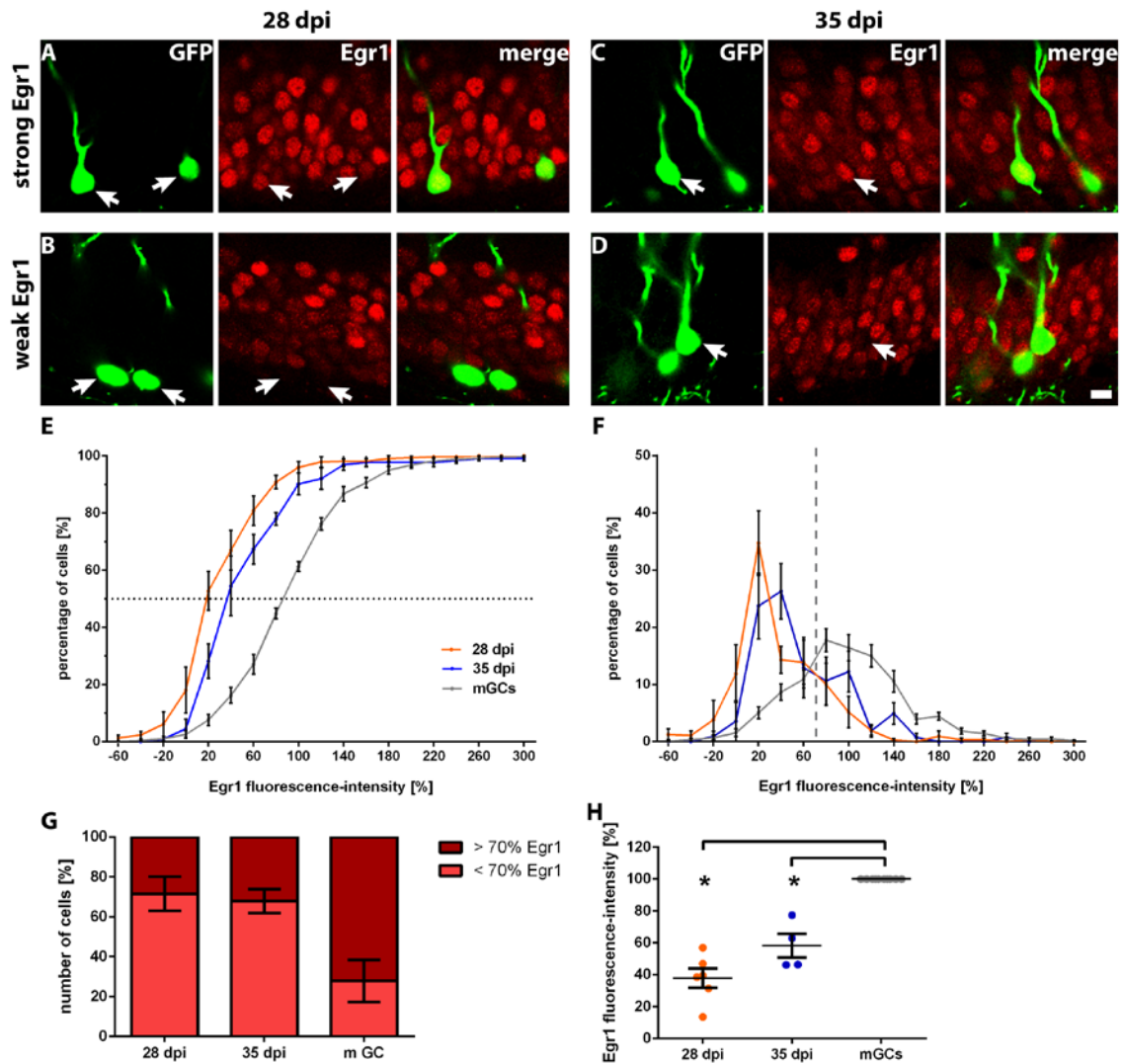


Figure 16: Cell age dependent Egr1 expression: Examples of retrovirally GFP labelled ABGCs with strong (A) and weak (B) Egr1 expression intensities at 28 dpi. Examples of retrovirally GFP labelled ABGCs with strong (C) and weak (D) Egr1 expression at 35 dpi. The cumulative Egr1 intensity for ABGCs at 28 dpi, 35 dpi and for mature GCs is depicted (E). The diagram depicts the distribution of Egr1 intensities of ABGCs at 28 dpi, 35 dpi and for mature GCs (F). Dashed line marks 70% Egr1 intensity. The columns depict the portion of GCs with either less or more than 70% nuclear Egr1 intensity.

ty at 28 dpi, 35 dpi and for mGCs (G). The dot plot shows the mean *Egr1* intensities of ABGCs at 28 dpi, 35 dpi in relation to the *Egr1* intensities of mature GCs (H). Animal number: (28 dpi)  $n = 6$ , (35 dpi)  $n = 5$ . Asterisks indicate significant difference from mature GCs. Kruskal-Wallis test, Dunn's multiple comparisons test, (28 dpi vs mGCs, 35 dpi vs mGCs)  $*P < 0.05$ . Scale bar (A-D) = 10  $\mu\text{m}$ .

## **8.2.2 Dendritic spine plasticity of adult-born granule cells following HFS**

The dendritic tree of each GC was analysed in a layer specific manner. Spine size of mushroom spines was measured in segments from the inner-, middle- and outer molecular layer (IML, MML and OML) of the ipsilateral hemisphere following 2h HFS. Only dendrites with connection to a soma, identified and analysed in the abovementioned results (Figure 16), were used in order to analyse cell specific changes across the IML, MML and OML. Mushroom spines were defined as “big” if the largest cross-sectional area of the spine head was larger than  $0.2 \mu\text{m}^2$  (see chapter 6.5). The percentage of big spines was calculated based on the total amount of mushroom spines. An ipsilateral ABGC at 28 dpi with its complete dendritic tree is depicted in Figure 17 (A, B) with matching samples of dendritic segments from IML, MML and OML. On the stimulated hemisphere, the percentage of big spines in the MML was significantly larger than in the IML and OML at 28 dpi and even more so at 35 dpi. The percentage of big spines in IML and OML was comparable (Figure 17, C+D). Interestingly, the highest percentage of big spines prevailed in the MML which had been subject to 2 h HFS.

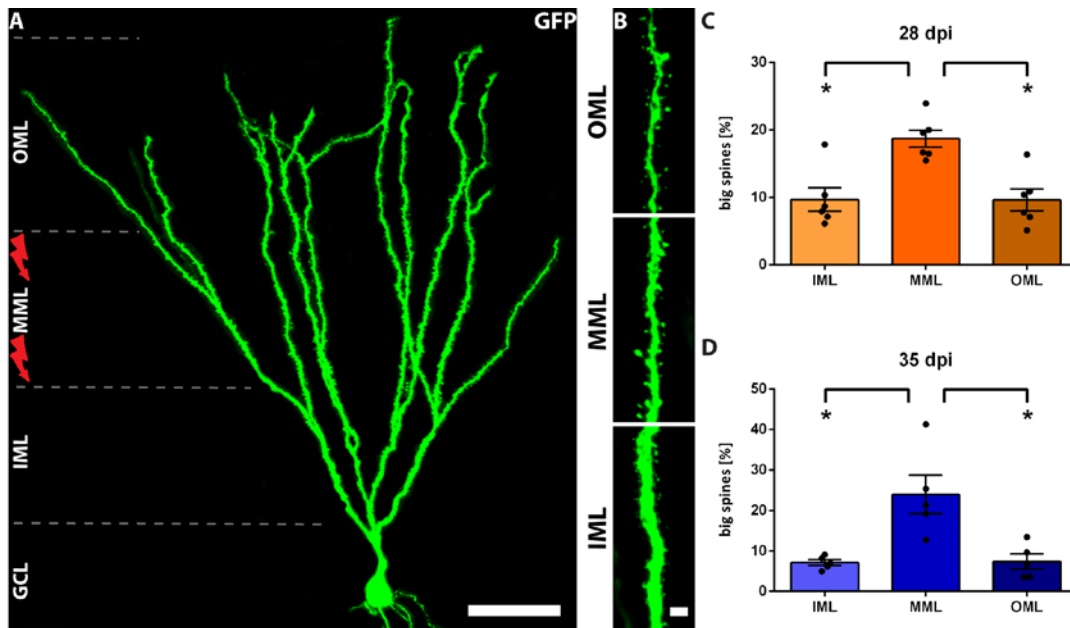


Figure 17: Layer specific structural plasticity of dendritic spines: GFP labelled dendritic tree sample of an ABGC at 28 dpi (A). Matching spine segments from IML, MML and OML of the cell shown in A (B). The average percentage of big spines in IML, MML and OML at 28 dpi (C) and at 35 dpi (D) in the stimulated hemisphere, each dot represents the average of one animal. Animal number: (28 dpi)  $n = 6$ , (35 dpi)  $n = 5$ . Asterisks indicate significant difference between layers. Kruskal-Wallis test,  $*P < 0.05$ . Scale bar (A) =  $50 \mu\text{m}$ , (B) =  $2 \mu\text{m}$ . IML= inner molecular layer, MML= middle molecular layer, OML= outer molecular layer, GCL= granule cell layer, lightning bolt indicates layer specific stimulation.

### 8.2.3 Correlation of Egr1 intensity and spine enlargement

The analysis of spine head enlargement and shrinkage was done in a cell specific manner. Thus, the structural dimensions of mushroom spines in the molecular layer could be correlated with the Egr1 expression intensity measured in the corresponding cell soma following the induction of heterosynaptic plasticity. The images in Figure 18 A-H show cells that are represented as dots in the graphs in Figure 18, I. For example the corresponding dots of the ABGC with weak Egr1 expression in the soma (Figure 19 E) and little variation in spine characteristics between IML, MML and OML (Figure 19 A) can be found at the leftmost pole of the linear fit (Figure 19 I - K). The

dots for the ABGC shown in Figure 19 B and F are placed at the rightmost pole of the linear fit. The analysis of spine size in high frequency stimulated ABGC revealed a trend toward the correlation between the percentage of big spines and the relative expression intensity of Egr1. The manner of correlation depended on the position in the molecular layer. A positive correlation between percentage of big spines and Egr1 intensity could be observed in the MML with an  $R^2$  of 0.09 (Figure 18 J). In the OML and IML the correlation was negative with a respective  $R^2$  of 0.12 for OML and 0.05 for IML (Figure 18 I+K). The positive trend in the MML indicated homosynaptic spine enlargement. The observed structural plasticity represents evidence for stimulation induced homosynaptic LTP in the MML. The negative tendency in OML and IML suggests heterosynaptic LTD induction. Spine shrinkage in OML and IML may therefore reflect heterosynaptic LTD in IML and OML. The changes in spine size were examined in adjacent dendritic segments, providing evidence for activity dependent homo- and heterosynaptic structural plasticity within the dendritic tree of individual GCs.

Next, it was analysed, if the amount of structural homo- and heterosynaptic structural plasticity could be correlated with the Egr1 expression intensity on the level of single identified ABGCs. In order to investigate this, the ABGCs from both age groups were split into two groups: Those with less than 70 %, and those with more than 70 % nuclear relative Egr1 intensity (Figure 18, L - N). This value was chosen as a threshold due to findings depicted in Figure 16, F: The majority of ABGCs expressed less than 70 % nuclear Egr1 intensity while the majority of mGCs expressed more than 70 % nuclear Egr1 intensity. In the MML, the cell group with more than 70 % Egr1 intensity expression appeared to have a significantly higher percentage of big spines than the group with less than 70 % Egr1 intensity (Figure 18, M). This shows a positive correlation between the expression intensity of Egr1 and the percentage of big spines in the MML. Contrary to this, in the cell group of ABGCs with more than 70 % Egr1 expression intensity a smaller percentage of big spines was observed in the OML as well as in the IML (Figure 18, L+N). From these findings, a negative correlation between Egr1 expression and the percentage of big spines can be deduced for the OML and IML indicating a concomitant heterosynaptic structural plasticity in these layers. ABGCs at 28 and 35 dpi were merged for this analysis because, when using the 70 % threshold, both pop-

ulations showed an almost identical cell distribution (Figure 16, G). Taken together, the results strongly indicate a link between structural homo- and heterosynaptic plasticity and Egr1 expression.

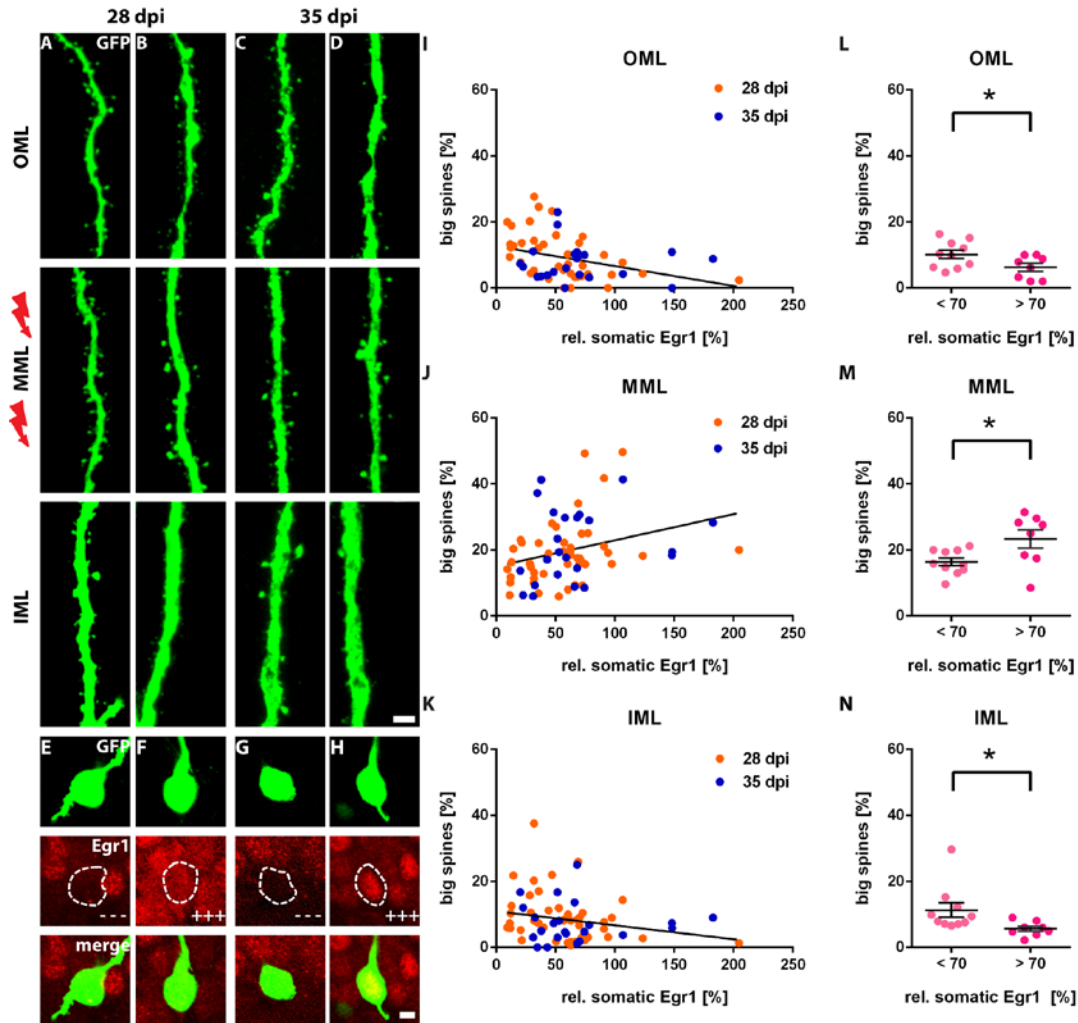


Figure 18: Correlation of Egr1 expression and dendritic spine size: Dendrite samples for IML, MML and OML from ABGCs at 28 dpi with weak (A, E) and strong (B, F) Egr1 expression. Dendrite samples from OML, MML and IML from ABGCs at 35 dpi with weak (C, G) and strong (D, H) Egr1 expression. The dot plots show the percentage of big spines in relation to the relative somatic Egr1 intensity in the OML (I), MML (J) and IML (K). 100 % equal the average Egr1 intensity of all mGCs. Each dot represents the averaged dendritic segments of one GC. Only GCs of the stimulated side are included. Regression analysis reveals: OML:  $R^2 = 0.12$ , MML:  $R^2 = 0.09$ , IML:  $R^2 = 0.05$ . The dot plots show the percentage of big spines from ABGCs at 28 and 35 dpi with



more or less than 70 % Egr1 intensity in the OML (L), MML (M) and IML (N). Each dot represents the average of one animal. Asterisks indicate significant difference. Wilcoxon test, \* $P < 0.05$ . Animal number: (28 dpi)  $n = 6$ , (35 dpi)  $n = 5$ . Scale bar (A - D) = 2  $\mu\text{m}$ , (E-H) = 5  $\mu\text{m}$ . IML = inner molecular layer, MML = middle molecular layer, OML = outer molecular layer, GCL = granule cell layer, lightning bolt indicates layer specific stimulation.

A correlation between nuclear Egr1 expression intensity and structural plasticity was found in ABGCs at 28 and 35 dpi. The strength of homo- and heterosynaptic structural plasticity in Egr1 positive cells was further investigated: A ratio of big spines between the MML and IML as well as the MML and OML was calculated for ABGC groups with more or less than 70 % nuclear Egr1 expression (Figure 19, A - B). This analysis was made with the merged data from ABGCs at 28 and 35 dpi, since it was previously shown, that the cell distribution at this threshold was near identical for both time points (Figure 16, G). Interestingly, the ratio of big spines between MML and IML was significantly higher in ABGCs with more than 70 % Egr1 intensity (Figure 19, A). This effect could also be seen for a comparison of MML and OML: ABGCs expressing more than 70 % nuclear Egr1 intensity appeared to have a significantly higher ratio of big spines than those with less than 70 % Egr intensity (Figure 19, B). This phenomenon is depicted in a schematic (Figure 19, C). On the left, an ABGC is shown with a typical distribution of small and large mushroom spines along the dendritic tree throughout the molecular layer. The nucleus is outlined, showing only a very low level of endogenous Egr1 expression before HFS<sup>48</sup>. On the right, two ABGCs after HFS are shown. The middle one expresses weak nuclear Egr1 intensity, the right one expresses strong nuclear Egr1 intensity. Spines that undergo change due to stimulation are highlighted in green. HFS applied to the medial perforant path and thus to the middle molecular layer is indicated with lightning bolts. In the GC with weak nuclear Egr1, the increase in spine size in the MML is not as pronounced as in the GC with strong Egr1 expression. Likewise, the decrease in spine size in the IML and OML is more distinct in the GC with strong nuclear Egr1. In conclusion, homosynaptic structural plasticity, indicated by an increase of big spines in the MML following HFS, positively correlated with nuclear Egr1 expression intensity. Heterosynaptic structural plasticity was apparent through a decrease in big

spines in the IML and OML. It showed a negative correlation to nuclear Egr1 expression intensity.

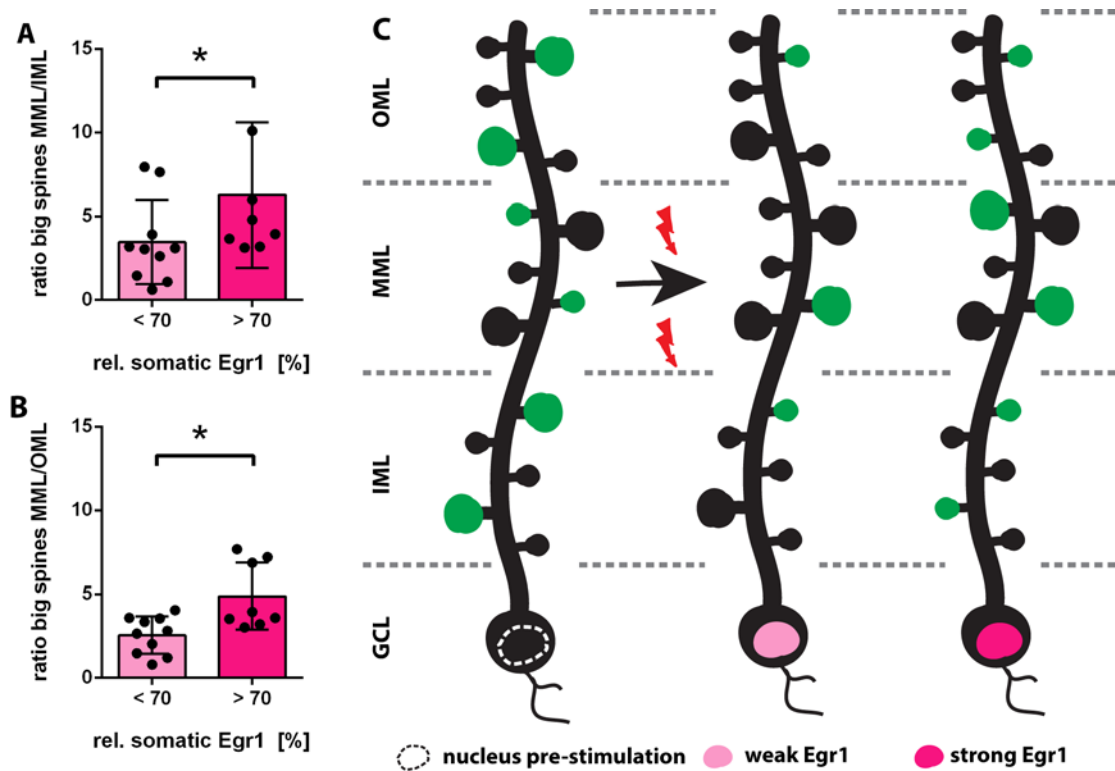


*Figure 19: Egr1 expression is linked to homo- and heterosynaptic structural plasticity: The ratio of big spines between the MML and IML (A), and between MML and OML (B) is shown from ABGCs of 28 and 35 dpi following HFS, separated in weak Egr1 positive (< 70 %) and strong Egr1 positive (> 70 %) cells. Each dot represents the average of one animal. Asterisks indicate significant difference. Mann-Whitney Test, \* $P < 0.05$ . Animal number: (28 dpi)  $n = 6$ , (35 dpi)  $n = 5$ . The schematic shows an unstimulated GC on the left and the change in GCs with weak (middle) or strong (right) nuclear Egr1 expression after stimulation (C). Spines that change after stimulation are highlighted green. Nuclear Egr1 expression intensity is marked in shades of pink. IML= inner molecular layer, MML= middle molecular layer, OML = outer molecular layer, GCL = granule cell layer, lightning bolt indicates layer specific stimulation.*

## **9 Discussion**

### **9.1 XdU project**

#### **9.1.1 Early retirement vs. ongoing function in maturing granule cells**

In this study, we aimed at analysing, to what degree maturing and matured ABGCs are functionally active and exhibit synaptic plasticity in mature rats. In the past, many studies focused on the fate of ABGCs during adolescence and early adulthood. However, the question whether or not ABGCs retire once their maturation is completed or which tasks the matured ABGCs maintain cannot be answered only by studying their immediate future during animal adolescence. In this study, three populations of ABGCs born and labelled with CldU and IdU 6, 12 and 35 weeks prior to death of 10 month old rats were examined. The animals were subjected to intracranial high frequency stimulation (HFS) to induce LTP in GCs of the hippocampus. After 48 h rest they were exposed to 5 min of novel environment. One hour later they were perfused. The expression of the IEG *Egr1* was analysed for the ABGCs of various cell ages and compared to that of mature GCs. It was found that although the stimulation was only applied on one side, a resulting increase of *Egr1* in ABGCs occurred in both hemispheres. It could be shown that this enhanced excitability is not an innate feature of all ABGCs but was in fact due to previous stimulation. Furthermore, the unilateral stimulation caused a heightened excitability of all considered groups of ABGCs to the same degree, independent of brain side and age. Lastly, the infrapyramidal ABGCs appeared to express an increased *Egr1* expression compared to the suprapyramidal ones. These results reveal a general high excitability of young and matured ABGCs in the mature rat. They are in contrast to the concept that mature ABGCs retire in the adult dentate gyrus as suggested by Alme and colleagues<sup>216</sup>. The prevailing state of knowledge about the fate of newborn GCs includes an extensive set of information about the earlier stages but less about the later phase of GC development. After about 4 - 6 weeks of maturation an ABGC has

reached a functional state of structural differentiation and integration<sup>48,184,217</sup>. In contrast to mature GCs, ABGCs exhibit a lower induction threshold and increased LTP amplitude<sup>47</sup>. This critical phase of high intrinsic excitability makes ABGCs susceptible to a preferential recruitment for memory tasks as well as to impart experience-induced plasticity<sup>47,96,196</sup>. This enhanced excitability declines in the following weeks until the ABGC can no longer be distinguished from prenatally born GCs<sup>184,218,219</sup>. Alme and colleagues even proposed an “early retirement” of mature GCs. In their study, two theories were hypothesised: If GCs were selectively tuned to an event (for example exposure to environment A), occurring within its critical phase, it would respond during the recall of this event and therefore exhibit activity (during re-exposure to environment A for example). On the other hand, if a GC were to retire early, it would not necessarily be reactivated whilst visiting an environment that was explored during its critical phase. As a result, rats were trained in 4 different or one single environment over the course of several weeks and then retested with exposure to either 4 different or only one environment on a single day. It appeared that exposure to multiple environments during testing but not during training significantly increased Arc expression. The conclusion to their experiment was that Alme and co-workers argued for an early retirement of GCs<sup>216</sup>. The observation in consequence to the Alme study that, if all mature GC retire, they would be “out of a job”<sup>220</sup> leads to the question how such a system, in which more than 90 % of all GCs are inactive<sup>216</sup>, could be so ubiquitous<sup>221</sup>? According to the earliest evolutionary studies, organisms only prevail, if their phenotype is superior to that of their competitors<sup>222</sup>. The energy necessary for the production and maintenance of thousands of mature but retired GCs could well have been spent elsewhere<sup>223</sup>. As a result, it cannot be probable that this vast population of mature GCs is without function. In accordance with this, several studies have found specific functionalities of mature GCs. It could be shown that old GCs are necessary for pattern completion. A mouse model, where the output of mature GCs was inhibited, rapid pattern completion was defected while pattern separation was intact as long as young GCs were functioning normally<sup>84</sup>. In computational models, mature GCs functioned as discriminators of specific information while young GCs, with a high excitability, received a wide range of input in an unspecific manner<sup>224</sup>. A contribution to hippocampus dependent memory encoding was discussed for mature GCs, proposing that mature GCs carry the engram of experiences dating fur-

ther back. This would allow the network to use certain sets of mature GCs to process new experiences in established contexts<sup>225,226</sup>. This stands in line with the hypothesis that mature GCs are more receptive to memories acquired during their immature state, because of a steadier connective network<sup>227</sup>. In a more recent study, mice were subjected to contextual fear conditioning. GCs that were active during this task were labelled with a fluorescence marker and channelrhodopsin. A fear response was later observed, when these cells were activated with light. Furthermore, it was shown that the tagged cells express electrophysiological features of mature GCs<sup>228</sup>. This finding strongly indicates that mature GCs participate in behaviour processes. In order to clarify the functional role of adult-generated GCs over time, three populations of ABGCs aged 6, 12 and 35 weeks, were studied in this thesis work. ABGCs aged 6 weeks stand at the end of the critical period<sup>47</sup>. In accordance with prior findings that ABGCs aged 4 - 6 weeks are more excitable<sup>47,96,196</sup>, the population of ABGCs that was XdU labelled 6 weeks ptd expressed heightened excitability after HFS. A general boost in activity by novel environment proved enough to enhance this population's activity after LTP induction. The other two ABGC populations of 12 and 35 weeks of age had proceeded further into maturity<sup>47</sup>. Interestingly, it could be shown that they reacted similarly to the youngest ABGC population. In conclusion, our results do not suggest a retirement of maturing ABGCs but indicate that ABGCs are functionally active and exhibit synaptic plasticity at least for 35 weeks of cell age in mature animals.

### **9.1.2 Excitability of adult born granule cells over time**

By using three ABGC populations of differing cell age, the development of excitability during their maturation can be studied. In this thesis, ABGCs were labelled 6, 12 and 35 weeks ptd in rats (Figure 3). After stimulation and novel environment (see chapter 7.1), the rats were perfused and brain tissue was immunohistochemically analysed for Egr1 expression. The measured Egr1 level was similar in all three ABGC populations. It appeared significantly higher than Egr1 intensity of unlabelled i.e. perinatally born GCs (Figure 10, A - D). As Egr1 intensity is a measure for synaptic activity and plasticity, these results indicate that ABGCs exhibit an enhanced phase of excitability and plasticity for a prolonged time period between 6 and 35 weeks of cell age. In order to address

the change in excitability of an ABGC contingent on its age, it is necessary to observe maturing ABGCs closely over time. A well-established method for assessing excitability is by staining IEGs, such as Egr1, Arc or Fos<sup>218,229</sup>. It is indispensable to know the expression pattern of these markers since it is dependent on cell age and phenotype as well as animal race and strain<sup>123,218</sup>. Even at very early stages of development, a small percentage of newborn GCs that are not yet fully integrated, express Egr1. This could indicate an endogenous expression pattern, which is independent of external stimulation<sup>48</sup>. A GCs capacity for physiological excitability starts when its synaptic integration is sufficiently complete. It has been shown that at least 3 weeks are necessary for the completion of this process<sup>48</sup>. From then on, GCs can be recruited to behaviourally relevant networks<sup>201</sup>. During the subsequent 4 - 6 weeks, enhanced excitability in ABGCs with a lower induction threshold of LTP has been described<sup>47</sup>. In a study where 2 month old mice were injected with BrdU and trained in the Morris water maze 1, 2, 4, 6 or 8 weeks later<sup>96</sup>. Spatial memory was tested 10 weeks after BrdU injection and the activation of ABGC was analysed via Fos and Arc expression patterns. 1 and 2 week old ABGCs expressed only a very low degree of IEG. This indicated insufficient integration for active participation in excitability. 4 week old ABGCs appeared to express similar amounts of Fos as mature GCs. This result was interpreted as the beginning of adequate integration and thus activity. Interestingly, a heightened excitability was documented for 6 - 8 week old ABGCs as their expression of the IEG was twice as large as mature GCs. Kee and colleagues argued that this proved a preferential recruitment of ABGCs during this time span<sup>96</sup>. In a follow up study the same group found a rather differing conclusion in contrast to these results. In this case, 2 month old mice received the same BrdU labelling but were now trained in the water maze 1, 5, 7.5 and 10 weeks later. The insufficient maturation of the youngest ABGCs was confirmed by limited Fos expression. Differing to prior results, no peak in recruitment was found in 5 - 10 week old ABGCs but a steady state of integration to spatial memory<sup>214</sup>. Furthermore, it was shown that it made no difference whether GCs were embryonically, postnatally or adult-generated, the likelihood to be recruited for spatial or contextual fear memory was similar<sup>214</sup>. In our study, HFS elicited equal amounts of Egr1 expression in 6, 12 and 35 week old ABGCs. In corroboration with the above mentioned results, no preferential activation of younger ABGCs could be observed. Although it must be kept in mind that the

abovementioned spatial memory studies<sup>96,230</sup> were performed on mice, whereas rats were used in my study. In this thesis work, ABGCs analysed 6, 12 and 35 weeks after XdU injection expressed similarly elevated levels of Egr1. When considering reports comparing mice and rats, a greater Egr1 expression following seizures and water maze training is to be especially expected at 3 weeks of GC age<sup>123</sup>. This would lead to an overestimation of excitation in the rat. In this case, however, older populations are compared. Further support for age independent recruitment was recently demonstrated: In a study using CldU and IdU injections to label 6 and 12 week old ABGCs, memory acquisition and retrieval was tested in rats with the Morris water maze. It was demonstrated that both younger and older ABGCs are activated in spatial memory processes<sup>231</sup>. These findings correspond directly to the equivalent excitation, assessed by Egr1 expression, elicited in the 6 and 12 week old ABGCs in my study. It can be concluded that ABGCs appear more excitable than perinatally born mature GCs and that ABGCs retain their enhanced excitability up to 35 weeks.

### **9.1.3 Influence of experience/stimulation on excitability reactivation**

The analysis on excitability in differently aged ABGCs after HFS performed in this study is part of a larger cooperative study about “Age dependent stability versus plasticity of adult-born granule cell excitability” by the group of Prof. Wickliffe Abraham in New Zealand<sup>209</sup> and the laboratory at the Frankfurt University. In the beginning, four populations of 4, 6, 12 and 35 week old ABGCs were labelled with CldU and IdU in 10 month old rats. They were subjected to 5 minutes of novel environment. After resting for one hour, the animals were perfused and Egr1 expression was analysed. As expected, the youngest ABGCs showed a high level of Egr1 expression. This was in accordance with prior studies<sup>47,96</sup>. Egr1 expression decreased incrementally in the 6 and 12 week old ABGCs. Fascinatingly, the 35 week old ABGCs expressed Egr1 at a similar level as the 4 week old ABGCs. Analogue experiments with 5 and 15 month old rats confirmed that this elevated excitability, observed in the 35 week old ABGCs, was due to the fact that the GCs were born when the animal was 2 months old. Thus, GCs born in a rat’s adolescence are unique as they express enhanced excitability throughout the

ensuing months<sup>209</sup>. Apart from this privileged population, the Egr1 expression of ABGCs appears to decline after the peak observed during the critical phase<sup>47,123</sup>. This trend was also documented in the experiments by Ohline et al described above<sup>209</sup>. Building on these observations, the experiments were repeated, with the exception that each animal was exposed to enriched environment for 10 consecutive nights and 5 minutes of novel environment prior to its death. It was demonstrated that resulting from this additional stimulation, the 4 week old ABGCs expressed even higher levels of Egr1. The Egr1 expression of the 6 and 12 week old ABGCs was raised to the same level as that of the 35 week old ABGCs, which did not increase further. Thus, the excitability levels of the 6 - 35 week old ABGCs became similar<sup>209</sup>. The rats analysed by me were treated in the same fashion as in the previous experiments but received HFS instead of enriched environment. The 4 week old population was omitted because the time point of labelling coincided with the surgery for stimulation electrode implantation. This could have affected this population in a confounding way. The effect of HFS on the 6 - 35 week old ABGCs was similar to that of enriched environment: A heightened but equivalent expression level of Egr1 could be observed in every ABGC population (Figure 12). The resulting enhanced excitability, due to exposure to enriched environment as well as to HFS, indicates that ABGCs can regain increased levels of activity even in mature stages of development. This increase is brought about by behavioural experience like exploration of enriched environment or physiological-like stimulation through HFS<sup>209</sup>. The results discussed here complement previous findings in a compatible study: rats were trained in the water maze for 8 or 16 weeks after BrdU injection and then perfused. Analysing the dendritic arbour of the labelled ABGCs revealed that spatial learning enhanced its complexity and increased spine number in both ABGCs populations<sup>232</sup>. This shows that maturing ABGCs retain the property for structural plasticity and that this process was activated by spatial learning<sup>209</sup>. Interestingly, in a behavioural study with rats, Penner et al found that adult (9 - 12 months) and aged rats (24 - 32 months) both had equivalent levels of Egr1 mRNA in the dentate gyrus. After exploratory behaviour, however, the increase in Egr1 mRNA in the DG of aged rats was significantly less than in adult rats<sup>233</sup>. This confirms that experience can rescue GCs from relative quiescence even at a very advanced age whilst simultaneously indicating that the degree of reactivation might become diminished in the senium of a rat.



#### **9.1.4 Bilateral excitation by unilateral stimulation**

The intracranial stimulation of the medial perforant path was only performed in one hemisphere. LTP induction was confirmed on the ipsilateral side immediately after HFS. Observation of the contralateral side by colleagues in New Zealand did not reveal LTP induction at this time point. Nevertheless, the expression of *Egr1* in ABGCs had increased in the hippocampus of both hemispheres (Figure 9). Similar stimulation protocols had not been reported to lead to contralateral LTP induction in prior experiments<sup>210</sup>. Microstimulation under fMRI surveillance had shown evidence for interhemispheric communication<sup>234</sup>. An extensive fMRI study provided further information on bilateral effects of unilateral LTP induction<sup>235</sup>. Sprague-Dawley rats were stimulated in the medial perforant path, albeit with a different stimulation protocol from the one used in my data, and analysed for subfield recruitment in the MRI. A bilateral activation could be observed and this was interpreted to be a result of augmented interhemispheric coupling via the mossy cell commissural pathway<sup>235</sup>. Experiments using HFS on one DG had yielded the result that *Egr1* expression directly after stimulation was only ipsilaterally increased<sup>149,150</sup>. This result was later reproduced by Bramham et al. In the same study it could be shown that after unilateral LTP induction, neurotrophins and *trk* (Tyrosine kinase) receptor mRNA were expressed equivalently in both sides<sup>236</sup>. Considering the analysis time difference (i.e. directly versus 6 - 35 weeks after LTP induction), these results do not contradict each other, but rather, could signify a diverging time course of *Egr1* expression in the two hemispheres. Given the strong functional connectivity between the hippocampi of both hemispheres (see Introduction), an affection of both hemispheres by unilateral HFS seems likely.

#### **9.1.5 Differences in *Egr1* expression between infra- and suprapyramidal blade**

In this study, 6 and 12 week old ABGCs of the infrapyramidal blade exhibited a higher *Egr1* expression compared to those of the suprapyramidal blade (Figure 14). The hippocampal formation arches through the brain starting from the median basis of the forebrain and ending close to the amygdala in the temporal lobe. In order to describe the

location of a GC in this C-shaped structure, two axes are used: The dorsoventral or septotemporal axis where the ventral, temporal pole is the one close to the amygdala. The transverse axis is perpendicular to the first one and describes the continuum of suprapyramidal-to-infrapyramidal-blade of the DG<sup>29,237</sup>. During the development of the DG, the settlement of GCs starts at the lateral end of the suprapyramidal blade. The infrapyramidal blade is established in the ensuing time<sup>238-240</sup>. The structure and connectivity differs between dorsal and ventral hippocampus. Among many other distinctions, the dorsal DG receives projections from the lateral and medial entorhinal cortex, the ventral DG is reached only by afferents from the medial entorhinal cortex<sup>241,242</sup>. The function of the DG is not homogenous along the dorsoventral axis. Early lesion studies have shown that the dorsal hippocampus is tasked with spatial learning and memory while the ventral hippocampus is crucial for anxiety-related and affective behaviour<sup>243-245</sup>. Unsurprisingly, several differences between the supra- and the infrapyramidal blade of the DG can be found. The projections from the entorhinal cortex also seem to distinguish between supra- and infrapyramidal blade as the suprapyramidal blade is preferentially reached by afferents from the lateral EC, and the infrapyramidal blade is rather projected to by the medial EC<sup>246,247</sup>. More GABAergic neurons were found in the suprapyramidal blade than in the infrapyramidal blade<sup>248</sup>. Electrophysiological experiments revealed that, compared to the suprapyramidal blade, the infrapyramidal blade generated a larger population spike whereas paired-pulse inhibition was weaker following perforant path stimulation<sup>249</sup>. Furthermore, Ambrogini et al. described more 2 week old BrdU labelled GCs supra- than infrapyramidally in Sprague Dawley rats<sup>250</sup>. In line with this, a higher percentage of DCX positive GCs in the suprapyramidal blade of the dorsal DG were found than in the remaining DG. In addition to this result, the infrapyramidal blade of the ventral DG appeared to show the lowest level of radial glia-like progenitor cells<sup>251</sup>. Interestingly, Snyder et al. observed more 4 week old BrdU labelled GCs in the infrapyramidal blade of Long Evans rats than in the suprapyramidal blade<sup>123</sup>. In a subsequent study of 13 month old rats, neurogenesis was found to be evenly distributed throughout the DG<sup>252</sup>. Scrutinising the distribution of 6 week old BrdU labelled GCs, Tashiro and colleagues found that exposure to enriched environment influenced GCs proliferation in the same degree along the septotemporal and transversal axis<sup>253</sup>. In this study a higher Egr1 expression of 6 and 12 week old ABGCs of the infrapyramidal blade compared to

those of the suprapyramidal blade was discovered. The Egr1 expression of the latter was at the same level as the unlabelled i.e. “mature” GCs. The 35 week old ABGCs showed similar Egr1 expression in both blades at a significantly higher level than the unlabelled GCs. The Egr1 expression of the unlabelled GCs was similar to that of unlabelled and labelled GCs in control animals (Figure 14). These results can be brought into beneficial context with findings from Schmidt et al<sup>36</sup>. Rats were trained in spatial navigation tasks and Egr1 expression was measured in GCs of the supra- and infrapyramidal blade. It was shown that Egr1 expression increased in the suprapyramidal blade with each increment of activity<sup>36</sup>. Interestingly, Egr1 and Arc expression remained at the same intermediate level in the infrapyramidal blade regardless of whether the animal stayed in the home cage or experienced a new environment<sup>36,254–257</sup>. Although Schmidt et al found more Egr1 in the suprapyramidal blade during spatial exploration; this is not in contrast to the results of greater Egr1 expression in the infrapyramidal blade after HFS outlined in this thesis. Since, according to Schmidt et al, the balance of Egr1 expression between supra and infra depends on the state of activation, it is possible that in the study outlined here, the constant level of Egr1 expression in the infrapyramidal blade preponderated, whilst in Schmidt’s case the activation induced an overweight of suprapyramidal Egr1 expression. Further studies will have to elaborate, in which way the balance of Egr1 expression is set by each stimulation protocol and behavioural experience. The observation that the suprapyramidal blade is more flexible in Egr1 expression, could mark a tendency of increased pattern separation in the suprapyramidal blade<sup>36</sup>.

### **9.1.6 Omission of cross reaction in single stainings**

The Thymidine analogues IdU and CldU were injected in amounts equivalent to the application of 50 mg/kg BrdU for the 35 week old ABGC and 200mg/kg BrdU for the 6 and 12 week old ABGCs. The amount which labels the maximum number of cells is 300 mg/kg<sup>258</sup>. According to previous studies, amounts equivalent to the latter cause a cross reaction between the used antibodies from BD Bioscience (mouse-anti-IdU, 347580) and Accurate (rat-anti-CldU, OBT 0030)<sup>156</sup>. In lower doses IdU and CldU have been reported not to cause any cross reaction in antibodies used for their visualisation<sup>259,260</sup>. The doses used in this experiment were closer to those used by Vega

& Petersen than to those of Cameron & McKay<sup>258,259</sup>. The very small percentage of cross reaction can therefore be tolerated. The more extensive cross reaction observed using the secondary AB Alexa Fluor goat-anti-mouse 488 and 568 in IdU/CldU co-stainings proved to be intolerable. The problem was solved by reverting to stainings where either IdU or CldU were analysed with Egr1 and NeuN, which meant the cross reaction of secondary AB could be omitted. The cross reaction of secondary AB has also been documented by other researchers who avoided this in a similar way<sup>261</sup>. IdU as well as CldU label fewer cells than BrdU, furthermore they are less soluble than BrdU and therefore require larger injection volumes. The potentially harmful effect of Thymidine analogues is more probable in greater quantities when the abovementioned cross reaction occurs. Large injection volumes have been shown to be stressful for the animal and therefore proven derogatory for studying adult neurogenesis<sup>116</sup>. Smaller doses in smaller volumes were used as a result (200 mg/kg in 20 mg/ml and 50 mg/kg in 50 mg/ml).

## 9.2 Spine project

In the second part of my thesis work, the plasticity of spine morphology was analysed. This project, called “spine project” was part of a larger study from Dr. Tassilo Jungenitz published in early 2018<sup>215</sup>. Rats were transfected with a GFP-expressing murine leukaemia retrovirus (RV-GFP) to label ABGC. 28 or 35 days afterwards, the animals were subjected to intrahippocampal high frequency stimulation and consecutively to transcardial perfusion. In my thesis work, I performed immunohistological stainings for Egr1 with an additional antibody against GFP to strengthen the signal. Egr1 expression intensity was measured in the same way as for the XdU labelled GCs (see chapter 6.4). The dendritic tree of GFP labelled GCs was analysed for mushroom spines by imaging dendritic segments from the inner-, middle- and outer molecular layer (IML, MML and OML) of the stimulated side in high resolution. Consecutively, a differentiation of mushroom spine size was made between small spines of  $< 0.2 \mu\text{m}^2$  and big spines of  $> 0.2 \mu\text{m}^2$  using a grid based approach. Layer specific differences in spine size and structural plasticity as well as possible correlations to stimulation induced Egr1 expression intensity were studied.

### 9.2.1 Age dependent functional integration of maturing adult born granule cells

The expression of *Egr1* together with numerous other IEGs such as *c-fos* and *Jun-B* has been shown to play a vital part in the maintenance of the late phase of LTP<sup>262–265</sup>. In this study, the IEG *Egr1* was chosen as a marker for activation following HFS. It has been established, that HFS protocols such as the one used in this study (see chapter 7.2.3) are capable of inducing LTP and as a result stimulate the expression of IEGs in the vast majority of GCs<sup>48,211</sup>. On the ipsilateral hemisphere, ABGCs at 28 and 35 dpi as well as mature GCs were analysed for stimulation induced *Egr1* expression intensity. The *Egr1* intensity of the mature GCs was significantly higher than that of the ABGCs. Viewing the average *Egr1* intensity of 50 % of each age grouped GC population, the ABGCs at 28 dpi expressed a relative *Egr1* intensity of 20 % which increased to approximately 40 % for the ABGC at 35 dpi. 50 % of the mature GC expressed an *Egr1* expression intensity of 90 % (Figure 16, E). 100 % relative *Egr1* expression intensity equals the average *Egr1* intensity of all mGCs. This age dependent increase of HFS induced IEG expression has also been observed in previous experiments where the IEGs *c-fos* and *Arc* were used in complement to *Egr1*<sup>48</sup>. In addition to 28 and 35 day old ABGC, further age groups at 21, 49, 63 and 77 dpi were analysed. An augmenting expression of *c-fos*, *Arc* and *Egr1* from 21 to 77 dpi in response to HFS was observed<sup>48</sup>. Since the methods implemented were identical to those of this study, the results are of great compatibility. Taken together, these results reflect the increasing functional integration of maturing GCs which corroborates with earlier results that new born GCs integrate slowly into the existing network<sup>266</sup>. Comparing the induced *Egr1* intensity of the ABGCs to that of mature GCs, a significantly higher expression intensity could be observed for the mature GCs (28 dpi:  $p = 0.0001$  and 35dpi:  $p = 0.0114$ , Figure 16, H). The same abundance of IEG expression following HFS was observed for *c-fos*, *Egr1* and *Arc* in a previous study, although IEG expression intensity in ABGC increased with maturation, it never reached the same level as that of perinatally born GC<sup>48</sup>.

## 9.2.2 Homo- and heterosynaptic spine plasticity in adult born granule cells following HFS

Homosynaptic plasticity describes an input-specific potentiation of synapses that received direct activation. In contrast, the weakening of synapses that were not stimulated during homosynaptic potentiation is coined heterosynaptic plasticity<sup>1</sup>. It has been demonstrated, that spine size and its synaptic capacity are positively correlated<sup>267</sup>. Furthermore it could be shown that increasing spine size is concomitant with LTP induction<sup>169</sup>. Spine shrinkage on the other hand, was shown to be associated with the induction of LTD<sup>268,269</sup>. In this study, dendritic segments from ABGC at 28 and 35 dpi were imaged within the IML, MML and OML of the DG. Analysis of mushroom spine size revealed a significantly higher percentage of big spines ( $> 0.2 \mu\text{m}^2$ ) in the stimulated MML than in the non-stimulated OML and IML (Figure 17, C+D), concurrent with the occurrence of homo- and heterosynaptic plasticity. Spine size changes were only observed for ABGCs of the ipsilateral (stimulated) hemisphere. Ipsilateral spine size changes can be compared to matching data from ABGCs of the contralateral hemisphere and to that from mature GCs gathered by Jungenitz and colleagues<sup>215</sup>. In the study of Jungenitz and colleagues<sup>215</sup>, a significant increase of big spines was found in the MML from 28 dpi on, and a significant decrease of big spines in the OML was shown starting at 35 dpi. A corresponding decreasing tendency in big spines could be shown in the IML at 35 dpi. These results clearly corroborate the findings made here (Figure 17, C+D). Small spines ( $< 0.2 \mu\text{m}^2$ ) were analysed as well. At 28 dpi a significant decrease of small spines in the MML of the ipsilateral side was found as well as a similar tendency at 35 dpi. Importantly, the overall spine density in each sublayer of the molecular layer, although increasing with maturation from 21 to 77 dpi, did not change after HFS<sup>215</sup>. This allows the conclusion, that it was indeed spine shrinkage and enlargement and not de novo formation that caused the structural changes<sup>215</sup>. Nevertheless, it cannot be determined whether either or both mechanisms are more relevant in structural plasticity following LTP induction<sup>270,271</sup>. The observed effect of spine enlargement in the MML reflects the homosynaptic potentiation of spines as a reaction to 2 h HFS of the MPP. The spine shrinkage that was found in the OML and possibly the IML corresponds to heterosynaptic depression as was described earlier by Abraham and col-

leagues<sup>1,269,272</sup>. Further evidence for homosynaptic potentiation has been presented through the analysis of F-actin. F-actin is a part of the cytoskeleton and has been shown to locally polymerize after LTP and depolymerize following LTD<sup>169,273</sup>. A layer specific stimulation-induced accumulation in the MML has been shown for F-actin, marking homosynaptic spine potentiation<sup>215,274</sup>. A decrease of F-actin in IML and OML has equally been portrayed, proposing a participation of F-actin in heterosynaptic plasticity<sup>215</sup>. Considering the observation that homosynaptic spine enlargement takes place in the MML and heterosynaptic spine shrinkage occurs in OML and possibly IML (Figure 17, C+D), whilst overall spine density remains stable<sup>215</sup>, it can be proposed that both phenomena form a balance. This corroborates previous suggestions, that heterosynaptic plasticity functions as a counter mechanism to homosynaptic potentiation in order to maintain homeostasis in the process of synaptic plasticity<sup>275</sup>

### **9.2.3 Homo- and heterosynaptic spine plasticity correlates with Egr1 expression intensity**

Mushroom spine size was analysed in a layer specific manner for individual GCs. The percentage of big spines of each GC was determined for each section of the molecular layer (Figure 18, I - K). Since spine analysis was performed in a cell specific way, the individual values could be correlated with somatic Egr1 expression intensity. An increased percentage of big spines was observed for ABGCs at 28 and 35 dpi following HFS in the MML. This finding indicates homosynaptic structural plasticity in the MML. A positive correlation between spine size and Egr1 expression intensity could be shown ( $R^2 = 0.09$ ) (Figure 18, J). In contrast, a lower percentage of big spines was found in the IML and OML, representing heterosynaptic structural depression. Accordingly, a negative correlation between spine size and Egr1 intensity arose with a respective  $R^2$  of 0.12 for OML and 0.05 for IML (Figure 18, I+K). Thereafter, the percentage of big spines was assessed in ABGCs at 28 and 35 dpi with more or less than 70 % nuclear Egr1 expression intensity (Figure 18, L-N). 70 % Egr1 intensity had been established as a threshold value (Figure 16, G). The majority of ABGCs at 28 and 35 dpi expressed less than 70 % while the majority of mGCs expressed more than 70 % Egr1 intensity. The distribution ABGCs below or above this threshold was nearly identical at 28 and 35 dpi.

Therefore, both time points were merged for the analysis of big spine percentages in GCs with more or less than 70 % Egr1 intensity: In the MML a significantly higher percentage of big spines was observed in ABGCs with > 70 % nuclear Egr1 expression intensity (Figure 18, M). In the IML and OML, a significantly smaller percentage of big spines was found in ABGCs with > 70 % Egr1 intensity (Figure 18, L+N). These results indicate a close link between nuclear Egr1 expression and homo-, as well as concomitant heterosynaptic structural plasticity. In order to further elaborate these findings, the ratio of big spines in ABGCs with more or less than 70 % nuclear Egr1 intensity was calculated for the MML and IML as well as for MML and OML (Figure 19, A+B). The effect of homosynaptic spine enlargement with collateral heterosynaptic spine shrinkage was found to be significantly stronger in ABGCs with > 70 % nuclear Egr1 intensity. The role of Egr1 expression in homo- and heterosynaptic structural plasticity must therefore be considered as highly influential. As to the causality of the link between nuclear Egr1 expression intensity and the strength of structural plasticity, previous studies can be cited: It has repeatedly been shown that Egr1 is indispensable for the maintenance of the late phase of LTP<sup>149,150</sup>. Furthermore it was found that increased expression of Egr1 by gain of function mutation promotes synaptic plasticity in the hippocampus<sup>276</sup>. The examination of Egr1 targets of transcription reveals that a large number of genes, influencing the regulation of synaptic plasticity, are being controlled by Egr1. These targets include genes associated with the actin cytoskeleton like Arc as well as neurotransmitter release and transport of vesicles<sup>277,278</sup>. Additionally, the transcriptional program of Egr1 includes genes associated with protein synthesis and degradation<sup>279,280</sup>. Taken together, the role of Egr1 in synaptic organisation takes place at several levels<sup>281</sup>. Our findings provide novel evidence that nuclear Egr1 expression intensity can be correlated with homo- and concomitant heterosynaptic structural plasticity. By partaking in the regulation of synaptic stabilisation, Egr1 supplies the prerequisites for a reliable correlation with synaptic strength.



## 10 Conclusion, clinical relevance and outlook

This work investigates the age dependence of ABGC excitability by the use of the IEG Egr1 as a immunohistological marker.

It comprises two projects: The XdU project centres on changing excitability in differently aged XdU labelled ABGCs after HFS. It is part of a larger cooperative study about “Age dependent stability versus plasticity of adult-born granule cell excitability” by the group of Prof. Wickliffe Abraham in New Zealand<sup>209</sup> in cooperation with the team of Prof. T. Deller from the Institute of clinical Neuroanatomy at the Goethe-University in Frankfurt.

The Spine project focuses on layer specific homo- and heterosynaptic plasticity of dendritic mushroom spines of GFP labelled AGBCs. It builds on previous results from Dr. T. Jungenitz from the Institute of clinical Neuroanatomy of the Goethe-University in Frankfurt: “Structural homo- and heterosynaptic plasticity in adult newborn rat hippocampal granule cells”<sup>215</sup>.

In the XdU project, ABGCs in rats had been labelled with XdU at 6, 12 and 35 week before DBS of the medial perforant path of the hippocampus in one hemisphere by the group of Prof. Wickliffe Abraham in New Zealand<sup>209</sup>. By measuring nuclear Egr1 expression intensities in ABGCs and mature GCs on fixed brain tissue, their change in excitability was analysed by me. It was found that enhanced Egr1 expression is not an innate feature of ABGCs but occurs following HFS. Interestingly, the unilateral stimulation resulted in a bilateral increase of excitability in ABGCs. Compared to mature GCs, ABGCs of 6, 12 and 35 weeks showed enhanced responsiveness to stimulation. Furthermore, it was shown that the infrapyramidal ABGCs express a higher level of Egr1 intensity up to 12 weeks than the suprapyramidal ones. At 35 weeks, the suprapyramidal reach an equally high level of Egr1 expression. Evaluated together, a rescue of excitability in ABGCs, from a low level of inactivity to a heightened level with enhanced Egr1 expression resulting from HFS of the MPP was shown.

Within the Spine project, ABGCs of 28 and 35 dpi were GFP labelled in rats via retroviral transduction, followed by unilateral HFS that was applied to the MPP of the hip-

pocampus by Dr. T. Jungenitz from the Institute of Clinical Neuroanatomy at the Goethe-University in Frankfurt. The analysis on fixed brain tissue was done by me. Dendritic mushroom spines were analysed for changes in size in a layer specific manner. Nuclear Egr1 was measured and used as a marker for excitability. The Egr1 expression intensity of ABGCs was significantly lower than that of mature GC with a slight increase from 28 to 35 day old ABGCs. It could be shown that large spines ( $> 0.2 \mu\text{m}^2$ ) increased in the MML and decreased in the IML and OML. This result indicated homosynaptic spine enlargement in the MML and heterosynaptic spine shrinkage in IML and OML. Plasticity in spine size correlated with nuclear Egr1 expression intensity. A positive correlation was found in the MML. For the concomitant heterosynaptic spine shrinkage in IML and OML a negative correlation to nuclear Egr1 intensity was found.

ABGCs can be rescued from low excitability to enhanced excitability by LTP induction and exceed the level of excitability of mature GCs at 6, 12 and 35 weeks. This contrasts the hypothesis that mature GCs lose their excitability<sup>216</sup>.

Following HFS, ABGCs of 28 and 35 dpi expressed a layer specific structural homosynaptic LTP and concomitant heterosynaptic LTD. This is in line with the general view that ABGCs in the critical phase of 4 - 6 weeks of age undergo an increasing integration into the pre-existing network while in a state of enhanced plasticity<sup>47,201</sup>. Comparing the results from both projects, it is indispensable to note that the stimulation protocol used in the Spine project induces the maximal possible stimulation intensity. It was chosen to exploit the peak potential of the ABGCs and mGCs. The finding that although ABGCs show strong excitability, they never reach the level of mGCs is in line with previous studies<sup>215</sup>. The stimulation protocol employed in the XdU project in contrast is far milder and reflects an approach based on behavioural stimulation. It was used in order to analyse the subtle differences in cell activation between mature and ABGCs under physiological conditions *in vivo*. ABGCs were found to express an enhanced excitability compared to mGCs resulting in a heightened susceptibility to mild stimulation. This confirms prior findings concerning the critical phase in ABGCs<sup>47,184,201,204</sup>.

For both the XdU labelled and the retrovirally labelled GCs, Egr1 was chosen as a marker for neuronal excitability. Egr1 has proven to be best suited for measuring GC

excitability<sup>48</sup>. Using the method for nuclear Egr1 intensity measurement described in 6.4 in correlation with a detailed spine size analysis, the results concerning homosynaptic plasticity (Figure 18) validate Egr1 as a solid marker for excitability.

Increasing evidence outlines the importance of Egr1 expression levels in neuropsychiatric disorders. Reduced levels of Egr1 and Egr1 mRNA were found in patients suffering major depressive disorders and schizophrenia as well as in a mouse model for depression<sup>158,282,283</sup>. The correct maturation of GC plays a vital role in mental health. A mouse model with an “immature dentate gyrus” exhibiting molecularly and electrophysiologically underdeveloped neurons expressed typical morphological traits as seen in brain tissue from patients suffering from schizophrenia and bipolar disorders<sup>284</sup>. In conclusion it can be said that the dynamics of Egr1 expression in ABGC maturation and their excitability due to different forms of stimulation are of potentially high clinical interest as they may provide important groundwork for the treatments of neuropsychiatric disorders. Future work will be needed to close the gap between fundamental research and clinical therapy.

Although adult hippocampal neurogenesis has been demonstrated to exist in humans, it is still heavily debated to what extent it persists throughout the human life span<sup>285</sup>. After findings from Spalding et. al., presenting evidence for hippocampal neurogenesis in humans throughout life, clinical use was seen in an even more promising light<sup>5</sup>. Interestingly, a re-assessment of the duration and extent of neurogenesis in humans was made very recently<sup>6</sup>. DCX and PSA-NCAM stainings in hippocampal neurons from tissue samples from epileptic surgery and neurologically healthy deceased revealed a sharp decrease of neurogenesis in the human brain in childhood. No neurogenesis could be detected in adults beyond puberty<sup>6</sup>. Contrasting to this, a study on whole hippocampi from cognitively healthy humans aged 14 - 79 revealed a decreasing but persisting adult neurogenesis<sup>7</sup>. These contrary results demand more clarification in the field of adult neurogenesis, especially when considering its role in neurodegenerative diseases as well as learning and memory<sup>44,63,64,68,85,87</sup>

## 11 Acknowledgements

At this point I would like to give thanks to all those people without whom this work would not have come into being.

I would like to thank my supervisor PD Dr. med. Stephan W. Schwarzacher, who lured me from the anatomical dissection course into this great field of research. The scientific conversations always kindled the fascination for neuroscience and provided wonderful support for this thesis.

Also, I want to thank Prof. Dr. med Thomas Deller for providing the opportunity and endorsement to do research in his institute.

I would like to thank Prof. Dr. Wickliffe Abraham from the Department of Psychology, University of Otago, New Zealand for letting me partake in his research as part of the collaboration between our two laboratories. I have enjoyed meeting you and I found our scientific conversations very inspirational. At this point I would like to thank Shane Ohline for providing the XdU labelled brain tissue and much useful information for my thesis.

Furthermore, I would like to thank my colleagues Dr. rer. nat. Tijana Radic, Andreas Strehl, Michael Rietsche, Martina Hütten, Dr. med. Peter Jedlicka, Christos Galanis, Aline Blistein, Sylvia Cienciala, Charlotte Nolte-Uhl, Heike Korff, Nadine Zahn and Anke Biczysko for enduring my countless questions, introducing me to lab work, showing me techniques and helping me with all the everyday problems. I am very grateful to have gotten to know you and to have won dear friends in the process.

I would like to thank my native-speaking godmother Paula Blake-Rath for making the huge effort of correcting this thesis as far as language is concerned.

A big thank you goes to my parents and family for their emotional, financial and motivational support throughout my studies.

Above all, I would like to give the most special thanks to Dr. rer. nat. Tassilo Jun- genitz, for letting me partake in his research and especially his never-ending help with topic, tech, statistics, methods, motivation and absolutely any problem I encountered from the moment I started working in the lab. You are the best part of Neuroscience I met in my life.

## 12 References

1. Abraham WC, Logan B, Wolff A, Benuskova L. “Heterosynaptic” LTD in the dentate gyrus of anesthetized rat requires homosynaptic activity. *J Neurophysiol.* 2007;98(2):1048-1051. doi:10.1152/jn.00250.2007
2. Paton JA, Nottebohm FN. Neurons generated in the adult brain are recruited into functional circuits. *Science.* 1984;225(4666):1046-1048.
3. Nottebohm F. The Road We Travelled: Discovery, Choreography, and Significance of Brain Replaceable Neurons. *Ann N Y Acad Sci.* 2004;1016(1):628-658. doi:10.1196/annals.1298.027
4. Eriksson PS, Perfilieva E, Björk-Eriksson T, et al. Neurogenesis in the adult human hippocampus. *Nat Med.* 1998;4(11):1313-1317. doi:10.1038/3305
5. Spalding KL, Bergmann O, Alkass K, et al. Dynamics of Hippocampal Neurogenesis in Adult Humans. *Cell.* 2013;153(6):1219-1227. doi:10.1016/j.cell.2013.05.002
6. Sorrells SF, Paredes MF, Cebrian-Silla A, et al. Human hippocampal neurogenesis drops sharply in children to undetectable levels in adults. *Nature.* March 2018. doi:10.1038/nature25975
7. Boldrini M, Fulmore CA, Tartt AN, et al. Human Hippocampal Neurogenesis Persists throughout Aging. *Cell Stem Cell.* 2018;22(4):589-599.e5. doi:10.1016/j.stem.2018.03.015
8. Chapouton P, Jagasia R, Bally-Cuif L. Adult neurogenesis in non-mammalian vertebrates. *BioEssays.* 2007;29(8):745-757. doi:10.1002/bies.20615
9. Kornack DR, Rakic P. Continuation of neurogenesis in the hippocampus of the adult macaque monkey. *Proc Natl Acad Sci U S A.* 1999;96(10):5768-5773.
10. Ernst A, Alkass K, Bernard S, et al. Neurogenesis in the striatum of the adult human brain. *Cell.* 2014;156(5):1072-1083. doi:10.1016/j.cell.2014.01.044
11. Gould E. How widespread is adult neurogenesis in mammals? *Nat Rev Neurosci.* 2007;8(6):481-488. doi:10.1038/nrn2147
12. Rakic P. Adult neurogenesis in mammals: an identity crisis. *J Neurosci.* 2002;22(3):614-618.

13. Gurunluoglu R. Giulio Cesare Aranzio (Arantius) (1530-89) in the pageant of anatomy and surgery. *J Med Biogr.* 2011;19(2):63-69.
14. Diemerbroeck I van. *Anatome Corporis Humani: Plurimis Novis Inventis Instructa.*; 1672.
15. Duvernoy H. *The Human Hippocampus ,(3rd Ed.)*. Springer-Verlag; 2005.
16. Amaral DG, Ishizuka N, Claiborne B. Neurons, numbers and the hippocampal network. *Prog Brain Res.* 1990;83:1-11.
17. Bliss T V, Lomo T. Long-lasting potentiation of synaptic transmission in the dentate area of the anaesthetized rabbit following stimulation of the perforant path. *J Physiol.* 1973;232(2):331-356.
18. Andersen P, Morris R, Amaral D, Bliss T, O'Keefe J. *The Hippocampus Book*. (Andersen P, Morris R, Amaral D, Bliss T, O'Keefe J, eds.). Oxford University Press; 2006. doi:10.1093/acprof:oso/9780195100273.001.0001
19. Andersen P. Organization of Hippocampal Neurons and Their Interconnections. In: *The Hippocampus*. Boston, MA: Springer US; 1975:155-175. doi:10.1007/978-1-4684-2976-3\_7
20. Yoganarasimha D, Rao G, Knierim JJ. Lateral entorhinal neurons are not spatially selective in cue-rich environments. *Hippocampus.* 2011;21(12):1363-1374. doi:10.1002/hipo.20839
21. Chao OY, Huston JP, Li J-S, Wang A-L, de Souza Silva MA. The medial prefrontal cortex-lateral entorhinal cortex circuit is essential for episodic-like memory and associative object-recognition. *Hippocampus.* 2016;26(5):633-645. doi:10.1002/hipo.22547
22. Moser EI, Kropff E, Moser M-B. Place cells, grid cells, and the brain's spatial representation system. *Annu Rev Neurosci.* 2008;31:69-89. doi:10.1146/annurev.neuro.31.061307.090723
23. Igarashi KM. The entorhinal map of space. *Brain Res.* 2016;1637:177-187. doi:10.1016/j.brainres.2015.10.041
24. Mody I, Köhr G, Otis TS, Staley KJ. The electrophysiology of dentate gyrus granule cells in whole-cell recordings. *Epilepsy Res Suppl.* 1992;7:159-168.
25. Spruston N, Johnston D. Perforated patch-clamp analysis of the passive membrane properties of three classes of hippocampal neurons. *J Neurophysiol.*

- 1992;67(3):508-529.
26. Staley KJ, Otis TS, Mody I. Membrane properties of dentate gyrus granule cells: comparison of sharp microelectrode and whole-cell recordings. *J Neurophysiol.* 1992;67(5):1346-1358.
  27. Buzsáki G. Memory consolidation during sleep: a neurophysiological perspective. *J Sleep Res.* 1998;7 Suppl 1:17-23.
  28. Sun GJ, Sailor KA, Mahmood QA, et al. Seamless reconstruction of intact adult-born neurons by serial end-block imaging reveals complex axonal guidance and development in the adult hippocampus. *J Neurosci.* 2013;33(28):11400-11411. doi:10.1523/JNEUROSCI.1374-13.2013
  29. Amaral DG, Scharfman HE, Lavenex P. The dentate gyrus: fundamental neuroanatomical organization (dentate gyrus for dummies). *Prog Brain Res.* 2007;163. doi:10.1016/S0079-6123(07)63001-5
  30. Jinde S, Zsiros V, Nakazawa K. Hilar mossy cell circuitry controlling dentate granule cell excitability. *Front Neural Circuits.* 2013;7. doi:10.3389/fncir.2013.00014
  31. Nò L de. *Studies on the Structure of the Cerebral Cortex II. Continuation of the Study of the Ammonic System.* Journal für Psychologie und Neurologie, 46; 1934.
  32. Sun GJ, Sailor KA, Mahmood QA, Chavali N, Christian KM, Song H. Seamless Reconstruction of Intact Adult-Born Neurons by Serial End-Block Imaging Reveals Complex Axonal Guidance and Development in the Adult Hippocampus. 2013;33(28):11400-11411. doi:10.1523/JNEUROSCI.1374-13.2013
  33. van Dijk RM, Huang S-H, Slomianka L, Amrein I. Taxonomic Separation of Hippocampal Networks: Principal Cell Populations and Adult Neurogenesis. *Front Neuroanat.* 2016;10:22. doi:10.3389/fnana.2016.00022
  34. Boss BD, Turlejski K, Stanfield BB, Cowan WM. On the numbers of neurons in fields CA1 and CA3 of the hippocampus of Sprague-Dawley and Wistar rats. *Brain Res.* 1987;406(1-2):280-287.
  35. Mulders WHAM, West MJ, Slomianka L. Neuron numbers in the presubiculum, parasubiculum, and entorhinal area of the rat. *J Comp Neurol.* 1997;385(1):83-94. doi:10.1002/(SICI)1096-9861(19970818)385:1<83::AID-CNE5>3.0.CO;2-8



36. Schmidt B, Marrone DF, Markus EJ. Disambiguating the similar: The dentate gyrus and pattern separation. *Behav Brain Res.* 2012;226(1):56-65. doi:10.1016/j.bbr.2011.08.039
37. Miller JF, Neufang M, Solway A, et al. Neural activity in human hippocampal formation reveals the spatial context of retrieved memories. *Science.* 2013;342(6162):1111-1114. doi:10.1126/science.1244056
38. Bjornsson CS, Apostolopoulou M, Tian Y, Temple S. It takes a village: constructing the neurogenic niche. *Dev Cell.* 2015;32(4):435-446. doi:10.1016/j.devcel.2015.01.010
39. Jin K, Zhu Y, Sun Y, Mao XO, Xie L, Greenberg DA. Vascular endothelial growth factor (VEGF) stimulates neurogenesis in vitro and in vivo. *Proc Natl Acad Sci U S A.* 2002;99(18):11946-11950. doi:10.1073/pnas.182296499
40. Schänzer A, Wachs F-P, Wilhelm D, et al. Direct stimulation of adult neural stem cells in vitro and neurogenesis in vivo by vascular endothelial growth factor. *Brain Pathol.* 2004;14(3):237-248.
41. Seri B, García-Verdugo JM, McEwen BS, Alvarez-Buylla A. Astrocytes give rise to new neurons in the adult mammalian hippocampus. *J Neurosci.* 2001;21(18):7153-7160.
42. Filippov V, Kronenberg G, Pivneva T, et al. Subpopulation of nestin-expressing progenitor cells in the adult murine hippocampus shows electrophysiological and morphological characteristics of astrocytes. *Mol Cell Neurosci.* 2003;23(3):373-382.
43. Alvarez-Buylla A, García-Verdugo JM, Tramontin AD. A unified hypothesis on the lineage of neural stem cells. *Nat Rev Neurosci.* 2001;2(4):287-293. doi:10.1038/35067582
44. Ming G, Song H. Adult neurogenesis in the mammalian brain. *Cell Press.* 2011;70(4):687-702. doi:10.1016/j.neuron.2011.05.001.Adult
45. Kempermann G, Song H, Gage FH. Neurogenesis in the Adult Hippocampus. *Cold Spring Harb Perspect Biol.* 2015;7(9):a018812. doi:10.1101/cshperspect.a018812
46. Brandt MD, Jessberger S, Steiner B, et al. Transient calretinin expression defines early postmitotic step of neuronal differentiation in adult hippocampal

- neurogenesis of mice. *Mol Cell Neurosci*. 2003;24(3):603-613.
47. Ge S, Yang C hao, Hsu K sen, Ming G li, Song H. A Critical Period for Enhanced Synaptic Plasticity in Newly Generated Neurons of the Adult Brain. *Neuron*. 2007;54(4):559-566. doi:10.1016/j.neuron.2007.05.002
  48. Jungenitz T, Radic T, Jedlicka P, Schwarzacher SW. High-frequency stimulation induces gradual immediate early gene expression in maturing adult-generated hippocampal granule cells. *Cereb Cortex*. 2014;24(7):1845-1857. doi:10.1093/cercor/bht035
  49. Squire LR. Memory systems of the brain: a brief history and current perspective. *Neurobiol Learn Mem*. 2004;82(3):171-177. doi:10.1016/j.nlm.2004.06.005
  50. Squire LR. The neuropsychology of human memory. *Annu Rev Neurosci*. 1982;5:241-273. doi:10.1146/annurev.ne.05.030182.001325
  51. Snyder JS, Soumier A, Brewer M, Pickel J, Cameron HA. Adult hippocampal neurogenesis buffers stress responses and depressive behaviour. *Nature*. 2011;476(7361):458-461. doi:10.1038/nature10287
  52. Nadel L, O'Keefe J, Black A. Slam on the brakes: A critique of Altman, Brunner, and Bayer's response-inhibition model of hippocampal function. *Behav Biol*. 1975;14(2):151-162. doi:10.1016/S0091-6773(75)90148-0
  53. McNaughton N, Gray JA. Anxiolytic action on the behavioural inhibition system implies multiple types of arousal contribute to anxiety. *J Affect Disord*. 2000;61(3):161-176.
  54. Lee I, Kesner RP. Encoding versus retrieval of spatial memory: double dissociation between the dentate gyrus and the perforant path inputs into CA3 in the dorsal hippocampus. *Hippocampus*. 2004;14(1):66-76. doi:10.1002/hipo.10167
  55. Gilbert PE, Kesner RP, Lee I. Dissociating hippocampal subregions: double dissociation between dentate gyrus and CA1. *Hippocampus*. 2001;11(6):626-636. doi:10.1002/hipo.1077
  56. Sutherland RJ, Whishaw IQ, Kolb B. A behavioural analysis of spatial localization following electrolytic, kainate- or colchicine-induced damage to the hippocampal formation in the rat. *Behav Brain Res*. 1983;7(2):133-153.
  57. Corkin S, Amaral DG, González RG, Johnson KA, Hyman BT. H. M.'s medial

- temporal lobe lesion: findings from magnetic resonance imaging. *J Neurosci*. 1997;17(10):3964-3979.
58. Bayer SA, Brunner RL, Hine R, Altman J. Behavioural effects of interference with the postnatal acquisition of hippocampal granule cells. *Nat New Biol*. 1973;242(120):222-224.
  59. Wojtowicz JM. Irradiation as an experimental tool in studies of adult neurogenesis. *Hippocampus*. 2006;16(3):261-266. doi:10.1002/hipo.20158
  60. Garcia ADR, Doan NB, Imura T, Bush TG, Sofroniew M V. GFAP-expressing progenitors are the principal source of constitutive neurogenesis in adult mouse forebrain. *Nat Neurosci*. 2004;7(11):1233-1241. doi:10.1038/nn1340
  61. Goodman T, Trouche S, Massou I, et al. Young hippocampal neurons are critical for recent and remote spatial memory in adult mice. *Neuroscience*. 2010;171(3):769-778. doi:10.1016/j.neuroscience.2010.09.047
  62. Mohapel P, Leanza G, Kokaia M, Lindvall O. Forebrain acetylcholine regulates adult hippocampal neurogenesis and learning. *Neurobiol Aging*. 2005;26(6):939-946. doi:10.1016/j.neurobiolaging.2004.07.015
  63. Kheirbek MA, Tannenholz L. NR2B-dependent plasticity of adult born granule cells is necessary for context discrimination. *J Neurosci*. 2012;257(5):2432-2437. doi:10.1016/j.immuni.2010.12.017.Two-stage
  64. Shors TJ, Townsend DA, Zhao M, Kozorovitskiy Y, Gould E. Neurogenesis may relate to some but not all types of hippocampal-dependent learning. *Hippocampus*. 2002;12(5):578-584. doi:10.1002/hipo.10103
  65. Shors TJ, Miesegaes G, Beylin A, Zhao M, Rydel T, Gould E. Neurogenesis in the adult is involved in the formation of trace memories. *Nature*. 2001;410(6826):372-376. doi:10.1038/35066584
  66. Tronel S, Belnoue L, Grosjean N, et al. Adult-born neurons are necessary for extended contextual discrimination. *Hippocampus*. 2012;22(2):292-298. doi:10.1002/hipo.20895
  67. Saxe MD, Battaglia F, Wang J-W, et al. Ablation of hippocampal neurogenesis impairs contextual fear conditioning and synaptic plasticity in the dentate gyrus. *Proc Natl Acad Sci U S A*. 2006;103(46):17501-17506. doi:10.1073/pnas.0607207103

68. Winocur G, Wojtowicz JM, Sekeres M, Snyder JS, Wang S. Inhibition of neurogenesis interferes with hippocampus-dependent memory function. *Hippocampus*. 2006;16(3):296-304. doi:10.1002/hipo.20163
69. Warner-Schmidt JL, Duman RS. Hippocampal neurogenesis: opposing effects of stress and antidepressant treatment. *Hippocampus*. 2006;16(3):239-249. doi:10.1002/hipo.20156
70. Dupret D, Revest J-M, Koehl M, et al. Spatial relational memory requires hippocampal adult neurogenesis. *PLoS One*. 2008;3(4):e1959. doi:10.1371/journal.pone.0001959
71. Zhang S, Cranney J. The role of GABA and anxiety in the reconsolidation of conditioned fear. *Behav Neurosci*. 2008;122(6):1295-1305. doi:10.1037/a0013273
72. Snyder JS, Hong NS, McDonald RJ, Wojtowicz JM. A role for adult neurogenesis in spatial long-term memory. *Neuroscience*. 2005;130(4):843-852. doi:10.1016/j.neuroscience.2004.10.009
73. Yau SY, Li A, So KF. Involvement of Adult Hippocampal Neurogenesis in Learning and Forgetting. *Neural Plast*. 2015;2015. doi:10.1155/2015/717958
74. Houser CR. Interneurons of the dentate gyrus: an overview of cell types, terminal fields and neurochemical identity. *Prog Brain Res*. 2007;163:217-232. doi:10.1016/S0079-6123(07)63013-1
75. Freund TF, Buzsáki G. Interneurons of the hippocampus. *Hippocampus*. 1996;6(4):347-470. doi:10.1002/(SICI)1098-1063(1996)6:4<347::AID-HIPO1>3.0.CO;2-I
76. O'Reilly RC, McClelland JL. Hippocampal conjunctive encoding, storage, and recall: avoiding a trade-off. *Hippocampus*. 1994;4(6):661-682. doi:10.1002/hipo.450040605
77. Hopfield JJ. Neural networks and physical systems with emergent collective computational abilities. *Proc Natl Acad Sci U S A*. 1982;79(8):2554-2558.
78. Treves A, Rolls ET. Computational analysis of the role of the hippocampus in memory. *Hippocampus*. 1994;4(3):374-391. doi:10.1002/hipo.450040319
79. Ruediger S, Vittori C, Bednarek E, et al. Learning-related feedforward inhibitory connectivity growth required for memory precision. *Nature*.

- 2011;473(7348):514-518. doi:10.1038/nature09946
80. Rolls ET. Pattern completion and pattern separation mechanisms in the hippocampus. *Neurobiol Basis Mem A Syst Attrib Process Anal.* 2015;7(October):77-113. doi:10.1007/978-3-319-15759-7\_4
  81. Leutgeb JK, Leutgeb S, Moser M-B, Moser EI. Pattern separation in the dentate gyrus and CA3 of the hippocampus. *Science.* 2007;315(5814):961-966. doi:10.1126/science.1135801
  82. Yassa MA, Stark CEL. Pattern separation in the hippocampus. *Trends Neurosci.* 2011;34(10):515-525. doi:10.1016/j.tins.2011.06.006
  83. Marín-Burgin A, Mongiat LA, Pardi MB, et al. Unique processing during a period of high excitation/inhibition balance in adult-born neurons. *Science.* 2012;335(6073):1238-1242. doi:10.1126/science.1214956
  84. Nakashiba T, Cushman JD, Pelkey KA, et al. Young dentate granule cells mediate pattern separation, whereas old granule cells facilitate pattern completion. *Cell.* 2012;149(1):188-201. doi:10.1016/j.cell.2012.01.046
  85. Zhao C, Deng W, Gage FH. Mechanisms and Functional Implications of Adult Neurogenesis. *Cell.* 2008;132(4):645-660. doi:10.1016/j.cell.2008.01.033
  86. Imayoshi I, Sakamoto M, Ohtsuka T, et al. Roles of continuous neurogenesis in the structural and functional integrity of the adult forebrain. *Nat Neurosci.* 2008;11(10):1153-1161. doi:10.1038/nn.2185
  87. Clelland CD, Choi M, Romberg C, et al. A functional role for adult hippocampal neurogenesis in spatial pattern separation. *Science.* 2009;325(5937):210-213. doi:10.1126/science.1173215
  88. Sahay A, Wilson DA, Hen R. Pattern separation: a common function for new neurons in hippocampus and olfactory bulb. *Neuron.* 2011;70(4):582-588. doi:10.1016/j.neuron.2011.05.012
  89. Akers KG, Martinez-Canabal A, Restivo L, et al. Hippocampal neurogenesis regulates forgetting during adulthood and infancy. *Science.* 2014;344(6184):598-602. doi:10.1126/science.1248903
  90. Fong BC, Slack RS. RB: An essential player in adult neurogenesis. *Neurogenes (Austin, Tex).* 2017;4(1):e1270382. doi:10.1080/23262133.2016.1270382
  91. Pierfelice T, Alberi L, Gaiano N. Notch in the vertebrate nervous system: an old

- dog with new tricks. *Neuron*. 2011;69(5):840-855. doi:10.1016/j.neuron.2011.02.031
92. Song H, Stevens CF, Gage FH. Astroglia induce neurogenesis from adult neural stem cells. *Nature*. 2002;417(6884):39-44. doi:10.1038/417039a
  93. Kuhn HG, Winkler J, Kempermann G, Thal LJ, Gage FH. Epidermal growth factor and fibroblast growth factor-2 have different effects on neural progenitors in the adult rat brain. *J Neurosci*. 1997;17(15):5820-5829.
  94. Olson AK, Eadie BD, Ernst C, Christie BR. Environmental enrichment and voluntary exercise massively increase neurogenesis in the adult hippocampus via dissociable pathways. *Hippocampus*. 2006;16(3):250-260. doi:10.1002/hipo.20157
  95. Jang M-H, Song H, Ming G. Regulation of adult neurogenesis by neurotransmitters. Gage FH, Kempermann G, eds. *Cold Spring Harb Lab Press*. 2008:Chapter 19.
  96. Kee N, Teixeira CM, Wang AH, Frankland PW. Preferential incorporation of adult-generated granule cells into spatial memory networks in the dentate gyrus. *Nat Neurosci*. 2007;10(3):355-362. doi:10.1038/nn1847
  97. Leuner B, Mendolia-Loffredo S, Kozorovitskiy Y, Samburg D, Gould E, Shors TJ. Learning enhances the survival of new neurons beyond the time when the hippocampus is required for memory. *J Neurosci*. 2004;24(34):7477-7481. doi:10.1523/JNEUROSCI.0204-04.2004
  98. Drapeau E, Montaron M-F, Aguerre S, Abrous DN. Learning-induced survival of new neurons depends on the cognitive status of aged rats. *J Neurosci*. 2007;27(22):6037-6044. doi:10.1523/JNEUROSCI.1031-07.2007
  99. Tashiro A, Makino H, Gage FH. Experience-specific functional modification of the dentate gyrus through adult neurogenesis: a critical period during an immature stage. *J Neurosci*. 2007;27(12):3252-3259. doi:10.1523/JNEUROSCI.4941-06.2007
  100. Bergami M, Masserdotti G, Temprana SG, et al. A Critical Period for Experience-Dependent Remodeling of Adult-Born Neuron Connectivity. *Neuron*. 2015;85(4):710-717. doi:10.1016/j.neuron.2015.01.001
  101. Kempermann G, Kuhn HG, Gage FH. More hippocampal neurons in adult mice

- living in an enriched environment. *Nature*. 1997;386(6624):493-495.  
doi:10.1038/386493a0
102. Nilsson M, Perfilieva E, Johansson U, Orwar O, Eriksson PS. Enriched environment increases neurogenesis in the adult rat dentate gyrus and improves spatial memory. *J Neurobiol*. 1999;39(4):569-578.
  103. Williams BM, Luo Y, Ward C, et al. Environmental enrichment: effects on spatial memory and hippocampal CREB immunoreactivity. *Physiol Behav*. 2001;73(4):649-658.
  104. Freund J, Brandmaier AM, Lewejohann L, et al. Emergence of individuality in genetically identical mice. *Science*. 2013;340(6133):756-759.  
doi:10.1126/science.1235294
  105. Zang J, Liu Y, Li W, et al. Voluntary exercise increases adult hippocampal neurogenesis by increasing GSK-3 $\beta$  activity in mice. *Neuroscience*. 2017;354:122-135. doi:10.1016/j.neuroscience.2017.04.024
  106. van Praag H, Kempermann G, Gage FH. Running increases cell proliferation and neurogenesis in the adult mouse dentate gyrus. *Nat Neurosci*. 1999;2(3):266-270.  
doi:10.1038/6368
  107. Tozuka Y, Fukuda S, Namba T, Seki T, Hisatsune T. GABAergic excitation promotes neuronal differentiation in adult hippocampal progenitor cells. *Neuron*. 2005;47(6):803-815. doi:10.1016/j.neuron.2005.08.023
  108. Sibbe M, Kulik A. GABAergic Regulation of Adult Hippocampal Neurogenesis. *Mol Neurobiol*. 2017;54(7):5497-5510. doi:10.1007/s12035-016-0072-3
  109. Deisseroth K, Singla S, Toda H, Monje M, Palmer TD, Malenka RC. Excitation-neurogenesis coupling in adult neural stem/progenitor cells. *Neuron*. 2004;42(4):535-552.
  110. Bruel-Jungerman E, Davis S, Rampon C, Laroche S. Long-term potentiation enhances neurogenesis in the adult dentate gyrus. *J Neurosci*. 2006;26(22):5888-5893. doi:10.1523/JNEUROSCI.0782-06.2006
  111. Chun SK, Sun W, Park J-J, Jung MW. Enhanced proliferation of progenitor cells following long-term potentiation induction in the rat dentate gyrus. *Neurobiol Learn Mem*. 2006;86(3):322-329. doi:10.1016/j.nlm.2006.05.005
  112. Tashiro A, Sandler VM, Toni N, Zhao C, Gage FH. NMDA-receptor-mediated,

- cell-specific integration of new neurons in adult dentate gyrus. *Nature*. 2006;442(7105):929-933. doi:10.1038/nature05028
113. Altman J, Das G. Autoradiographic and histological evidence of postnatal hippocampal neurogenesis in rats. *J Comp Neurol*. 1965;124(3):319-335.
  114. Kuhn HG, Dickinson-Anson H, Gage FH. Neurogenesis in the dentate gyrus of the adult rat: age-related decrease of neuronal progenitor proliferation. *J Neurosci*. 1996;16(6):2027-2033.
  115. Heine VM, Maslam S, Joëls M, Lucassen PJ. Prominent decline of newborn cell proliferation, differentiation, and apoptosis in the aging dentate gyrus, in absence of an age-related hypothalamus-pituitary-adrenal axis activation. *Neurobiol Aging*. 2004;25(3):361-375. doi:10.1016/S0197-4580(03)00090-3
  116. Mirescu C, Gould E. Stress and adult neurogenesis. *Hippocampus*. 2006;16(3):233-238. doi:10.1002/hipo.20155
  117. Veena J, Srikumar BN, Raju TR, Shankaranarayana Rao BS. Exposure to enriched environment restores the survival and differentiation of new born cells in the hippocampus and ameliorates depressive symptoms in chronically stressed rats. *Neurosci Lett*. 2009;455(3):178-182. doi:10.1016/j.neulet.2009.03.059
  118. Sportiche N, Suntsova N, Methippara M, et al. Sustained sleep fragmentation results in delayed changes in hippocampal-dependent cognitive function associated with reduced dentate gyrus neurogenesis. *Neuroscience*. 2010;170(1):247-258. doi:10.1016/j.neuroscience.2010.06.038
  119. Jessberger S, Zhao C, Toni N, Clemenson GD, Li Y, Gage FH. Seizure-associated, aberrant neurogenesis in adult rats characterized with retrovirus-mediated cell labeling. *J Neurosci*. 2007;27(35):9400-9407. doi:10.1523/JNEUROSCI.2002-07.2007
  120. Arvidsson A, Collin T, Kirik D, Kokaia Z, Lindvall O. Neuronal replacement from endogenous precursors in the adult brain after stroke. *Nat Med*. 2002;8(9):963-970. doi:10.1038/nm747
  121. Thored P, Wood J, Arvidsson A, Cammenga J, Kokaia Z, Lindvall O. Long-term neuroblast migration along blood vessels in an area with transient angiogenesis and increased vascularization after stroke. *Stroke*. 2007;38(11):3032-3039. doi:10.1161/STROKEAHA.107.488445



122. Kempermann G, Kronenberg G. Depressed new neurons--adult hippocampal neurogenesis and a cellular plasticity hypothesis of major depression. *Biol Psychiatry*. 2003;54(5):499-503.
123. Snyder JS, Choe JS, Clifford MA, et al. Adult-Born Hippocampal Neurons Are More Numerous, Faster Maturing, and More Involved in Behavior in Rats than in Mice. *J Neurosci*. 2009;29(46):14484-14495. doi:10.1523/JNEUROSCI.1768-09.2009
124. Brown JP, Couillard-Després S, Cooper-Kuhn CM, Winkler J, Aigner L, Kuhn HG. Transient expression of doublecortin during adult neurogenesis. *J Comp Neurol*. 2003;467(1):1-10. doi:10.1002/cne.10874
125. Gleeson JG, Lin PT, Flanagan LA, Walsh CA. Doublecortin is a microtubule-associated protein and is expressed widely by migrating neurons. *Neuron*. 1999;23(2):257-271.
126. Cremer H, Chazal G, Lledo PM, et al. PSA-NCAM: an important regulator of hippocampal plasticity. *Int J Dev Neurosci*. 2000;18(2-3):213-220.
127. Cremer H, Chazal G, Golidis C, Represa A. NCAM is essential for axonal growth and fasciculation in the hippocampus. *Mol Cell Neurosci*. 1997;8(5):323-335. doi:10.1006/mcne.1996.0588
128. Seki T, Arai Y. Distribution and possible roles of the highly polysialylated neural cell adhesion molecule (NCAM-H) in the developing and adult central nervous system. *Neurosci Res*. 1993;17(4):265-290.
129. Mullen RJ, Buck CR, Smith AM. NeuN, a neuronal specific nuclear protein in vertebrates. *Development*. 1992;116(1):201-211.
130. Oliver G, Sosa-Pineda B, Geisendorf S, Spana EP, Doe CQ, Gruss P. Prox 1, a prospero-related homeobox gene expressed during mouse development. *Mech Dev*. 1993;44(1):3-16.
131. Iwano T, Masuda A, Kiyonari H, Enomoto H, Matsuzaki F. Prox1 postmitotically defines dentate gyrus cells by specifying granule cell identity over CA3 pyramidal cell fate in the hippocampus. *Development*. 2012;139(16):3051-3062. doi:10.1242/dev.080002
132. Lavado A, Lagutin O V, Chow LML, Baker SJ, Oliver G. Prox1 is required for granule cell maturation and intermediate progenitor maintenance during brain

- neurogenesis. *PLoS Biol.* 2010;8(8). doi:10.1371/journal.pbio.1000460
133. Lanahan A, Worley P. Immediate-early genes and synaptic function. *Neurobiol Learn Mem.* 1998;70(1-2):37-43. doi:10.1006/nlme.1998.3836
  134. Cole AJ, Saffen DW, Baraban JM, Worley PF. Rapid increase of an immediate early gene messenger RNA in hippocampal neurons by synaptic NMDA receptor activation. *Nature.* 1989;340(6233):474-476. doi:10.1038/340474a0
  135. Guzowski JF, McNaughton BL, Barnes CA, Worley PF. Environment-specific expression of the immediate-early gene Arc in hippocampal neuronal ensembles. *Nat Neurosci.* 1999;2(12):1120-1124. doi:10.1038/16046
  136. Okuno H. Regulation and function of immediate-early genes in the brain: beyond neuronal activity markers. *Neurosci Res.* 2011;69(3):175-186. doi:10.1016/j.neures.2010.12.007
  137. Bozon B, Davis S, Laroche S. Regulated transcription of the immediate-early gene Zif268: mechanisms and gene dosage-dependent function in synaptic plasticity and memory formation. *Hippocampus.* 2002;12(5):570-577. doi:10.1002/hipo.10100
  138. Link W, Konietzko U, Kauselmann G, et al. Somatodendritic expression of an immediate early gene is regulated by synaptic activity. *Proc Natl Acad Sci U S A.* 1995;92(12):5734-5738.
  139. Ramírez-Amaya V, Vazdarjanova A, Mikhael D, Rosi S, Worley PF, Barnes CA. Spatial exploration-induced Arc mRNA and protein expression: evidence for selective, network-specific reactivation. *J Neurosci.* 2005;25(7):1761-1768. doi:10.1523/JNEUROSCI.4342-04.2005
  140. Hall J, Thomas KL, Everitt BJ. Cellular imaging of zif268 expression in the hippocampus and amygdala during contextual and cued fear memory retrieval: selective activation of hippocampal CA1 neurons during the recall of contextual memories. *J Neurosci.* 2001;21(6):2186-2193.
  141. Vann SD, Brown MW, Erichsen JT, Aggleton JP. Fos imaging reveals differential patterns of hippocampal and parahippocampal subfield activation in rats in response to different spatial memory tests. *J Neurosci.* 2000;20(7):2711-2718.
  142. Christy B, Nathans D. Functional serum response elements upstream of the

- growth factor-inducible gene *zif268*. *Mol Cell Biol*. 1989;9(11):4889-4895.
143. Swirnoff AH, Milbrandt J. DNA-binding specificity of NGFI-A and related zinc finger transcription factors. *Mol Cell Biol*. 1995;15(4):2275-2287.
  144. Lemaire P, Vesque C, Schmitt J, Stunnenberg H, Frank R, Charnay P. The serum-inducible mouse gene *Krox-24* encodes a sequence-specific transcriptional activator. *Mol Cell Biol*. 1990;10(7):3456-3467.
  145. Hughes P, Dragunow M. Induction of immediate-early genes and the control of neurotransmitter-regulated gene expression within the nervous system. *Pharmacol Rev*. 1995;47(1):133-178.
  146. Beckmann AM, Wilce PA. Egr transcription factors in the nervous system. *Neurochem Int*. 1997;31(4):477-510-6.
  147. Davis S, Bozon B, Laroche S. How necessary is the activation of the immediate early gene *zif 268* in synaptic plasticity and learning? *Behav Brain Res*. 2003;142(1-2):17-30. doi:10.1016/S0166-4328(02)00421-7
  148. Sukhatme VP, Cao XM, Chang LC, et al. A zinc finger-encoding gene coregulated with *c-fos* during growth and differentiation, and after cellular depolarization. *Cell*. 1988;53(1):37-43.
  149. Richardson CL, Tate WP, Mason SE, Lawlor PA, Dragunow M, Abraham WC. Correlation between the induction of an immediate early gene, *zif/268*, and long-term potentiation in the dentate gyrus. *Brain Res*. 1992;580(1-2):147-154.
  150. Abraham WC, Mason SE, Demmer J, et al. Correlations between immediate early gene induction and the persistence of long-term potentiation. *Neuroscience*. 1993;56(3):717-727. doi:10.1016/0306-4522(93)90369-Q
  151. Plath N, Ohana O, Dammermann B, et al. *Arc/Arg3.1* is essential for the consolidation of synaptic plasticity and memories. *Neuron*. 2006;52(3):437-444. doi:10.1016/j.neuron.2006.08.024
  152. Jones MW, Errington ML, French PJ, et al. A requirement for the immediate early gene *Zif268* in the expression of late LTP and long-term memories. *Nat Neurosci*. 2001;4(3):289-296. doi:10.1038/85138
  153. Veyrac A, Gros A, Bruel-jungerman E, Rochefort C. *Zif268/egr1* gene controls the selection, maturation and Functional Integration of Adult Hippocampal Newborn Neurons By Learning. *PNAS*. 2013:1-6.

doi:10.1073/pnas.1220558110/-

/DCSupplemental.www.pnas.org/cgi/doi/10.1073/pnas.1220558110

154. Sisti HM, Glass AL, Shors TJ. Neurogenesis and the spacing effect: Learning over time enhances memory and the survival of new neurons. *Learn Mem.* 2007;14(5):368-375. doi:10.1101/lm.488707
155. Miller MW, Nowakowski RS. Use of bromodeoxyuridine-immunohistochemistry to examine the proliferation, migration and time of origin of cells in the central nervous system. *Brain Res.* 1988;457(1):44-52.
156. Leuner B, Glasper ER, Gould E. Thymidine analog methods for studies of adult neurogenesis are not equally sensitive. *J Comp Neurol.* 2009;517(2):123-133. doi:10.1002/cne.22107.Thymidine
157. Zeng C, Pan F, Jones LA, et al. Evaluation of 5-ethynyl-2'-deoxyuridine staining as a sensitive and reliable method for studying cell proliferation in the adult nervous system. *Brain Res.* 2010;1319:21-32. doi:10.1016/j.brainres.2009.12.092
158. Kee N, Sivalingam S, Boonstra R, Wojtowicz JM. The utility of Ki-67 and BrdU as proliferative markers of adult neurogenesis. *J Neurosci Methods.* 2002;115(1):97-105.
159. Geraerts M, Eggermont K, Hernandez-Acosta P, Garcia-Verdugo J-M, Baekelandt V, Debyser Z. Lentiviral vectors mediate efficient and stable gene transfer in adult neural stem cells in vivo. *Hum Gene Ther.* 2006;17(6):635-650. doi:10.1089/hum.2006.17.635
160. Livet J, Weissman TA, Kang H, et al. Transgenic strategies for combinatorial expression of fluorescent proteins in the nervous system. *Nature.* 2007;450(7166):56-62. doi:10.1038/nature06293
161. Malenka RC, Bear MF. LTP and LTD: an embarrassment of riches. *Neuron.* 2004;44(1):5-21. doi:10.1016/j.neuron.2004.09.012
162. Bailey CH, Kandel ER, Harris KM. Structural Components of Synaptic Plasticity and Memory Consolidation. *Cold Spring Harb Perspect Biol.* 2015;7(7):a021758. doi:10.1101/cshperspect.a021758
163. Escobar ML, Derrick B. *Long-Term Potentiation and Depression as Putative Mechanisms for Memory Formation.*; 2007.
164. Malenka RC. Synaptic plasticity in the hippocampus: LTP and LTD. *Cell.*

- 1994;78(4):535-538.
165. Bliss T V, Collingridge GL. A synaptic model of memory: long-term potentiation in the hippocampus. *Nature*. 1993;361(6407):31-39. doi:10.1038/361031a0
  166. Kessels HW, Malinow R. Synaptic AMPA receptor plasticity and behavior. *Neuron*. 2009;61(3):340-350. doi:10.1016/j.neuron.2009.01.015
  167. Keinänen K, Wisden W, Sommer B, et al. A family of AMPA-selective glutamate receptors. *Science*. 1990;249(4968):556-560.
  168. Engert F, Bonhoeffer T. Dendritic spine changes associated with hippocampal long-term synaptic plasticity. *Nature*. 1999;399(6731):66-70. doi:10.1038/19978
  169. Matsuzaki M, Honkura N, Ellis-Davies GCR, Kasai H. Structural basis of long-term potentiation in single dendritic spines. *Nature*. 2004;429(6993):761-766. doi:10.1038/nature02617
  170. Bourne JN, Sorra KE, Hurlburt J, Harris KM. Polyribosomes are increased in spines of CA1 dendrites 2 h after the induction of LTP in mature rat hippocampal slices. *Hippocampus*. 2007;17(1):1-4. doi:10.1002/hipo.20238
  171. van Harrevelde A, Fifkova E. Rapid freezing of deep cerebral structures for electron microscopy. *Anat Rec*. 1975;182(3):377-385. doi:10.1002/ar.1091820311
  172. Bozon B, Davis S, Laroche S. Regulated transcription of the immediate-early gene *Zif268*: mechanisms and gene dosage-dependent function in synaptic plasticity and memory formation. *Hippocampus*. 2002;12(5):570-577. doi:10.1002/hipo.10100
  173. Abraham WC, Mason-Parker SE, Bear MF, Webb S, Tate WP. Heterosynaptic metaplasticity in the hippocampus in vivo: a BCM-like modifiable threshold for LTP. *Proc Natl Acad Sci U S A*. 2001;98(19):10924-10929. doi:10.1073/pnas.181342098
  174. Bowden JB, Abraham WC, Harris KM. Differential effects of strain, circadian cycle, and stimulation pattern on LTP and concurrent LTD in the dentate gyrus of freely moving rats. *Hippocampus*. 2012;22(6):1363-1370. doi:10.1002/hipo.20972
  175. Bienenstock EL, Cooper LN, Munro PW. Theory for the development of neuron selectivity: orientation specificity and binocular interaction in visual cortex. *J*

- Neurosci.* 1982;2(1):32-48.
176. Abraham WC, Williams JM. LTP maintenance and its protein synthesis-dependence. *Neurobiol Learn Mem.* 2008;89(3):260-268. doi:10.1016/j.nlm.2007.10.001
  177. Jedlicka P. Synaptic plasticity, metaplasticity and BCM theory. *Bratisl Lek Listy.* 2002;103(4-5):137-143.
  178. Claiborne BJ, Amaral DG, Cowan WM. A light and electron microscopic analysis of the mossy fibers of the rat dentate gyrus. *J Comp Neurol.* 1986;246(4):435-458. doi:10.1002/cne.902460403
  179. Frotscher M, Seress L, Schwerdtfeger WK, Buhl E. The mossy cells of the fascia dentata: a comparative study of their fine structure and synaptic connections in rodents and primates. *J Comp Neurol.* 1991;312(1):145-163. doi:10.1002/cne.903120111
  180. Gu Z, Lamb PW, Yakel JL. Cholinergic Coordination of Presynaptic and Postsynaptic Activity Induces Timing-Dependent Hippocampal Synaptic Plasticity. *J Neurosci.* 2012;32(36):12337-12348. doi:10.1523/JNEUROSCI.2129-12.2012
  181. Faulkner RL, Jang M-H, Liu X-B, et al. Development of hippocampal mossy fiber synaptic outputs by new neurons in the adult brain. *Proc Natl Acad Sci U S A.* 2008;105(37):14157-14162. doi:10.1073/pnas.0806658105
  182. Acsády L, Kamondi A, Sík A, Freund T, Buzsáki G. GABAergic cells are the major postsynaptic targets of mossy fibers in the rat hippocampus. *J Neurosci.* 1998;18(9):3386-3403.
  183. Amaral DG. Synaptic extensions from the mossy fibers of the fascia dentata. *Anat Embryol.* 1979;(155):241-251.
  184. Zhao C. Distinct Morphological Stages of Dentate Granule Neuron Maturation in the Adult Mouse Hippocampus. *J Neurosci.* 2006;26(1):3-11. doi:10.1523/JNEUROSCI.3648-05.2006
  185. Shapiro LA, Upadhyaya P, Ribak CE. Spatiotemporal profile of dendritic outgrowth from newly born granule cells in the adult rat dentate gyrus. *Brain Res.* 2007;1149:30-37. doi:10.1016/j.brainres.2006.07.032
  186. Harris KM, Kater SB. Dendritic spines: cellular specializations imparting both

- stability and flexibility to synaptic function. *Annu Rev Neurosci.* 1994;17:341-371. doi:10.1146/annurev.ne.17.030194.002013
187. Nimchinsky EA, Sabatini BL, Svoboda K. Structure and function of dendritic spines. *Annu Rev Physiol.* 2002;64:313-353. doi:10.1146/annurev.physiol.64.081501.160008
188. Sala C, Pièch V, Wilson NR, Passafaro M, Liu G, Sheng M. Regulation of dendritic spine morphology and synaptic function by Shank and Homer. *Neuron.* 2001;31(1):115-130.
189. Nimchinsky EA, Sabatini BL, Svoboda K. Structure and function of dendritic spines. *Annu Rev Physiol.* 2001;64:313-353. doi:10.1146/annurev.physiol.64.081501.160008
190. Bosch M, Hayashi Y. Structural plasticity of dendritic spines. *Curr Opin Neurobiol.* 2012;22(3):383-388. doi:10.1016/j.conb.2011.09.002
191. Toni N, Teng EM, Bushong E a, et al. Synapse formation on neurons born in the adult hippocampus. *Nat Neurosci.* 2007;10(6):727-734. doi:10.1038/nn1908
192. Matsuzaki M, Ellis-Davies GC, Nemoto T, Miyashita Y, Iino M, Kasai H. Dendritic spine geometry is critical for AMPA receptor expression in hippocampal CA1 pyramidal neurons. *Nat Neurosci.* 2001;4(11):1086-1092. doi:10.1038/nn736
193. Takumi Y, Matsubara A, Rinvik E, Ottersen OP. The arrangement of glutamate receptors in excitatory synapses. *Ann N Y Acad Sci.* 1999;868:474-482.
194. Espósito MS, Piatti VC, Laplagne DA, et al. Neuronal Differentiation in the Adult Hippocampus Recapitulates Embryonic Development. *J Neurosci.* 2005;25(44):10074-10086. doi:10.1523/jneurosci.3114-05.2005
195. Ge S, Sailor KA, Ming G, Song H. Synaptic integration and plasticity of new neurons in the adult hippocampus. *J Physiol.* 2008;586(16):3759-3765. doi:10.1113/jphysiol.2008.155655
196. Mongiat LA, Espósito MS, Lombardi G, Schinder AF. Reliable activation of immature neurons in the adult hippocampus. *PLoS One.* 2009;4(4). doi:10.1371/journal.pone.0005320
197. Overstreet Wadiche L, Bromberg DA, Bensen AL, Westbrook GL. GABAergic signaling to newborn neurons in dentate gyrus. *J Neurophysiol.* 2005;94(6):4528-

4532. doi:10.1152/jn.00633.2005
198. Overstreet-Wadiche LS, Bromberg DA, Bensen AL, Westbrook GL. Seizures accelerate functional integration of adult-generated granule cells. *J Neurosci.* 2006;26(15):4095-4103. doi:10.1523/JNEUROSCI.5508-05.2006
  199. Wang L-P, Kempermann G, Kettenmann H. A subpopulation of precursor cells in the mouse dentate gyrus receives synaptic GABAergic input. *Mol Cell Neurosci.* 2005;29(2):181-189. doi:10.1016/j.mcn.2005.02.002
  200. Ge S, Goh ELK, Sailor KA, Kitabatake Y, Ming G, Song H. GABA regulates synaptic integration of newly generated neurons in the adult brain. *Computer (Long Beach Calif).* 2006;144(5):724-732. doi:10.1038/jid.2014.371
  201. Schmidt-Hieber C, Jonas P, Bischofberger J. Enhanced synaptic plasticity in newly generated granule cells of the adult hippocampus. *Nature.* 2004;429(6988):184-187. doi:10.1038/nature02553
  202. Cull-Candy SG, Leszkiewicz DN. Role of distinct NMDA receptor subtypes at central synapses. *Sci STKE.* 2004;2004(255):re16. doi:10.1126/stke.2552004re16
  203. Nácher J, Varea E, Miguel Blasco-Ibáñez J, et al. N-methyl-d-aspartate receptor expression during adult neurogenesis in the rat dentate gyrus. *Neuroscience.* 2007;144(3):855-864. doi:10.1016/j.neuroscience.2006.10.021
  204. Snyder JS, Kee N, Wojtowicz JM. Effects of adult neurogenesis on synaptic plasticity in the rat dentate gyrus. *J Neurophysiol.* 2001;85(6):2423-2431.
  205. Wang LP, Li F, Wang D, et al. NMDA receptors in dopaminergic neurons are crucial for habit learning. *Neuron.* 2011;72(6):1055-1066. doi:10.1016/j.neuron.2011.10.019
  206. Liu L, Wong TP, Pozza MF, et al. Role of NMDA receptor subtypes in governing the direction of hippocampal synaptic plasticity. *Science.* 2004;304(5673):1021-1024. doi:10.1126/science.1096615
  207. Vivar C, Potter MC, Choi J, et al. Monosynaptic inputs to new neurons in the dentate gyrus. *Nat Commun.* 2012;3(2012):1107. doi:10.1038/ncomms2101
  208. Buttner-Ennever J. The Rat Brain in Stereotaxic Coordinates, 3rd edn. By George Paxinos and Charles Watson. (Pp. xxxiii+80; illustrated; f\$69.95 paperback; ISBN 0 12 547623; comes with CD-ROM.) San Diego: Academic Press. 1996. *J Anat.* 1997;191(2):315-317. doi:10.1046/j.1469-7580.1997.191203153.x



209. Ohline SM, Wake KL, Hawkrigde M-V, et al. Adult-born dentate granule cell excitability depends on the interaction of neuron age, ontogenetic age and experience. *Brain Struct Funct.* 2018;223(845):1-16. doi:10.1007/s00429-018-1685-2
210. Abraham WC, Logan B, Greenwood JM, Dragunow M. Induction and experience-dependent consolidation of stable long-term potentiation lasting months in the hippocampus. *J Neurosci.* 2002;22(21):9626-9634.
211. Steward O, Wallace CS, Lyford GL, Worley PF. Synaptic activation causes the mRNA for the IEG Arc to localize selectively near activated postsynaptic sites on dendrites. *Neuron.* 1998;21(4):741-751.
212. Cahill SP, Yu RQ, Green D, Todorova E V, Snyder JS. Early survival and delayed death of developmentally-born dentate gyrus neurons. *Hippocampus.* 2017;27(11):1155-1167. doi:10.1002/hipo.22760
213. Merkle CM, Jian C, Mosa A, Tan Y-F, Wojtowicz JM. Homeostatic regulation of adult hippocampal neurogenesis in aging rats: long-term effects of early exercise. *Front Neurosci.* 2014;8:174. doi:10.3389/fnins.2014.00174
214. Stone SSD, Teixeira CM, Zaslavsky K, et al. Functional convergence of developmentally and adult-generated granule cells in dentate gyrus circuits supporting hippocampus-dependent memory. *Hippocampus.* 2011;21(12):1348-1362. doi:10.1002/hipo.20845
215. Jungenitz T, Beining M, Radic T, et al. Structural homo- and heterosynaptic plasticity in mature and adult newborn rat hippocampal granule cells. *Proc Natl Acad Sci U S A.* April 2018. doi:10.1073/pnas.1801889115
216. Alme CB, Buzzetti RA, Marrone DF, et al. Hippocampal Granule Cells Opt for Early Retirement. *Hippocampus.* 2010;1123(20):1109-1123. doi:10.1002/hipo.20810
217. Radic T, Jungenitz T, Singer M, et al. Time-lapse imaging reveals highly dynamic structural maturation of postnatally born dentate granule cells in organotypic entorhino-hippocampal slice cultures. *Sci Rep.* 2017;7:43724. doi:10.1038/srep43724
218. Jessberger S, Kempermann G. Adult-born hippocampal neurons mature into activity-dependent responsiveness. *Eur J Neurosci.* 2003;18(10):2707-2712.

- doi:10.1111/j.1460-9568.2003.02986.x
219. Laplagne DA, Kamienkowski JE, Espósito MS, et al. Similar GABAergic inputs in dentate granule cells born during embryonic and adult neurogenesis. *Eur J Neurosci.* 2007;25(10):2973-2981. doi:10.1111/j.1460-9568.2007.05549.x
  220. Aimone JB, Deng W, Gage FH. Put them out to pasture? What are old granule cells good for, anyway? *Hippocampus.* 2010;20(10):1124-1125. doi:10.1002/hipo.20867
  221. Hevner RF. Evolution of the mammalian dentate gyrus. *J Comp Neurol.* 2016;524(3):578-594. doi:10.1002/cne.23851
  222. Darwin CR. *The Origin of Species by Means of Natural Selection, or the Preservation of Favoured Races in the Struggle for Life, 6th Edn.* John Murray, London, UK; 1872.
  223. Kutschera U, Niklas KJ. The modern theory of biological evolution: an expanded synthesis. *Naturwissenschaften.* 2004;91(6):255-276. doi:10.1007/s00114-004-0515-y
  224. Kropff E, Yang SM, Schinder AF. Dynamic role of adult-born dentate granule cells in memory processing. *Curr Opin Neurobiol.* 2015;35:21-26. doi:10.1016/j.conb.2015.06.002
  225. Deng W, Aimone JB, Gage FH. New neurons and new memories: how does adult hippocampal neurogenesis affect learning and memory? *Nat Rev Neurosci.* 2010;11(5):339-350. doi:10.1038/nrn2822
  226. Aimone JB, Wiles J, Gage FH. Computational influence of adult neurogenesis on memory encoding. *Neuron.* 2009;61(2):187-202. doi:10.1016/j.neuron.2008.11.026
  227. Bischofberger J. Young and excitable: new neurons in memory networks. *Nat Neurosci.* 2007;10(3):273-275. doi:10.1038/nn0307-273
  228. Ryan TJ, Roy DS, Pignatelli M, Arons A, Tonegawa S. Engram cells retain memory under retrograde amnesia. *Science (80- ).* 2015;348(6238):1007-1013. doi:10.1126/science.aaa5542
  229. Williams JM, Beckmann AM, Mason-Parker SE, Abraham WC, Wilce PA, Tate WP. Sequential increase in Egr-1 and AP-1 DNA binding activity in the dentate gyrus following the induction of long-term potentiation. *Brain Res Mol Brain*

- Res.* 2000;77(2):258-266.
230. Stone SSD, Teixeira CM, Zaslavsky K, et al. Functional convergence of developmentally and adult-generated granule cells in dentate gyrus circuits supporting hippocampus-dependent memory. *Hippocampus*. 2011;21(12):1348-1362. doi:10.1002/hipo.20845
  231. Tronel S, Lemaire V, Charrier V, Montaron M-F, Abrous DN. Influence of ontogenetic age on the role of dentate granule neurons. *Brain Struct Funct*. 2015;220(2):645-661. doi:10.1007/s00429-014-0715-y
  232. Lemaire V, Tronel S, Montaron M-F, Fabre A, Dugast E, Abrous DN. Long-lasting plasticity of hippocampal adult-born neurons. *J Neurosci*. 2012;32(9):3101-3108. doi:10.1523/JNEUROSCI.4731-11.2012
  233. Penner M, Parrish R, Hoang L, Roth T, Lubin F, Barnes C. Age-related changes in *Egr 1* transcription and DNA methylation within the hippocampus. *Hippocampus*. 2016;26(8):n/a-n/a. doi:10.1002/hipo.22583
  234. Canals S, Beyerlein M, Merkle H, Logothetis NK. Functional MRI evidence for LTP-induced neural network reorganization. *Curr Biol*. 2009;19(5):398-403. doi:10.1016/j.cub.2009.01.037
  235. Alvarez-Salvado E, Pallarés V, Moreno A, Canals S. Functional MRI of long-term potentiation: imaging network plasticity. *Philos Trans R Soc Lond B Biol Sci*. 2014;369(1633):20130152. doi:10.1098/rstb.2013.0152
  236. Bramham CR, Southard T, Sarvey JM, Herkenham M, Brady LS. Unilateral LTP triggers bilateral increases in hippocampal neurotrophin and trk receptor mRNA expression in behaving rats: evidence for interhemispheric communication. *J Comp Neurol*. 1996;368(3):371-382. doi:10.1002/(SICI)1096-9861(19960506)368:3<371::AID-CNE4>3.0.CO;2-2
  237. Gaarskjaer FB. Organization of the mossy fiber system of the rat studied in extended hippocampi. II. Experimental analysis of fiber distribution with silver impregnation methods. *J Comp Neurol*. 1978;178(1):73-88. doi:10.1002/cne.901780105
  238. Piatti VC, Espósito MS, Schinder AF. The timing of neuronal development in adult hippocampal neurogenesis. *Neuroscientist*. 2006;12(6):463-468. doi:10.1177/1073858406293538

239. Angevine JB. Time of neuron origin in the hippocampal region. An autoradiographic study in the mouse. *Exp Neurol Suppl*. October 1965:Suppl 2:1-70.
240. Altman J, Bayer SA. Migration and distribution of two populations of hippocampal granule cell precursors during the perinatal and postnatal periods. *J Comp Neurol*. 1990;301(3):365-381. doi:10.1002/cne.903010304
241. Witter MP, Groenewegen HJ, Lopes da Silva FH, Lohman AH. Functional organization of the extrinsic and intrinsic circuitry of the parahippocampal region. *Prog Neurobiol*. 1989;33(3):161-253.
242. van Groen T, Miettinen P, Kadish I. The entorhinal cortex of the mouse: organization of the projection to the hippocampal formation. *Hippocampus*. 2003;13(1):133-149. doi:10.1002/hipo.10037
243. Moser E, Moser MB, Andersen P. Spatial learning impairment parallels the magnitude of dorsal hippocampal lesions, but is hardly present following ventral lesions. *J Neurosci*. 1993;13(9):3916-3925.
244. Kjelstrup KG, Tuvnes FA, Steffenach H-A, Murison R, Moser EI, Moser M-B. Reduced fear expression after lesions of the ventral hippocampus. *Proc Natl Acad Sci U S A*. 2002;99(16):10825-10830. doi:10.1073/pnas.152112399
245. Bannerman DM, Rawlins JNP, McHugh SB, et al. Regional dissociations within the hippocampus--memory and anxiety. *Neurosci Biobehav Rev*. 2004;28(3):273-283. doi:10.1016/j.neubiorev.2004.03.004
246. Teng E, Squire LR. Memory for places learned long ago is intact after hippocampal damage. *Nature*. 1999;400(6745):675-677. doi:10.1038/23276
247. Tamamaki N. Organization of the entorhinal projection to the rat dentate gyrus revealed by Dil anterograde labeling. *Exp brain Res*. 1997;116(2):250-258.
248. Woodson W, Nitecka L, Ben-Ari Y. Organization of the GABAergic system in the rat hippocampal formation: a quantitative immunocytochemical study. *J Comp Neurol*. 1989;280(2):254-271. doi:10.1002/cne.902800207
249. Scharfman HE, Sollas AL, Smith KL, Jackson MB, Goodman JH. Structural and functional asymmetry in the normal and epileptic rat dentate gyrus. *J Comp Neurol*. 2002;454(4):424-439. doi:10.1002/cne.10449
250. Ambrogini P, Cuppini R, Cuppini C, et al. Spatial learning affects immature

- granule cell survival in adult rat dentate gyrus. *Neurosci Lett*. 2000;286(1):21-24.
251. Jinno S. Topographic differences in adult neurogenesis in the mouse hippocampus: A stereology-based study using endogenous markers. *Hippocampus*. 2011;21(5):467-480. doi:10.1002/hipo.20762
252. Snyder JS, Ramchand P, Rabbett S, Radik R, Wojtowicz JM, Cameron HA. Septo-temporal gradients of neurogenesis and activity in 13-month-old rats. *Neurobiol Aging*. 2011;32(6):1149-1156. doi:10.1016/j.neurobiolaging.2009.05.022
253. Tashiro A, Makino H, Gage FH. Experience-specific functional modification of the dentate gyrus through adult neurogenesis: a critical period during an immature stage. *J Neurosci*. 2007;27(12):3252-3259. doi:10.1523/JNEUROSCI.4941-06.2007
254. Chawla MK, Guzowski JF, Ramirez-Amaya V, et al. Sparse, environmentally selective expression of Arc RNA in the upper blade of the rodent fascia dentata by brief spatial experience. *Hippocampus*. 2005;15(5):579-586. doi:10.1002/hipo.20091
255. Ramirez-Amaya V, Marrone DF, Gage FH, Worley PF, Barnes CA. Integration of new neurons into functional neural networks. *J Neurosci*. 2006;26(47):12237-12241. doi:10.1523/JNEUROSCI.2195-06.2006
256. Satvat E, Schmidt B, Argraves M, Marrone DF, Markus EJ. Changes in task demands alter the pattern of zif268 expression in the dentate gyrus. *J Neurosci*. 2011;31(19):7163-7167. doi:10.1523/JNEUROSCI.0094-11.2011
257. Vazdarjanova A, Ramirez-Amaya V, Insel N, et al. Spatial exploration induces ARC, a plasticity-related immediate-early gene, only in calcium/calmodulin-dependent protein kinase II-positive principal excitatory and inhibitory neurons of the rat forebrain. *J Comp Neurol*. 2006;498(3):317-329. doi:10.1002/cne.21003
258. Cameron HA, McKay RD. Adult neurogenesis produces a large pool of new granule cells in the dentate gyrus. *J Comp Neurol*. 2001;435(4):406-417.
259. Vega CJ, Peterson DA. Stem cell proliferative history in tissue revealed by temporal halogenated thymidine analog discrimination. *Nat Methods*. 2005;2(3):167-169. doi:10.1038/nmeth741

260. Burns KA, Kuan C-Y. Low doses of bromo- and iododeoxyuridine produce near-saturation labeling of adult proliferative populations in the dentate gyrus. *Eur J Neurosci.* 2005;21(3):803-807. doi:10.1111/j.1460-9568.2005.03907.x
261. Tronel S, Charrier V, Sage C, Maitre M, Leste-Lasserre T, Abrous DN. Adult-born dentate neurons are recruited in both spatial memory encoding and retrieval. *Hippocampus.* 2015;25(11):1472-1479. doi:10.1002/hipo.22468
262. Abraham WC, Mason SE, Demmer J, et al. Correlations between immediate early gene induction and the persistence of long-term potentiation. *Neuroscience.* 1993;56(3):717-727.
263. Davis S, Bozon B, Laroche S. How necessary is the activation of the immediate early gene *zif268* in synaptic plasticity and learning? *Behav Brain Res.* 2003;142(1-2):17-30.
264. Fleischmann A, Hvalby O, Jensen V, et al. Impaired long-term memory and NR2A-type NMDA receptor-dependent synaptic plasticity in mice lacking c-Fos in the CNS. *J Neurosci.* 2003;23(27):9116-9122.
265. Bramham CR, Worley PF, Moore MJ, Guzowski JF. The Immediate Early Gene *Arc/Arg3.1*: Regulation, Mechanisms, and Function. *J Neurosci.* 2008;28(46):11760-11767. doi:10.1523/JNEUROSCI.3864-08.2008
266. Temprana SG, Mongiat LA, Yang SM, et al. Delayed coupling to feedback inhibition during a critical period for the integration of adult-born granule cells. *Neuron.* 2015;85(1):116-130. doi:10.1016/j.neuron.2014.11.023
267. Reymann KG, Frey JU. The late maintenance of hippocampal LTP: requirements, phases, “synaptic tagging”, “late-associativity” and implications. *Neuropharmacology.* 2007;52(1):24-40. doi:10.1016/j.neuropharm.2006.07.026
268. Zhou Q, Homma KJ, Poo M. Shrinkage of dendritic spines associated with long-term depression of hippocampal synapses. *Neuron.* 2004;44(5):749-757. doi:10.1016/j.neuron.2004.11.011
269. Oh WC, Parajuli LK, Zito K. Heterosynaptic structural plasticity on local dendritic segments of hippocampal CA1 neurons. *Cell Rep.* 2015;10(2):162-169. doi:10.1016/j.celrep.2014.12.016
270. Popov VI, Davies HA, Rogachevsky V V, et al. Remodelling of synaptic morphology but unchanged synaptic density during late phase long-term

- potentiation (LTP): a serial section electron micrograph study in the dentate gyrus in the anaesthetised rat. *Neuroscience*. 2004;128(2):251-262. doi:10.1016/j.neuroscience.2004.06.029
271. Wosiski-Kuhn M, Stranahan AM. Transient increases in dendritic spine density contribute to dentate gyrus long-term potentiation. *Synapse*. 2012;66(7):661-664. doi:10.1002/syn.21545
272. Abraham WC, Bliss TVP. An analysis of the increase in granule cell excitability accompanying habituation in the dentate gyrus of the anesthetized rat. *Brain Res*. 1985;331(2):303-313. doi:10.1016/0006-8993(85)91556-2
273. Okamoto K-I, Nagai T, Miyawaki A, Hayashi Y. Rapid and persistent modulation of actin dynamics regulates postsynaptic reorganization underlying bidirectional plasticity. *Nat Neurosci*. 2004;7(10):1104-1112. doi:10.1038/nn1311
274. Fukazawa Y, Saitoh Y, Ozawa F, Ohta Y, Mizuno K, Inokuchi K. Hippocampal LTP is accompanied by enhanced F-actin content within the dendritic spine that is essential for late LTP maintenance in vivo. *Neuron*. 2003;38(3):447-460.
275. Chistiakova M, Bannon NM, Chen J-Y, Bazhenov M, Volgushev M. Homeostatic role of heterosynaptic plasticity: models and experiments. *Front Comput Neurosci*. 2015;9:89. doi:10.3389/fncom.2015.00089
276. Penke Z, Morice E, Veyrac A, et al. Zif268/Egr1 gain of function facilitates hippocampal synaptic plasticity and long-term spatial recognition memory. *Philos Trans R Soc B Biol Sci*. 2013;369(1633):20130159-20130159. doi:10.1098/rstb.2013.0159
277. Minatohara K, Akiyoshi M, Okuno H. Role of Immediate-Early Genes in Synaptic Plasticity and Neuronal Ensembles Underlying the Memory Trace. *Front Mol Neurosci*. 2016;8(January):78. doi:10.3389/fnmol.2015.00078
278. Koldamova R, Schug J, Lefterova M, et al. Genome-wide approaches reveal EGR1-controlled regulatory networks associated with neurodegeneration. *Neurobiol Dis*. 2014;63:107-114. doi:10.1016/j.nbd.2013.11.005
279. Baumgärtel K, Tweedie-Cullen RY, Grossmann J, Gehrig P, Livingstone-Zatchej M, Mansuy IM. Changes in the proteome after neuronal Zif268 overexpression. *J Proteome Res*. 2009;8(7):3298-3316. doi:10.1021/pr801000r

280. James AB, Conway A-M, Morris BJ. Regulation of the neuronal proteasome by Zif268 (Egr1). *J Neurosci.* 2006;26(5):1624-1634. doi:10.1523/JNEUROSCI.4199-05.2006
281. Duclot F, Kabbaj M. The Role of Early Growth Response 1 (EGR1) in Brain Plasticity and Neuropsychiatric Disorders. *Front Behav Neurosci.* 2017;11. doi:10.3389/fnbeh.2017.00035
282. Covington HE, Lobo MK, Maze I, et al. Antidepressant effect of optogenetic stimulation of the medial prefrontal cortex. *J Neurosci.* 2010;30(48):16082-16090. doi:10.1523/JNEUROSCI.1731-10.2010
283. Kimoto S, Bazmi HH, Lewis DA. Lower expression of glutamic acid decarboxylase 67 in the prefrontal cortex in schizophrenia: contribution of altered regulation by Zif268. *Am J Psychiatry.* 2014;171(9):969-978. doi:10.1176/appi.ajp.2014.14010004
284. Hagihara H, Takao K, Walton NM, Matsumoto M, Miyakawa T. Immature Dentate Gyrus: An Endophenotype of Neuropsychiatric Disorders. *Neural Plast.* 2013;2013:1-24. doi:10.1155/2013/318596
285. Kempermann G, Gage FH, Aigner L, et al. Human Adult Neurogenesis: Evidence and Remaining Questions. *Cell Stem Cell.* April 2018. doi:10.1016/j.stem.2018.04.004



## 13 Curriculum Vitae

Marie-Violet L. Hawkrige \*1. Juli 1992



### Bildung

---

#### Goethe Universität Frankfurt am Main

Dritter Abschnitt der ärztlichen Prüfung (Note: 1,0) Dez 17

Zweiter Abschnitt der ärztlichen Prüfung (Note: 2,0) Okt 16

Erster Abschnitt der ärztlichen Prüfung: Physikum (Note: 1,5) Sep 13

#### Freie Waldorfschule Ulm, Deutschland

Aug 98 – Jul 11

Abitur: Notendurchschnitt: 1,2

### Berufserfahrung

---

#### St. Katharinen Krankenhaus Frankfurt

seit Jan 18

Assistenzärztin für Chirurgie

#### Sana Klinikum Offenbach

Okt 16 - Okt 17

Praktisches Jahr: mit Sono Kurs, BLS Kurs und Mikrochirurgie Kurs

Tertial in der Gastroenterologie, Radiologie und Diabetologie

Wahltertial in der Plastischen Chirurgie

Halbes Tertial in der Unfall- und Allgemeinchirurgie

#### Yonsei Universität, Severance Hospital in Seoul, Süd Korea

Mär17 - Apr 17

Praktisches Jahr:

Halbes Tertial in der Brustchirurgie und im

Department of Intensive Care and Trauma Surgery

### **Klinik für Sportmedizin, Hand- & Unfallchirurgie des Clemenshospital Münster**

Zwei Famulaturen auf Station, im OP und in der Ambulanz Jul 14 + Aug 15

### **Klinikum Heidenheim**

Famulatur auf der Station für Kardiologie Jan 15

Famulatur in der Praxis für Allgemein- und Anthroposophische Medizin Jan 16

Sechswöchiges Pflegepraktikum für Medizinstudenten Aug12– Sep 12

### **Bürgerhospital Frankfurt**

Feb12 – Aug12

Sechswöchiges Pflegepraktikum für Medizinstudenten (Diabetologie)

### **Cadmus Lifesharing Association, Great Barrington, USA**

Jun 09 – Jul 09

Sechswöchiges Sozialpraktikum in einer Einrichtung für Behinderte

### **Margarete Steiff GmbH, Giengen a. d. Brenz**

Jun 08 – Jul 08

Sechswöchiges Industriepraktikum im Entwicklungszentrum

Design und Herstellung eines eigenen Teddybärs

### **MEY Bodywear**

Sep 06

Im Rahmen: "Junior Akademie des Regierungspräsidium Tübingen"

Programmierung und Anwendung von CNC Nähmaschinen

Materialberechnung

## **Extracurriculäres Engagement**

---

**Kurs „Chirurgische Zugangswege“ der Goethe-Universität Frankfurt** Mär 15

Praktischer Kurs zu unfallchirurgischen Zugangswegen an der Leiche

**Osteosynthesekurs der Goethe-Universität Frankfurt**

Dez 15

Praktischer Kurs zu Osteosynsetechniken am Kunstknochen

**Hiwi Tätigkeiten in der Anatomie**

Mai 13 – Jul 15

Lehre im Präpariersaal über alle Themenbereiche der Anatomie

**Sommerschule der Goethe Universität Frankfurt**

Jul 13

Programm zur Eliteförderung für das Physikum

## **Praktische Projektarbeiten**

„The four poster bed“	2009
„The oriental carpet“	2006
Jeweils einjähriges Projekt mit Herstellung eines Himmelbetts und eines Teppichs je mit theoretischem Teil auf Englisch	

## **Stipendien**

---

<b>DAAD-PROMOS Stipendium</b>	2017
1.850€ für den zweimonatigen PJ- Aufenthalt in Seoul, Süd Korea	
<b>FPF-Promotionsstipendium der Goethe Universität Frankfurt</b>	2014
1.800€ für die Finanzierung der Dissertation im Freisemester	
<b>Stipendium des Deutsch-Französischen Jugendwerkes</b>	2009
Schüleraustausch nach Frankreich ins Lycée Internationale de Strasbourg	

## **Fähigkeiten und Interessen**

---



FELASA B (Experimentatorenfortbildung für Versuchstiere), Laborerfahrung bei Arbeit mit Ratten und Mäusen

Gute Kenntnisse von Word, Excel, Graphpad Prism, ImageJ und ImedOne. Grundkenntnisse SAP

## 14 Schriftliche Erklärung

Ich erkläre ehrenwörtlich, dass ich die dem Fachbereich Medizin der Johann Wolfgang Goethe-Universität Frankfurt am Main zur Promotionsprüfung eingereichte Dissertation mit dem Titel

Enhanced excitability and structural plasticity of maturing adult-born granule cells after LTP induction in the hippocampus.

In der Dr. Senckenbergischen Anatomie, Institut für Anatomie I (Klinische Neuroanatomie) unter Betreuung und Anleitung von PD Dr. Stephan Schwarzacher mit Unterstützung durch Prof. Dr. Thomas Deller ohne sonstige Hilfe selbst durchgeführt und bei der Abfassung der Arbeit keine anderen als die in der Dissertation angeführten Hilfsmittel benutzt habe. Darüber hinaus versichere ich, nicht die Hilfe einer kommerziellen Promotionsvermittlung in Anspruch genommen zu haben.

Ich habe bisher an keiner in- oder ausländischen Universität ein Gesuch um Zulassung zur Promotion eingereicht\*. Die vorliegende Arbeit wurde bisher nicht als Dissertation eingereicht.

Vorliegende Ergebnisse der Arbeit wurden in folgendem Publikationsorgan veröffentlicht:

S.M. Ohline, K.L. Wake, M.-V. Hawkrigde, M.F. Dinnunhan, R.U. Hegemann, A. Wilson, L. Schoderboeck, B.J. Logan, T. Jungenitz, S.W. Schwarzacher, S.M. Hughes, W.C. Abraham, Adult-born dentate granule cell excitability depends on the interaction of neuron age, ontogenetic age and experience. Brain Structure and Function, 223, 1-16, 2018

---

(Ort, Datum)

---

(Unterschrift)

\*) im Falle des Nichtzutreffens entfernen